TAMPEREEN TEKNILLINEN YLIOPISTO
TAMPERE UNIVERSITY OF TECHNOLOGY

OSCAR RODERA GARCIA

DAMAGE ONSET MODELLING OF CURVED COMPOSITE LAMINATES

Master of Science thesis

Examiner: Assistant Professor Mikko Kanerva, M.Sc. Jarno Jokinen, Dr. Donato Di Vito
Examiner and topic approved by the Faculty Council of the Faculty of Tampere
on 26th September 2018

ABSTRACT

OSCAR RODERA GARCIA: Damage onset modelling of curved composite laminates
Tampere University of Technology
Master of Science thesis, 92 pages, 17 Appendix pages
September 2018
Master's Degree Programme in Materials Science and Engineering, MSc (Tech)
Major: Plastics and elastomers
Examiner: Assistant Professor Mikko Kanerva, M.Sc. Jarno Jokinen, Dr. Donato Di Vito
Keywords: Fibre Reinforced Polymer (FRP) composites, World Wide Failure Exercise, Failure criteria, Fracture modelling, Damage onset, UMAT/VUMAT subroutines, Uniaxial test, Impact test.

Fibre Reinforced Polymer (FRP) composites are widely used in industry applications (e.g. aerospace, automotive), which require a high accuracy in terms of damage prediction and identification. Knowing the material behaviour under several loading conditions constitutes the key to understand and predict how failure initiates in FRP composites. The aim of this study is to carry out an analysis of damage onset over a semi-cylindrical structure (E-Glass/Polyester) subjected to impact of a rigid object. The first step in this thesis focuses on assessment and selection of the most relevant failure criteria from the two first exercises of the World Wide Failure Exercise (WWFE-I and II) [1]. Experimental and numerical tests under tensile (study of the material behaviour under 2D stresses) and impact loading (study test under 3D stresses) are carried out on curved specimens. The chosen failure criteria involve different failure modes (fibre and inter-fibre failure modes). The aforementioned criteria were implemented in Abaqus by using the UMAT and VUMAT subroutines. Finally, the experimental and numerical results were compared, in order to define the criterion with the best applicability over a wide range of mechanical applications.

PREFACE

All of the work presented in my Master Thesis was conducted in the modelling group of Laboratory of Materials Science at the Tampere University of Technology.
The theory base has been key to understand future steps in the Master Thesis. The finite element tool has allowed me knowing the composite material world in a detail and faster way. The experience has demonstrated that the modelling has to be always subjected to experimental tests, which allows contrasting results and draw firm conclusions. I would like to thank my work instructors M.Sc. Jarno Jokinen and Dr. Donato Di Vito for their excellent guidance during this process. They have contributed in my understanding and development process in the research field. I also wish to thank my supervisor Assistant Professor Mikko Kanerva for having trusted in me to carry out this important work. I would not have been able to conduct this research, without their cooperation. Thanks also to project Luxturrim5G (Business Finland, 10098/31/2016) for its financial and research support.
Finally, I would also like to thank my family and The Circle for being my motivation during more than six months which I have been working in this project.

Tampere, 24.09.2018

Óscar Rodera García

CONTENTS

LIST OF FIGURES

LIST OF TABLES

LIST OF ABBREVIATIONS AND SYMBOLS

2D	Two-dimensional
3D	Three-dimensional
FEM	Finite Element Method
FE	Finite Element
DOF	Degree of Freedom
FEA	Finite Element Analysis
GRP	Glass Fiber Reinforced Plastic
FRP	Fiber Reinforced Polymer
CFRP	Carbon fiber Reinforced Polymer
GFRP	Glass fiber Reinforced Polymer
WWFE	World Wide Failure Exercise
SR	Stress Ratio
PCR	Property Correlation Ratios
UD	Unidirectional
SDV	State Dependent Variable
FF	Fiber Failure
IFF	Inter Fiber Failure
Eff	Effort
NWF	Non-Woven Fabric
FMC	Failure Mode Concept
MCT	Multi Continuum Theory
ICAN	Integrated Composite Analyser
CODSTRAN	Composite Structural Analyser

σ_1,σ_{11}	Stress in fiber direction $N/(mm)^2$
σ_2,σ_{22}	Stress in transverse direction to fibers $N/(mm)^2$
$\sigma_3\sigma_{33}$	Stress in transverse direction to fibers $N/(mm)^2$
σ_4,τ_{12}	Stress shear in transversal plane to fibers $N/(mm)^2$
σ_5,τ_{13}	Stress shear in transversal plane to fibers $N/(mm)^2$
σ_6,τ_{23}	Stress shear in parallel plane to fibers $N/(mm)^2$

σ_A^+	Hashin tensile failure stress in fiber direction $N/(mm)^2$
σ_A^+	Hashin tensile failure stress in fiber direction $N/(mm)^2$
σ_A^-	Hashin compressive failure stress in fiber direction $N/(mm)^2$
σ_T^+	Hashin tensile failure stress transverse to fiber direction $N/(mm)^2$
σ_T^-	Hashin compressive failure stress transverse to fiber direction $N/(mm)^2$
τ_T/σ_{nt}	Hashin transverse failure stress shear $N/(mm)^2$
τ_A/σ_{ln}	Hashin axial failure shear $N/(mm)^2$
$I_1, I_2, I_3, I_4, I_5, I_6$	UD Invariants
C_{ii}	Stiffness matrix constants
$p_{vp}^+, p_{vp}^-, p_{vv}^-$	Puck inclination parameters
$m_{\sigma f}$	Magnification factor
E_1, E_2, E_3	Young's modulus in fiber and transverse fiber direction $N/(mm)^2$
G_i	In-plane shear modulus $N/(mm)^2$
f_E	Stress exposure
f_{EIFF}	Puck stress exposure in inter fiber failure mode
f_{EFF}	Puck stress exposure in fiber failure mode
f_S	Stretch factor
σ_{nn}	Puck stress in transversal and horizontal plane to fibers $N/(mm)^2$
τ_{nt},τ_{n1}	Puck stress shear tensor in transversal plane to fibers $N/(mm)^2$
$R_\parallel^t$, $R_\parallel^c$	Cuntze and Puck tensile and compression strength parallel to fibers $N/(mm)^2$
$R_\perp^t$, $R_\perp^c$	Cuntze and Puck tensile and compression strength transversal to fibers $N/(mm)^2$
$R_{\parallel\perp}$	Cuntze and Puck in-plane shear strength $N/(mm)^2$
$b_\perp^t$,$b_{\parallel\perp}$	Cuntze fiction-related b-parameters
m	Cuntze interaction exponent
$Subcript - f$	Fiber

1. INTRODUCTION

A few decades ago, the industry was dominated mainly by metallic materials. However, composite materials have achieved great progress due to developments such as weight reduction, durability, additional functionality and design freedom. The combination of fibre reinforced with the matrix has allowed to comply with the final properties required. The composite materials imply heterogeneity, anisotropy and various modes of failure. Unlike isotropic materials, fibre reinforced polymer (FRP) composites exhibit a more complex behaviour against failure. For that, an analysis more accurate of the material mechanic is required in order to make up for the demands of the industry. However, the study of failure in FRP composites needs to a coordination of its theory because of the large numbers of failure criteria involved currently. This complexity is being overcome through the powerful computational systems, which allow implement and model the failure approaches by using finite element method software. They search to get results comparable with experimental ones. Therefore, with the objective of contributing in establishing a design tool more effective in the sector, this thesis focuses on analysing and predicting the damage onset over a curved structure made up with fiber reinforced polymer composite (E-Glass/polyester).

2. REMARKS ON MECHANICS OF MATERIALS

Composite materials are structural materials constituted by two or more components combined at a macroscopic level; they are generally defined as not soluble in each other. One component is called the reinforcing phase (it forms fibres, particles or flakes) and the other one the matrix phase (it is a continuous material). The composites are classified by means of reinforcement geometry (particulate, flake and fibers) or by the type of matrix (polymer, metal, ceramic and carbon). The selection of type of composite depends on which industrial application it will carry out.
This thesis will focus on studying a composite material composed by fibers as reinforcing phase and polymer as matrix phase. The fibers can be continuous (fibers set up the ply with large and non-cut filaments) or discontinuous (fibers set up the ply with shorter and cut filaments). The polymers are classified into thermosets and thermoplastics. The thermosets are soluble and infusible after curing due to the chains are joints with strong covalent bonds. While the thermoplastic polymers are manufacture at high temperature and pressure because of the weakness of theirs bonds (van der Waals type). Typical examples of thermosets are epoxies, polyesters, phenolic and polyamide; and thermoplastics include polyethylene, polystyrene PEEK and polypropylene sulphide (PPS).

2.1 Stress and strain definitions

A laminate is constructed by staking a number of plies in the thickness direction. The design and analysis of the stacked structures, require of knowledges of the stresses and strain in the plies. In addition, the design tools (such as failure theories, stiffness models or optimization algorithms) need also to know the relations and values of stresses ans strains, which allow understanding the mechanical analysis of a lamina. Unlike the isotropic material, a ply displacement in the fiber direction generate a distinct deformation than a displacement in the transversal direction to the fibers. These deformation in the ply are more complex when the displacement is applied with a direction angle less to 90°.
The mechanical structure supports external forces, which result in internal forces inside of the body. It is indispensable to know the values and direction of these

internal forces, since they have to be less the material strengths of the structure. These strengths of a material are defined as the intensity of load per unit area that it give rise to the stress concept. If a body in equilibrium with external forces is taken, a component of force is acting over a cross-section of this body of very small area. This force has tangential and normal components over this plane, which are divided into the infinitesimal area in order to get stresses in the tangential and normal direction in respect of the cross-section. If a coordinate system x-y-z is taken (axis-x in normal direction and axis-y and -z in tangential direction), the definition of the stresses would be (figure 2.2-A) [46]:

$$\sigma_x = \lim_{\triangle A \to 0} \frac{\triangle P_x}{\triangle A}$$

$$\tau_{xy} = \lim_{\triangle A \to 0} \frac{\triangle P_y}{\triangle A}$$

$$\tau_{xz} = \lim_{\triangle A \to 0} \frac{\triangle P_z}{\triangle A}$$

Similarly, stresses are defined by taking an infinitesimal cuboid, which represents better all directions of a body. Nine different stresses are represented over the cuboid, which has three stresses in each face with different directions.
Both the stress of the internal structure and its strains have to be known. Because the analysis of stresses require finding deformations. The strain is defined as the relative change in the size and shape of a body. They are also defined on an infinitesimal cuboid, whose lengths of the sides change under loads. This change is related to a normal strain and the distortion corresponds to the shear strains. The strains are related to the displacements, which are defined as (figure 2.2-B) [46]:

$$u = u(x, y, z) = displacementinx - directionatpoint(x, y, z)$$

$$v = u(x, y, z) = displacementiny - directionatpoint(x, y, z)$$

$$w = u(x, y, z) = displacementinz - directionatpoint(x, y, z)$$

If the strains in each direction is defined as the change of its correspond lengths and the partial derivatives are taken, the strains in each direction are:

$$\varepsilon_x = \lim_{AB \to 0} \frac{A'B' - AB}{AB}$$

$$-> \varepsilon_x = \frac{\partial u}{\partial x}$$

$$\varepsilon_y = \lim_{AD \to 0} \frac{A'D' - AD}{AD}$$

$$-> \varepsilon_y = \frac{\partial v}{\partial y}$$

$$\gamma_{xy} = \lim_{AB \to 0} \frac{P'B'}{A'P'} + \lim_{AD \to 0} \frac{Q'D'}{A'Q'}$$

$$-> \gamma_{xy} = \frac{\partial u}{\partial y} + \frac{\partial v}{\partial x}$$

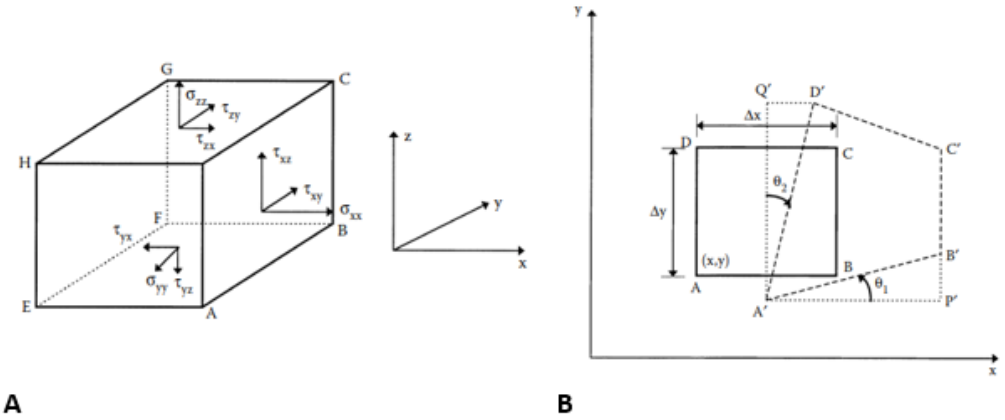

Figure 2.1 *(A) Stresses on an infinitesimal cuboid; (B) Normal and shearing strains on an infinitesimal area in the x-y plane.*

The stress-strain relationship for anisotropic material follow the Hooke law by means its constants, which can be different for each anisotropic material. Figure 2.2-A shows the stress-strain relationships in a 1-2-3 orthogonal Cartesian system. The matrix C (6x6) represent the material stiffness and its inverting matrix is the compliance matrix (strain-stress relationships). The material implemented in this thesis is orthotropic, which has three mutually perpendicular planes of material symmetry. These planes would imply also three mutually perpendicular planes of elastic symmetry. Figure 2.2-B shows the stiffness matrix of the orthotropic material, which presents nine independent elastic constants with the poisson rations ($\nu_{1,2,3}$), young modulus ($E_{1,2,3}$) and shear modulus ($G_{1,2,3}$) of each direction. This kind of material is typical in plies of continuous fiber composites.

$$\begin{bmatrix}\sigma_1\\ \sigma_2\\ \sigma_3\\ \tau_{23}\\ \tau_{31}\\ \tau_{12}\end{bmatrix}=\begin{bmatrix}C_{11} & C_{12} & C_{13} & C_{14} & C_{15} & C_{16}\\ C_{21} & C_{22} & C_{23} & C_{24} & C_{25} & C_{26}\\ C_{31} & C_{32} & C_{33} & C_{34} & C_{35} & C_{36}\\ C_{41} & C_{42} & C_{43} & C_{44} & C_{45} & C_{46}\\ C_{51} & C_{52} & C_{53} & C_{54} & C_{55} & C_{56}\\ C_{61} & C_{62} & C_{63} & C_{64} & C_{65} & C_{66}\end{bmatrix}\begin{bmatrix}\varepsilon_1\\ \varepsilon_2\\ \varepsilon_3\\ \gamma_{23}\\ \gamma_{31}\\ \gamma_{12}\end{bmatrix},$$

A

$$[C]=\begin{bmatrix}\frac{1-\nu_{23}\nu_{32}}{E_2E_3\Delta} & \frac{\nu_{21}+\nu_{23}\nu_{31}}{E_2E_3\Delta} & \frac{\nu_{31}+\nu_{21}\nu_{32}}{E_2E_3\Delta} & 0 & 0 & 0\\ \frac{\nu_{21}+\nu_{23}\nu_{31}}{E_2E_3\Delta} & \frac{1-\nu_{13}\nu_{31}}{E_1E_3\Delta} & \frac{\nu_{32}+\nu_{12}\nu_{31}}{E_1E_3\Delta} & 0 & 0 & 0\\ \frac{\nu_{31}+\nu_{21}\nu_{32}}{E_2E_3\Delta} & \frac{\nu_{32}+\nu_{12}\nu_{31}}{E_1E_3\Delta} & \frac{1-\nu_{12}\nu_{21}}{E_1E_2\Delta} & 0 & 0 & 0\\ 0 & 0 & 0 & G_{23} & 0 & 0\\ 0 & 0 & 0 & 0 & G_{31} & 0\\ 0 & 0 & 0 & 0 & 0 & G_{12}\end{bmatrix}$$

where

$$\Delta=\left(1-\nu_{12}\nu_{21}-\nu_{23}\nu_{32}-\nu_{13}\nu_{31}-2\nu_{21}\nu_{32}\nu_{13}\right)/\left(E_1E_2E_3\right).$$

B

Figure 2.2 *(A) Stress-strain relations in anisotropic materials; (B) Orthotopic stiffness matrix.*

2.2 Introduction on failure criteria

Once the stress and strain and their relationships are known, the failure theories can employed in order to study better the behaviour of laminates. The failure in composites is fairly complex, since it may not be catastrophic. Although some plies of a laminate fail, other plies from the same laminate can still keep the stiffness and strength of the structure under the same loading condition. The degradation of stiffness and the strength of the laminate depends on the failrue criteria employed. The failure theories, where the main criteria involved in this thesis are backed up, are:

The second-degree polynomial expansion, which represents mathematical form of the failure through the stress tensor. For orthotropic material, the shear and normal stress have to be independent of the shear stress sign. In consequence, the shear strengths are assumed uncoupled and the failure criteria would be with the following form:$(F_1\sigma_1 + F_2\sigma_2 + F_3\sigma_3) + (F_{11}\sigma_1^2 + F_{22}\sigma_2^2 + F_{33}\sigma_3^2 + F_{44}\sigma_4^2 + F_{55}\sigma_5^2 + F_{66}\sigma_6^2) = 1$ [11]. The Mohr fracture hypothesis for brittle material is based in determining the combination of shear and normal stress that can cause the failure in the material. For that, the Mohr circle determines the principle stresses due to the shear and normal stress, and it is capable to obtain the plane angle where these stresses occur [57]. The failure mode concept is based on macro-mechanical invariants which consider failure in fibres and in matrix. The strength failure conditions are based on the material symmetry requirements of UD material, which is isotropic transversally [12].

3. FAILURE CRITERIA

The section 3 will focus on setting a scene for an investigation and analysis about the status of fiber reinforced polymer composites (FRPs) failure theories by means the World Wide Failure Exercise (WWFE). This exercise involves different kind of composite materials, lay-ups and loading conditions for each test case. The failure criteria presented in WWFE are implemented under bi-directional (2D) and tri-directional (3D) state of stress into a collection of test cases proposed by the organisers. In order to carried out the target of this work, an assessment will be done for determining which of the present criteria are optimal to predict the damage onset into the study case, presented in the section 4.

3.1 Overview about the World Wide Failure Exercise - I

Composite materials are currently well integrated into industry, but engineers and researches communities constantly face with challenges related to manufacturing industrial processing and composite material continuum mechanic behaviour. Then, an expert meeting was held at United Kingdom in 1991 with the aim of achieving a level of confidence in the failure prediction of the FRP by resulting in the World Wide Failure Exercise (WWFE). The participants from different countries concluded that:

• There were not evident predictions of failure provided by the present criteria at ply or laminate level.

• There were not enough connections between the definitions of failure at ply level and structural applications in the industry.

In consequence, the World Wide Failure Exercise carried on as coordinated study by experts on the field. Its target resided on knowing how accurately the strength of a FRP laminate was be able to be predicted. For that, a first exercise, which was named as World Wide Failure Exercise−I, was carried out. From 1996 to 2004, the WWFE-I participants focused on the implementation of the WWFE-I failure criteria into FRP composites under two-dimensional (2D) state of stresses. Each involved criterion was analysed in the different 2D test cases, which were based on a specific 2D loading condition, lay-up and material. Given the huge number of criteria and test cases, the exercise procedure followed these four points for establishing

the final conclusions:
1. Identification of the best failure theories for FRP;
2. Application of the theories to the different test cases;
3. Theories comparison with each other and with the experimental results;
4. Ranking of the theories based on the achieved results;

However, two important points were taken into account due to the differences between research community and industry to develop this procedure. Partly because of their implementations of technical methods and approaches and partly, because of companies could resistance themselves to set new limitations in the failure prediction, since they had been investing a lot of money in project already started. They could already have established design and qualification procedures. Thus, the members chose a strategy divided into two sequential stages named Part A and Part B.

Part A
The part-A was planned to contain the details of the test cases and the different prediction chosen by the first exercise organisers. This was supported by a several papers, which provided deep descriptions of each criterion. The prediction of strengths and stress versus strain curves for each test case was exposed by mean the experimental data provided. Finally, a comparison was carried out between the approaches of the failure criteria and prediction made in each test case.

Part B
After carrying out the part A, a second procedure assessed the work done until then. For that, the experimental results from the test cases were described in more detail by means an evaluation of their developments. In addition, the comparison of each criterion with each experimental test case was improved by discussing their performances in order to do a refinement of the criteria mathematical approach according to the experimental data. Finally, an overall comparison of the experimental and approached results was published by establishing a degree of validation in the failure criteria so that the engineering communities could use it.

The WWFE-I involves sixteen failure criteria shown in figure 3.2. In order to deal with as many cases as possible, authors used fourteen test cases in the first exercise, as shoen in table 3.1. Each test case employees one loading condition, material and lay-up, which were established to develop an analysis as accurate as possible.

Table 3.1 *14 loading conditions, lay-ups and materials of the WWFE-I.*

Test Cases	Lay-up	Material	Loading conditions
1	0°	E-glass/LY556 epoxy	σ_y versus τ_{xy} envelope
2	0°	T300/BSL914C carbon/epoxy	σ_x versus τ_{xy} envelope
3	0°	E-glass/MY750 epoxy	σ_y versus σ_x envelope
4	(±30°/90°)	E-glass/LY555 epoxy	σ_y versus σ_x envelope
5	(±30°/90°)	E-glass/LY555 epoxy	σ_y versus τ_{xy} envelope
6	(0°/ ± 45°/90°)	AS4/3501-6 carbon/epoxy	σ_y versus σ_x envelope
7	(0°/ ± 45°/90°)	AS4/3501-6 carbon/epoxy	Stress-strain curves for σ_y:σ_x= 1:0
8	(0°/ ± 45°/90°)	AS4/3501-6 carbon/epoxy	Stress-strain curves for σ_y:σ_x= 2:1
9	±55°	E-glass/MY750 epoxy	σ_y versus σ_x envelope
10	±55°	E-glass/MY750 epoxy	Stress-strain curves for σ_y:σ_x= 1:0
11	±55°	E-glass/MY750 epoxy	Stress-strain curves for σ_y:σ_x= 2:1
12	(0°/90°)	E-glass/MY750 epoxy	Stress-strain curves for σ_y:σ_x= 0:1
13	±45°	E-glass/MY750 epoxy	Stress-strain curves for σ_y:σ_x= 1:1
14	±45°	E-glass/MY750 epoxy	Stress-strain curves for σ_y:σ_x= 1:-1

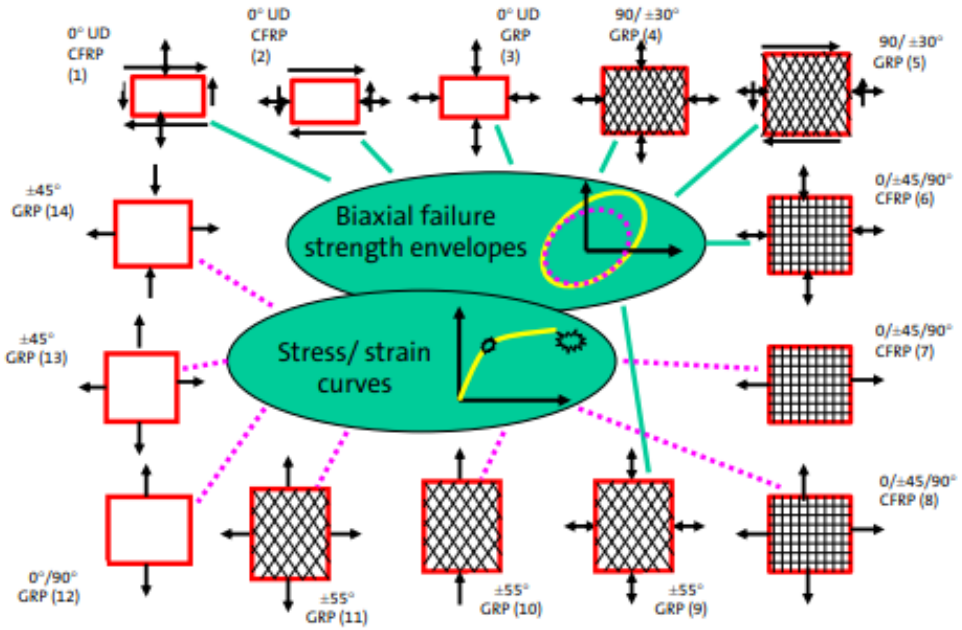

Figure 3.1 *14 loading conditions, lay-ups and materials of the WWFE-I ,[38].*

Through fourteen test cases above and with the scope to face the lack of confidence in the failure criteria, the following more specific issues were tackled:

- Use of micro-mechanics for prediction properties.
- Prediction of 2D modes of failure.
- Prediction of the biaxial failure envelopes for a variety of laminates.
- Matrix failure in tension, shear and compression.
- Material non-linearity.

- Post-failure modelling under 2D stresses.
- Prediction of fibre failure.

3.1.1 Contributors and failure theories

Table 3.2 shows the fourteen criteria which were chosen to analyse failure of composite materials. Most of these failure theories were modified during the second stage (Part B) of the exercise for failure theory could predict much better the experimental results. A more extensive and specific description of the theories are shown below (which are involved for both part A and part B of the WWFE-I).

Table 3.2 *Involved failure criteria of the WWFE-I.*

Contributors/ Theory	Organisation	Approach
L.J. Hart-Smith	Boeing, USA	10% rules theory
R. Cuntze et. al.	MAN Technologies Germany	Failure Mode Concept(Puck)
T. Bogetti et. al.	U.S. Army Research Laboratory (USA)	Maximum Strain Theory
Hansen et. al.	Alfred University (USA)	Multi-continuum theory
Z-M Huang	Tongi University (China)	Bridging model
Chamis C.C. et. al.	NASA Lewis (USA)	Micro-mechanics analyses
Eckold G.C.	AEA Technology (U.K.)	British Standard pressure vessel
Edge E.C.	Military Aircraft Division Warton (U.K.)	In-house design method
Hart Smith J.	Douglass Products Division (Canada)	Tresca and Maximum strain theory
McCartney L.N.	National Physical Laboratory (U.K.)	'Damage Mechanics'
Puck et. al.	Technische Hochchule (Germany)	Physically based 3D phenomenological models
Rotem A.	Faculty of Mechanical Engineering (Israel)	Interactive matrix and fibre failure theory
Sun C.T. et. al.	Purdue University (USA)	Linear and non-linear analysis.
Tsai S.W. et. al.	Aeronautics and Astronautics Dept. (USA)	Interactive progressive quadratic failure criterion
Wolfe et. al.	Department of Civil Engineering (Ohio, USA)	Maximum strain energy method
Zinoviev P. et. al.	Institute of Composite Technologies (Moscow, Russia)	Maximum stress theory

TSAI THEORY

Tsai developed a method to apply failure criteria to laminated composites. Failure mode was applied at points close to the initiation of failure under non-homogeneous stresses. Then a ply-by-ply analysis process was used to evaluate the capacity of laminate under higher loads. This process was based on repeated until the ultimate strength of the whole laminate is reached. The method was based on quadratic criterion with a mathematically rigorous framework and gave a basis to cater for 3D failure cases. In the part B, author introduced a new method of analysing the post-initial failure response. This theory was developed at Aeronautics and Astronautics Department in Stanford University (California, USA) [49].

WOLFE THEORY

Wolfe and Butalia developed a method for biaxial loading conditions by predicting

the stress/strain response, failure onset and progression in composite laminates. It involved longitudinal, transversal and shear stresses. Authors implemented the non-linear behaviour of the plies through a piecewise cubic spline interpolation scheme. This method evolved a strain-energy based failure criterion for orthotropic materials and an iterative incremental constitutive law to predict failure progression. In the part B, the author revised predictions for the majority of the test cases. This work was carried out at Civil Engineering Department in Ohio State University (Ohio, USA) [8].

EDGE THEORY

Edge presented an approach based on the stress-based Grant-Sanders method for predicting the initial and final failure in stress/strain curves. This method employed a ply-by-ply analysis with discrete failure criterion by considering only shear-tension and compression for matrix and fibre, respectively. Author implemented secant modulus versus strain curves for modelling the non-linear stiffness assuming that failed plies unload gradually. In the part B, author included the shear-compression interaction theory and the delamination criterion. It was developed at Military Aircraft Division Warton (UK) [22, 23].

ROTEM THEORY

Rotem failure criterion analysed the failure in matrix and fibre separately under in-plane loads, but there was not a possibility of inter-laminar failure. Predictions of laminate failure were based on the total stress in each ply by connecting the rotated stresses to the failure criterion. On the other hand, adjacent plies contributed to the strength of the ply by the bridging effect and therefore through an experimental factor. This theory was developed in collaboration with Hashin. In the part B, author considered the effects of matrix degradation on the stress-strain curves. It was developed at Faculty of Mechanical Engineering of Israel (Haifa, Israel) [60, 34].

SUN THEORY

Sun and Tao criterion employed the linear laminate theory to predict failure envelopes in uni and multi-directional composites by considering both material non-linearity and progressive matrix cracking. Authors employed a shear-lag analysis and Finite Element Analysis (FEA),which allowed to predict the stress/strain components and progressive matrix cracking. Different analyses were carried out, both a linear analysis (employed a derivation of the Hashin-Rotem ply failure criteria) and a non-linear analysis (based on finite element analysis for elastic/plastic material properties and progressively increasing matrix crack density). In the part B, a minor correction to the stress-strain curves was made. Authors developed this

theory at School of Aeronautics and Astronautics in Purdue University (Indiana, USA) [63, 34].

ECKOLD THEORY

Ecklod worked on designing a method used in the prevailing code for the design of glass-fibre-reinforced plastic (GRP), named as BS4994 approach. This approach was based on a strain-based criterion to get long-term design allowable. BS4994 approach was implemented into materials, which resist aggressive environments, thermal stresses (since it takes them into account when there is a mismatch due to thermal expansion between individual layers), ultimate strength (the code is not concerned with its prediction, only the mechanical properties and the approach to the laminate design was taken) and non-linear properties (stress-strain curves were limited to 0.5% strain). It had very small modification in part B and it was developed at AEA Technology (Harwell, UK) [21].

MCCARTNEY THEORY

McCarteney employed an analysis based on the prediction of ply crack formation and failure in laminates. Author employed the thermal residual stresses, which appeared due to thermal expansion effects between plies. The solutions of the model allowed to predict three important concepts in the criterion mathematical approach. The dependence of crack density on the value of the applied stress, the effective elastic constants on applied stress and the non-linear stress/strain behaviour associated with damage. In the part B, the applicability was extended to include angle ply and quasi-isotropic laminates. In addition, the maximum fibre strain limit was included as a criterion for fibre dominated failure. All these approaches were worked out at national Physical Laboratory (London, UK) [51].

HART-SMITH THEORY

Hart-Smith [31] carried out three different works. The first one was based on a generalized Tresca model [32] (it was constituted by five non-interactive strain limits, longitudinal and transverse strains combined with an in-plane shear strain limit). In the second one, author developed a 2-D interpretation of the widely used Maximum Strain and Truncated Maximum Strain failure theory [33] (it was based on the same failure criterion for metals, implemented to fibre/polymer composites). The third one implemented a generalisation of Hart-Smith's well known Ten Percent Rule [30] (rule based on reducing the number of measured properties needed when there were neither calculators nor desk-top computer). As for the part B, the author considered the effects of various methods of reducing failed ply moduli in the behaviour of the stress-strain curves. All of them were developed at Douglass Products Division

(Longbeach, USA).

PUCK THEORY

Puck developed a mechanistic theory that distinguishes between various modes of failure. The author employed two fracture criteria (fibre fracture and inter-fibre fracture). Through the inter-facial failure criteria the author could provide realistic stresses to failure and indicate their directions. The failure mode was based on degradation of plies stiffness after crack initiation with increasing load until either one of the fibre from one ply breaks or an inclined wedge-shaped inter-fibre crack appears, which leads to the failure of the whole laminate. This work was developed at Technische Hochchule (Darmstadt, Germany) [55].

CUNTZE THEORY

Cuntze focused on two aspects of failure prediction about initiation of the failure of a unidirectional ply and the non-linear progressive failure. The author employed the Failure Mode Concept (FMC) for failure conditions based on five failure mechanisms (two fibre failure (FF) and three inter-fibre failure (IFF)). In the part B, author carried out some simplifications of failure criteria and of computer code to get greater stresses. It is important to poit out that there was a very good correlation between predictions and the test data for UD plies and satisfactory correlation for laminates under Fiber Failure (FF). Cuntze theory was developed at MAN Technologies Germany [15, 13].

HUANG THEORY

Huang employed a micro-mechanical prediction procedure named 'bridging model' to define the 'instantaneous stiffness matrix'. Through this model the stress increments exerted on each ply were got and the stress increments with the constituent fiber and matrix were related each other. The author adopted a maximum normal stress criterion to predict the failure and to understand the progressive failure mode. This criterion established that if any of the constituent stresses achieved their maximum stress, it was considered that the ply has failed and the overall stiffness matrix of the laminate was reduced. Another key point was that the residual thermal stresses (consequence of lack in relationships between the coefficients of thermal expansion in fiber and matrix) was incorporated into his analysis. This development was taken place at Tongi University (Shanghai, China) [42].

BOGETTI THEORY

Bogetti employed the Maximum Strain theory in a full 3D form, by taking into account the non-linear shear stress-strain response of the lamina. There were minor

changes during the part B. It was developed at U.S. Army Research Laboratory [5, 6].

MAYES THEORY
Mayes and Hansen utilized a multi-continuum theory (MCT) to develop the stress-interactive failure criteria. This theory employed a non-linear shear behaviour in lamina, a formulated interactive failure criterion at the fiber and matrix constituent level and a finite element method to obtain the stresses at 3D level. There were no modificationsc during the part B for this theory, except fine-tuning modes of failure. It was developed at Naval Surface Warfare Center, West Bethesda (Alfred University) [43, 50].

CHAMIS THEORY
Integrated Composite Analyser (ICAN) and Composite Structural Analyser (COD-STRAN) have been developed by Chamis and his group in NASA to allow the analysis of complex structures. Both programs were based on micro-mechanics relationships to predict the ply properties and were developed at NASA Lewis (Cleveland, USA) [25, 26].

ZINOVIEV THEORY
Zinoviev employed the well known maximum stress criterion to develop his own theory. Author employed unloading behaviour factor of cracked laminates and the geometric non-linearity when there is changes in pay angle due to increasing deformation. This theory was developed at Instiute of Composite Technologies (Moscow, Russia) [71, 72].

3.1.2 Achievements and Gaps of the First exercise

The main and important results after finishing the WWFE-I concluded that:

- It established the limits of applicability of the failure theories and generated a benchmark for their accuracy.

- It gathered theories and practice on the failure in composites in order to achieve agreement in the results.

- It built the foundations to increase confidence in the theory of failure in the composite material.

- Through part B, it was possible to improve theories which had not been modified from the beginning (around 50% of all theories were modified). Thus, part B allowed to focus on gaps of theoretical and experimental development and understanding related to failure theory.

On the other hand, the weaknesses in the prediction of the failure criteria involved are due to two important points. These points, which involves other failure techniques, were not able to study neither implement them during the first exercise because of a lack of methodology and of 3D state of stress:

- Failure of Damaged Laminates that it involves: Damage evolution, matrix cracks initiation and crack density evolution, effects of ply thickness, effects of ply stacking sequence, cracking under thermal loading, failure at stress concentration (e.g. open holes), statistical and probabilistic nature of failure and leakage prediction.

- Failure under 3D state of stress which bases on: Applicability of composite failure criteria to isotropic materials, effects of pressure on shear strength and deformation of UD lamina, failure of unidirectional (UD) ply under hydrostatic pressure, Effect of through-thickness stress on biaxial failure of UD lamina, effects of 3D stresses on the failure of multi-directional laminates, deformation of laminates under hydrostatic pressure, 3D elastic constants of multi-directional laminates, effects of lay-up on through-thickness strength of laminates and failure under combined through-thickness and shear of laminates.

3.2 The World Wide Failure Exercise - II

The WWFE-I achieved important progresses in prediction the strength in FRP composites that allowed setting the bases of the involved failure criteria and their applicability into real test cases. In consequence, the predictions obtained under 2D loads in-plane were accepted by the engineers and reseacher communities. However, these same communities requested to resolve real applications in effective manner (bolted joints, impact loadings and ballistic penetration, thick composites, high pressure equipment...), which involved failures of composite materials under 3D state of stresses. New authors and some of the members from WWFE-I were carried out a second exercise, named as World Wide Failure Exercise-II (WWFE-II) in order to overcoming mentioned deficiency. Therefore, the aim of the exercise was established

level of confidence in the accuracy of the predictive tools that allowed to wonder how well the models could predict the failure under 3D situations.
Obviously, WWFE-II involved new failure criteria, adaptation of criteria used in WWFE-I and new test cases with different loading conditions, materials and lay-ups. The procedure of the WWFE-II was developed and divided in two areas like in WWFE-I:

Part A
In this part, authors involved of WWFE-II selected the test cases, in which their criteria were applied. This application of each failure criterion followed a coordinated scheme focused on performance. It took into account the failure modes employed, linearity of the analysis and criterion implementation into the finite element software. Finally, the results were analysis by comparing the failure envelopes with the stress-strain curves with the objective of showing weakness and strengths of the failure criteria over the test cases under 3D loading conditions.

Part B
Part B of WWFE-II represents the conclusion drawn of the part-A. It carried out an assessment of the performance of the involved failure criteria by predicting the response of FRP composites under 3D states of stress. A comparison between the results of the approached criteria and experimental test cases was made. Then, a classification procedure of the criteria was carried out by means a quantitative and qualitative assessment in order to identify each criterion as a tool which is capable to be used in industry. this assessment analysed the degree of maturity and capacity of each failrue criterion.
Table 3.3 shows the twelve experimental test cases which were selected by the authors for carrying out the WWFE-II. Each test case involved one different loading condition, lay-up and material.

Table 3.3 *12 loading Conditions, Lay-ups and materials of the WWFE-II.*

Test Cases	Lay-up	Material	Loading conditions
1	Polymer	MY750 epoxy	σ_x versus σ_z (with $\sigma_y = \sigma_z$) envelope
2	0°	T300/PR319	τ_{12} versus σ_2 (with $\sigma_1 = \sigma_2 = \sigma_3$) envelope
3	0°	T300/PR319	$\gamma 12$ versus σ_2 (with $\sigma_1 = \sigma_2 = \sigma_3$) envelope
4	0°	T300/PR319	Shear stress-strain curves $(\tau_{12} - \gamma 12)(for \sigma_1 = \sigma_2 = \sigma_3 = -600MPa)$ envelope
5	(90°)	E-glass/MY750 epoxy	σ_2 versus σ_3 (with $\sigma_1 = \sigma_3$) envelope
6	(0°)	S-glass/epoxy	σ_1 versus σ_3 (with $\sigma_2 = \sigma_3$) envelope
7	(0°)	A-S carbon/epoxy	σ_1 versus σ_3 (with $\sigma_2 = \sigma_3$) envelope
8	(±35°)	E-glass/MY750 epoxy	σ_y versus σ_z (with $\sigma_x = \sigma_z$) envelope
9	(±35°)	E-glass/MY750 epoxy	Stress-strain curves ($\sigma_y - \varepsilon_x$ and $\sigma_z = \sigma_x$=-100 MPa.
10	(0°/90°/ ± 45°)	IM7/8551-7	τ_{yz} versus σ_z (with $\sigma_y = \sigma_x = 0$) envelope
11	(0°/90°)	IM7/8551-7	τ_{yz} versus σ_z (with $\sigma_y = \sigma_x = 0$) envelope
12	(0°/90°)	IM7/8551-7	Stress-strain curves ($\sigma_z - \varepsilon_z$, σ_z-σ_x and σ_z-σ_x) for $\sigma_y = \sigma_x = 0$.

The selected materials were make up with carbon and glass fibres and five types of matrix (polymer, MY750, epoxy, 319 and 8551-7). Test cases involved a isotropic material in the test 1, unidirectional plies from the test 2 to 7 and multi-directional laminates from the test 8 to 12. In order to compare the experimental results from the test cases with failure approaches accurately, various 3D state of stresses were developed, as shown in figure 3.2. On the one hand, stress-strain curves were employed in the test cases 4, 9 and 12. On the other hand, three 3D strength envelopes (test 1, 2 and 3), four loading conditions in the through-thickness direction (test 5, 6, 7 and 8) and two shear loading (test 10 and 11) were applied.

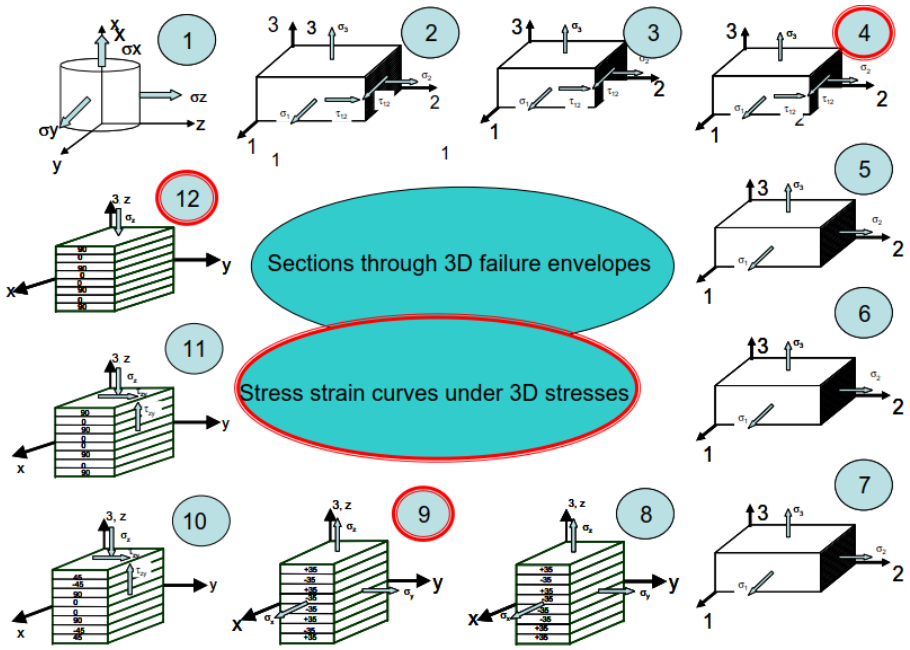

Figure 3.2 *12 loading conditions, lay-ups and materials of the WWFE-II [37].*

3.2.1 Contributors and failure theories

Table 3.4 shows the twelve criteria which were chosen to analyse failure over the test cases selected. Most of these failure theories were modified during the second stage (Part B) of the exercise for failure theory could predict much better the experimental results. A more extensive and specific description of the theories are shown afterwards.

Table 3.4 *Involved failure criteria of the WWFE-II.*

Contributors/ Theory	Organisation	Approach
Bogetti, Staniszewski, Burns, Hoppel, Gillespie and Tierney	U.S. Army Research Laboratory (USA)	3D Maximum strain theory
Carrere, Laurin and Maire	ONERA/DMSC (France)	Micromechanical based hybrid mesoscopic (MHM) 3D approach
Cuntze	Retired Engineer (Germany)	Failure mode concept (FMC) model
Huang, Jin and Ha	Hanyang University (S. Korea)	Micromechanics of failure (MMF) model
Nelson, Hansen, Mayes and Kenik	Firehole Technologies, Wyoming University, Alfred University (USA)	Multi-continuum micro-mechanics theory (MCT)
Zhou and Huang	Tongji University (China)	Anisotropic plasticity and generalised max stress
Kress	ETZ Zurich (Switzerland)	Hashin's model
Pinho, Darvizeh, Robinson, Schuecker, Camanho, Vyas and Robinson	Imperial Collage (UK), University of Porto (Portugal)	3D physically based constitutive model
Deuschle and Kroplin and Puck	Stuttgart University (Germany)	Physically based 3D phenomenological model
Rotem	Technion University (Israel)	Interactive matrix and fibre failure theory
Zand, Wolfe, Butalia, Schoeppner and Doudican	Ohio State University, AFRL, Wright-Patterson, AFB Ohio (USA)	Maximum strain energy method.
Ye and Zhang	Lancaster University, Manchester University (UK)	Christensen's theory

BOGETTI THEORY

Bogetti el al. modelled the tri-axial material behaviour of composite to predict the effective laminate stress/strain response. Its material non-linearity was explained at the ply level, and constitutive relations for each of the principal directions were defined with the Ramberg-Osgood equations [3]. Ply failure predictions were based on the established maximum strain failure criterion [65, 58]. Failure of material occurs when the strain in the principal ply strain direction ($\varepsilon_1, \varepsilon_2, \varepsilon_3, \varepsilon_4, \varepsilon_5$ and ε_6) exceeded its corresponding allowable level by comparing strains in the main six directions (longitudinal, transversal, normal and three shear directions) with their maximum tensile/compressive strain in each direction. This criterion was created in U.S. Army Research Laboratory (USA) [7].

CARRERE THEORY

Carrere et al. employed a micro-mechanics based hybrid mesoscopic (MHM) 3D approach considering the non-linear shear stress-strain response of the lamina. It also improved the determination of laminate final failure under complex tri-axial loadings. This approach was described both at the scale of the ply and at the mesoscopic scale (on treating micro-mechanical aspects). It introduced the progressive aspect of failure based on the concept that after the first ply failure, the mechanical properties of the failed ply got progressively worse. Thus, the stiffness of the laminate was reduced and leads to overloading of other plies. This criterion was created in ONERA/DMSC (France) [9].

CUNTZE THEORY

Cuntze developed a model under tri-axial loading, named as 'Failure Mode Concept' (FMC) [12, 13, 14, 16]. Cuntze model was implemented within a UD material with symmetries of the transversally isotropic material, where five basic (mode) strengths and five elasticity properties were involved. Its characterisation required five independent basic ply strengths. $R_{\parallel}^{t,c}(= X^{c,t})$ as tensile and compression strength parallel to the fibres. $R_{\perp}^{t}(= Y^{t})$ and $R_{\perp}^{c}(= Y^{c})$ as tensile and compressive strength transversal to the fibre direction and $R_{\perp\parallel}(= S)$ as in-plane shear strength. His model consisted of 5 failure modes: two fibre failure (FF) modes (FF1 and FF2, which respectively stand for tension and compression mode) and three inter-fibre failure (IFF) modes (with IFF1 as transverse tension, IFF2 as transverse compression and IFF3 shear). These modes were called inter-fiber failure modes since they indicated failure in the interface region between matrix and fibre. Two friction-related parameters ($b_{\parallel\perp}$ and $b_{\perp}^{t}$) had to be employed due to micro-mechanical nature of this model, since the macro-scopic values of strength were not used. This criterion was created in retired engineer association (Germany) [12].

TSAI THEORY

For the WWFE-II, Sung Hyu Ha et al. developed a model by combining a micromechanics-based constituent progressive damage model and a macroscopic failure behaviour (FMM) of composite laminates under multi-axial mechanical loading. By means of the FMM, the constitutive failure and the progress damage were obtained. His model focused on the micro-structure of a UD ply to get material properties and to calculate microscopic stresses within fibre and matrix from macro-level ply stresses. Distribution within the fibre, matrix as well as inter-facial area of microscopic stresses were related to the macroscopic stresses and the temperature increment [44]. The failure approach was based on the maximum longitudinal stress failure criterion for the fibre and on a modified Von Mises failure criterion for the matrix. This criterion was created in Hanyang University (S. Korea) [28].

HANSEN TEHORY

Hansen developed a multi-continuum and micro-mechanics based theory (MCT). It took non-linear shear laminar behaviour into account, employed equations of continuum damage mechanics, plasticity theory and mapping algorithm. The theory algorithm was based on a structural analysis of the composite for determining relationships between the material and failure constituent properties by decomposing the ply into matrix and fibre. A tangent operator was derived to ensure computational efficiency during the Newton-Raphson method in finite element method. The failure mode for both matrix and fibre was carried out through MCT decomposition.

This criterion was created in Firehole Technologies, Wyoming University and Alfred University (USA) [29, 52].

HASHIN THEORY

Hashin joined to the WWFE-II and he worked out a failure criterion that forms a set of branches of the failure surfaces. Each failure surface modelled a specific failure mode in order to overcome the deficiencies of the previous criteria. They were: Maximum-stress and strain criterion (that did not consider stress-interacting effects and established non-conservative predictions) and the criteria provided by Tsai [48], Tsai and Wu [64] and Hoffman [39] (which did not predict failure mode that is necessary to develops the damage progression analysis). The criterion consisted in two primary failure mode: fibre mode (the composite fails due to fibre rupture in tension or fibre buckling in compression) and the matrix mode (a plane crack parallel to the fibres occurs) by using a quadratic approximation. Each failure mode was discussed separately by subdividing into tensile and compressive form. This criterion was created in ETZ Zurich (Switzerland) [47, 47].

HUANG THEORY

Huang developed a micro-mechanics based method by combining the bridging model, the anisotropic plasticity and generalised Maximum Stress theories with a single theoretical framework. The method provided a basis for obtaining the laminate moduli and strengths from the constituent fibre and matrix properties. The failure criterion for both matrix and fibre was based on the condition of maximum stress. Failure occurs if the combined three principal stresses are larger or the same as the uni-axial tensile strength by considering both compressive and tensile modes. This criterion was created in Tongji University (China) [41, 40].

PINHO THEORY

Pinho developed a method through the hybrid damage based on physical principles and micro-mechanical aspects to make predictions of the tri-axial failure envelopes and stress-strain curves of the WWFE-II test cases. The different modes of failure were divided into: fibre failure mode, in-plane inter-fiber failure mode and through-the-thickness failure mode by showing matrix failure, fibre kinking and fibre tensile failure. For each mode the matrix failure and accumulation of cracks in the plies were related to the fracture energy during propagation of failure. Failure model at the ply level predicted that failure stress increases linearly with hydrostatic pressure (due to compressive stresses and volumetric deformation). The matrix failure criterion was based on an adaptation of the MOHR-Coulomb criterion of UD plies. The fibre failure was dominated by the fibre kinking due to matrix failure that triggers

the formation of kink bands. This criterion was created in Imperial Collage (U.K.) and University of Porto (Portugal) [53, 54].

PUCK THEORY

Puck developed a mechanistic theory that distinguished between various modes of failure like in the first exercise. The author used two fracture criteria (fiber fracture and inter-fiber fracture) leading to a continuous and gradual loss of stiffness after initiation of cracking. His theory was based on two set of equations, on for fibre failure (FF) and another for inter-fiber failure (IFF). Failure model was based on a simple maximum stress failure condition for fibre failure and a plane parallel to fibres governed by stresses and inclined an fracture angle theta (θ) under the stresses σ_n, τ_{nt} and τ_{n1} for the inter-fibre failure mode. This criterion was created in Stuttgart University (Germany) [17, 18].

ROTEM THEORY

Rotem continued to develop his approach based on 'Interactive matrix and fibre failure theory' in association with Hashin. His contribution represented two separate failure criteria, one intended for fibres and the other for matrix. Fibrous composite materials for this model assumed that laminate had many unidirectional plies, fibers are much stiffer and stronger than matrix and fibers are parallel and evenly distributed into the lamina. The tension strength is considered to be dependent on the adhesion properties between matrix and fibre, and in compression the authors assumed that fibres underwent micro-buckling due to the iso-static pressure. This criterion was created in Technion University (Israel) [60, 59].

WOLFE THEORY

Wolfe and Butalia employed a strain energy based failure theory specifically developed for fibrous composite laminates under multi-axial loading. The model also considered the effect of the hydrostatic stress. For the ply analysis, the material was considered to behave orthographically in order to describe the relationship between stresses and strain. Failure criterion focused on a failure mode interaction by using experimental data for fibre failure and by the approach proposed by Shandu [67] for tensile failure matrix. This criterion was created in Ohio State University, AFRL, Wright-Patterson and AFB Ohio (USA) [69].

CHRISTENSEN THEORY

Ye and Zhang employed Christensen method to address the 12 cases in the second World Wide Failure Exercise. The original model was a material failure theory created for isotropic materials, and its purpose was to offer a wide scale failure criterion

applicable to both ductile and brittle materials. It was constituted by two-property form, which was calibrated with uni-axial tensile and compressive strengths. Laminate failure criterion of Christensen was carried out via the matrix-controlled and the fibre-controlled failure modes separately. The prediction of fibre composite failure by combining the present stress analysis and Christensen failure criteria was predicted by the homogenization of a heterogeneous composite lamina. This criterion was created in Lancaster University and Manchester University (U.K.) [68, 70].

3.3 Assessment

Once the failure criteria involved in WWFE-I and WWFE-II have been explained. An assessment for determining which criteria are the most accurate in order to predict the damage onset in the two experiments performed in this thesis (uni-axial tensile test and impact test over a curved specimen). Material and stacking sequence of the specimen are shown in the chapter 4. For that, a selection procedure has to be carried out among all failure criteria explained so far. The procedure is based on the following steps:

- First, a comparison of material and loading characteristics between the case studies of the thesis work and each test case from the WWFE-I and WWFE-II is carried out. This allows to discard the test cases, which are not related to the experimental tests (tensile and impact test cases) in term of the loading condition as primary reason (lay-ups and materials secondary). This first discarding phase is based on qualitative assessment.
- After limiting all test cases into the test cases of interest, a second discarding phase will be developed for the final selection of the failure criteria. This analysis consists of a qualitative and a quantitative assessment. The first one is focused on getting the level of weakness or strength for each failure theory regarding the selected test cases. The quantitative assessment is based on numerical comparison between the experimental and numerical results. Both assessments must complement each other to set the final conclusion.

3.3.1 The WWFE-I criteria

The organisers of WWFE-I carried out the part B of the exercise to develop and revise more accurately the approaches in the 14 test cases. After achieving a better correlation with the 14 test cases listed in table 3.1, the qualitative and quantitative

assessment can be developed. Through assessment, the most feasible criteria will be defined for thesis analysis cases.
The first analysis case of the thesis is the tensile case, explained in section 4.2. In the tensile test case, the loading condition is based on applying one load component in the longitudinal direction of the laminate. Thus, if the first direction of the laminate takes a stance with the direction-x, the loading condition according to the tensile test reads the following way: $\sigma_x, \sigma_y, \sigma_z : 1, 0, 0$.
By following the 14 test cases of WWFE-I listed in the table 3.1, the loading conditions which match with the description of required prediction for the tensile case are the test cases number 7 and 10.
With respect to material and lay-up, the test case 7 and 10 present the characteristics of multi-directional laminate and E-glass/resin components. Thus, the test cases, which will be employed for the assessment of WWFE-I approaches for this thesis, are:
• Test case 7: lay-up of $(0°/ \pm 45°/90°)$, AS4/3501-6 carbon/epoxy material and stress-strain curves for σ_y:σ_x= 1:0 as loading condition.
• Test case 10: lay-up of $(\pm 55°)$, E-glass/MY750 epoxy material and stress-strain curves for σ_y:σ_x= 1:0 as loading condition.
After choosing the two most appropriate test cases of WWFE-I, the second step can be carried out by developing the qualitative and then a quantitative assessment.

Qualitative Assessment

The qualitative analysis remarks the correlation between theoretical prediction of all theories and experimental results for each test case. Then, between each failure theory and experimental data for the 14 test cases through the Appendix A and B of [36] respectively. Because this thesis will focus on the tensile test by means of the chosen test cases 7 and 10, the assessment will employ the correlation of the appendix A of [36], whose evaluation is summarized in table 3.5 and explained elaborately hereunder:
This evaluation explain the predictions of all theories which were shown superimposed with the experimental results for the test cases 7 and 10 in figures 3.3 and 3.5 especially. This analysis is not deterministic but is necessary to steer this thesis in the selection of the criteria. The places where weakness of all theoretical predictions occur are showed by classifying them in a level of confidence with the following weakness levels: Fundamental, significant or minor.

Test Case 7

• Bogetti: Predicted the shape of stress-strain curve very close to the experimental curve. Theory predicted small steps in the curve which were not seen in the exper-

iments, **Minor Weakness**.

• Chamis: Fit the experiment at small strain. Predicted low stiffness and strength, **Significant Weakness**.

• Cunzte: Predicted the shape and magnitude of stress-strain curve very close to the experimental curve. After revised curves, predicted curves were softer than measured data, **Minor Weakness**.

• Eckold: Did not offer prediction, **Fundamental Weakness**.

• Edge: Theory fit well the shape and magnitude of stress-strain curves, but did not offer prediction, **Fundamental Weakness**.

• Hart-Smith: Predicted the shape of stress-strain curve and fibre failure very close to the experimental curve. Poisson strain response were softer than measured data, **Minor Weakness**.

• Huang: Theory had significant effects by thermal stresses on final fibre tension failure, **Significant Weakness**.

• Mayes: Theory predicted final strength close to the experimental result. Theory developed large axial and hoop strains, **Significant Weakness**.

• McCartney: Predicted the shape of stress-strain curve very close to the experimental curve in the part B revision. But the theory does handle heat dominated failure, **Significant Weakness**.

• Puck: Theory predicted the shape and magnitude of stress-strain curve very good regarding to the experimental curve.

• Rotem: Theory had problems in predicting response beyond onset of initial failure, **Significant Weakness**.

• Sun: Theory fit well the shape and magnitude of stress-strain curves. Its strength prediction is similar to that using linear analysis, **Minor Weakness**.

• Tsai: Predicted the shape of stress-strain curve very close to the experimental curve and improved accuracy in part B. Part B did not change the oversoft strain prediction, **Minor Weakness**.

• Wolfe: Through the part B, theory predicted good the experimental curves. But it had steps in curves and premature final failure, **Significant Weakness**.

• Zinoviev: Theory predicted the magnitude of the stress at final failure very close to the experimental curve.

Test Case 10

• Bogetti: Theory predicted very well part of the non-linear curves and the initial modulus. But theory achieved one fifth of the measured hoop strain and one seventh of the measured axial strain, **Significant Weakness**.

• Chamis: Predicted the shape of stress-strain curve very close to the experimental curve just at low strain, **Fundamental Weakness**.

• Cunzte: Predicted the shape and magnitude of stress-strain curve very close to the experimental curve up to approx 3% strain. But theory was not able to get leakage prediction and a usual non-linearity before failure, **Significant Weakness**.
• Eckold: Theory did not predicted the shape of stress-strain curve and failure modes close to the experimental curve, **Fundamental Weakness**.
• Edge: Approach predicted the shape and magnitude of stress-strain curve in a good agreement with experiment up to approx 3% strain. However, there were problem for fitting the experimental curves at large strains, **Fundamental Weakness**.
• Hart-Smith: Theory obtained conservative stress and strain at failure. Theory predicted very soft stress-strain curves, **Minor Weakness**. For Hart-Smith 2 and 1, theory did not offer prediction, **Fundamental Weakness**.
• Huang: Approach predicted part of the non-linear behaviour and stresses 50% lower than measured, **Significant Weakness**.
• Mayes: Approach predicted part of the non-linear behaviour and stresses 50% lower than measured, **Significant Weakness**.
• McCartney: Theory predicted stress-strain curve very far away from the experiment due to being over-stiff, **Significant Weakness**.
• Puck: Theory predicted the shape and magnitude of stress-strain curve very close to the experiment up to approx. 4%. It had problem to capture final predicted strength (50% of measured final failure strain), **Significant Weakness**.
• Rotem: Theory predicted non-linear curves, but terminated at approx. 1.5% strain (less than 20% of measured at final failure), **Significant Weakness**.
• Sun: Approach captured part of the non-linear behaviour, but it predicted failure strains more than 5 time lower than measured data, **Significant Weakness**.
• Tsai: The magnitude of the stress at final failure matched well to the leakage experimental stress. The revised theory produced a horizontal plateau not seen in experiment through the part B, **Minor Weakness**.
• Wolfe: Theory predicted part of the non-linear behaviour and initial modulus very well. But curve terminated at approx. 1.5% strain (one fifth of the measured hoop strain and one seventh of the measured axial strain), **Significant Weakness**.
• Zinoviev: Theory predicted the magnitude of the stress at final failure well to the leakage experimental stress. Nevertheless, approach reproduced approx. 55% of the actual stress-strain response, **Significant Weakness**.

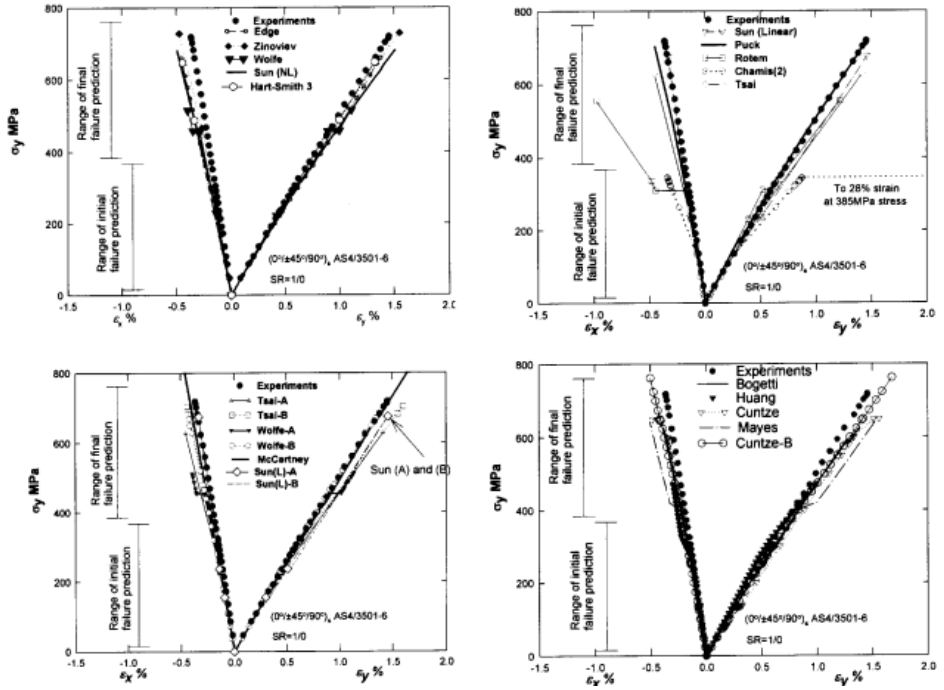

Figure *3.3 Comparison between the predicted and measured stress strain curves for AS4/3501-6 laminate under uni-axial tension (revised Part B theories) [36].*

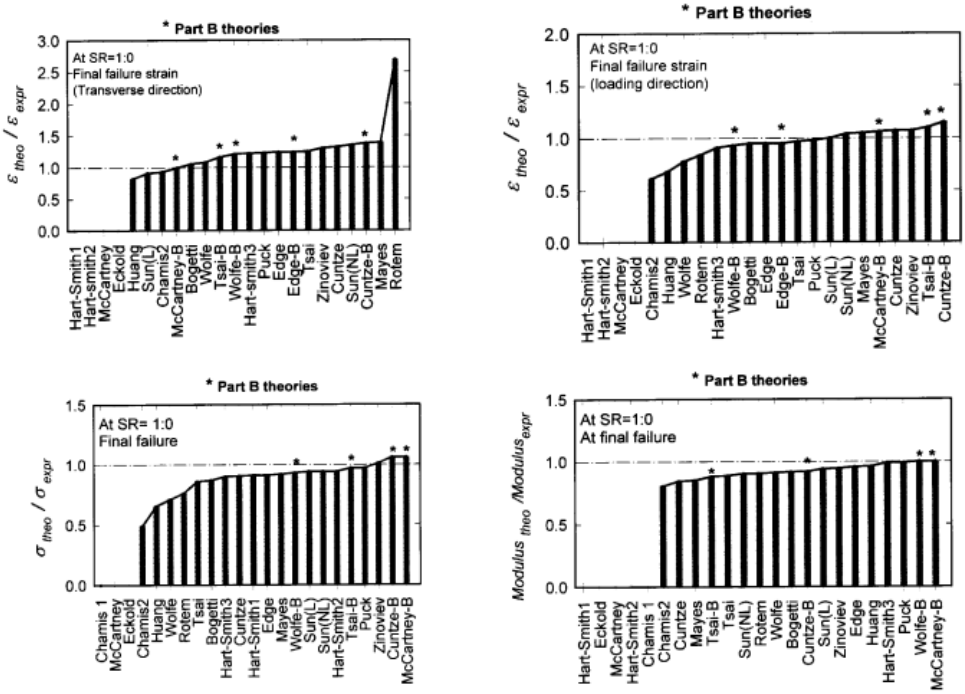

Figure *3.4 A bar chart showing the ratio of predicted to measured values of failure strains, strength and modulus for AS4/3501-6 laminate under uni-axial tension (revised Part B theories) [36].*

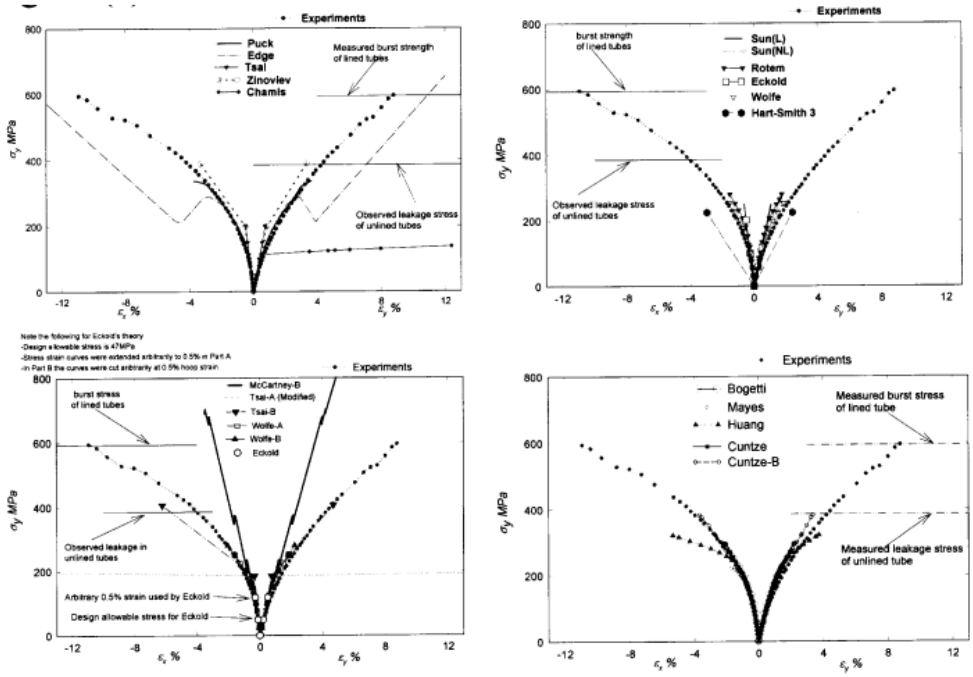

Figure 3.5 *Comparison between the predicted and measured stress strain curves for E-glass/MY750 laminate under uni-axial tension (revised Part B theories) [36].*

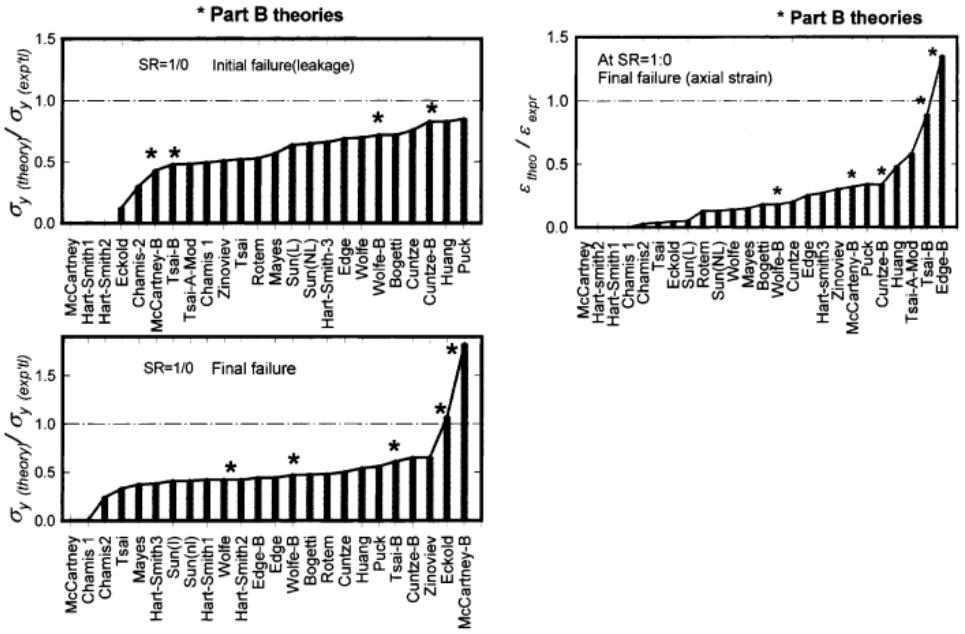

Figure 3.6 *A bar chart showing the ratio of predicted to measured values of failure strains, strength and modulus for E-glass/MY750 laminate under uni-axial tension (revised Part B theories) [36].*

Table 3.5 *Involved failure criteria of the WWFE-II.*

Theory	Test Case 7	Test case 10
Tsai	Minor (original,Pt. B)	Significant, Minor (Pt. B)
Wolfe and Butalia	Significant, No Weakness (B)	Significant (original,Pt. B)
Edge	No Weakness	Fundamental
Rotem	Significant	Significant
Sun	Minor (L,NL)	Significant (L, NL)
Eckold	No Comments	Fundamental
McCartney	Fundamental (original, Pt. B)	Significant (original, Pt. B)
Hart-Smith	Minor (3)	Minor (3)
Puck	No Weakness	No minus points
Cuntze	Significant, Minor (Pt. B)	Significant (original, Pt. B)
Huang	Significant	Significant
Mayes	Significant (original, Pt. B)	Significant (original, Pt. B)
Bogetti	Minor	Significant

Quantitative Assessment

The capabilities of the theories were assessed in a quantitative way. This assessment is based on a systematic comparison of the predicted strengths and deformations against the experimental data. The WWFE authors selected five ranking categories which cover major scenarios and variables to describe the failure behaviour in a laminate/ply under applied loads. These categories were:

1. Biaxial strength of unidirectional plies.
2. Initial bi-axial strengths of multi-directional laminates.
3. 'Final' strengths of multi-directional laminates.
4. Deformation (stress-strain curves) of multi-directional laminates.
5. Ability to predict the general trends observed in the test data.

Building on the categories, the first, third and fifth are not related with our interest test cases due to current work focuses on the onset damage and its derivations. For this reason, these categories were discarded for this work. For this reason, these categories were discarded for this work. The features related to the initial strengths and deformations of the failure will be evaluated since the damage initiation in laminates can have a strong dependency with them [36].

In the quantitative assessment, WWFE authors employed the stress ratios (SRs) to cover as many experiential points in each of the test cases as possible. These SRs correspond with one or various specific mechanical features- which is measured for

one test case. WWFE uses two kind envelopes to plot and compare the experimental and approach results under the same loading condition. If a test case is analysed by biaxial failure strength envelope, different points with the coordinates x and y of the graphic are established as SRs to compare themselves with the experimental points from the measured data. If a test case is analysed by stress/strain curves, the SRs would correspond with a mechanical feature which is analysed for this specific test case.
For making the table where results are shown it is necessary to establish the Property Correlation Ratios (PCRs). These ratios are the numbers employed to measure how far the results between theoretical approaches and test cases are for each SR in each test case. The WWFE authors employed a non-numerical conversion to classify the different level of closeness. The following percentages differ the graduation levels:

- Grade A: The prediction lies between ±10% and ±50% of the experimental value.
- Grade B: The prediction lies below 50% or above 150% of the experimental value.
- Grade C: No solution offered.

The comparison process is based on the prediction between the tests and approaches results, where the prediction with value 1 (e.g. PCR=1) would correspond with the perfect match. As the results separate each other, the prediction value distance itself from the value 1 both upwards and downwards.
The results separate each other, the prediction value distance itself from the value 1 both upwards and downwards. These distance between the prefect match (PCR=1) and values results constituent the level of under-prediction or over-prediction of the different theories in each SR. The over- and under-prediction are shown in the figures 3.4 and 3.6.
After understanding the parameters of the quantitative assessment, the results for each category are explained bellow:

Ranking Category 2 - predicting 'initial strengths of multi-directional laminates'

The experimental data obtained non-extensive but sufficient information to able to compare it with the current theories. The figure C-2 and table C-2 from appendix C of [36] showed that the majority of theories (approx. 85%) were not able to predict results with ±10% grade A score. In general terms, Bogetti, Zinoviev and wolfe-B obtained better performance under combined grade A and B scores for all test features (SRs).
From a more specific point of view, Wolfe, Mayes and Huang-B theories developed the closest results to the measured data with the grade B score for the test case 7 by

evaluating initial failure stress feature. Nevertheless, the effects of residual thermal stresses arising from cooling after curing and moisture content were not used within the predictions due to the difficulty of assessing its accuracy.
For the Test Case 10, WWFE authors carried out the analysis of the unlined failure stress, axial/hoop strain ratio at leakage, axial strain at leakage and hoop strain at leakage features. The results showed that Puck, Cuntze-B and Huang-B theories achieved the Grade A and B scores by predicting these features in general terms. Speciality, Puck and Cuntze-B could predict the axial/hoop strain ratio at leakage feature in their approaches above ±10% of the experimental value. Thus they demonstrate to be the theories closest to the experimental curves so far for predicting the initial strengths of multi-directional laminates. These correlations are shown in the table 3.6.

Table 3.6 *Ratios of predicted to measured values of the initial failure properties (second ranking category).*

Measured Parameters	Initial failure stress	Unlined Failure Stress	Axial/hoop strain ratio at leakage	Axial strain at leakage	Hoop strain at leakage
Test Cases	7	10	10	10	10
Exp. Data	400 MPa	386MPa	1.11	-4.85	4.36
Theory					
Tsai	0.45	0.52	0.6	0.1	0.17
Wolfe and Butalia	0.6	0.7	0.8	0.3	0.4
Edge	0.09	0.12	0.52	0.02	0.05
Rotem	0.58	0.53	0.78	0.31	0.4
Sun (L)	0.39	0.64	0.52	0.1	0.25
Eckold	NA	0.12	0.52	0.02	0.05
McCartney	1.04	0.43	0.52	0.08	0.16
Hart-Smith	NA	NA	NA	NA	NA
Puck	0.43	0.85	0.92	0.77	0.83
Cuntze (B)	0.34	0.83	0.91	0.55	0.61
Huang (B)	0.66	0.51	0.89	0.68	0.76
Mayes	0.59	0.57	0.91	0.34	0.37
Bogetti	0.56	0.72	0.83	0.42	0.50

Ranking Category 4 - predicting 'deformation of multi-directional laminates'

In fibre-dominated cases, the results demonstrated that many of failure theories were able to predict non-linear stress-strain curves very well. However, the large non-linear deformations for angle-ply specimen were predicted with grade B scores more than grade A scores. Puck achieved the highest number of Grade A scores (39% of cases). Zinoviev theory obtained the highest total number of combined grade A plus grade B scores in this category, being closer to ±50% of the experimental values.
On the other hand, Puck, Edge and Edge-B approaches got to describe the non-linear behaviour at moderate levels of strain in the best manner (grade A) regarding the measured data by means the strain ratio and strains features (in the two main

Table 3.7 *Ratios of predicted to measured values of multi-directional laminates (fourth ranking category).*

Measured Parameters	Final strain ε_x	Dinal strain ε_y	Strain ratio $-\varepsilon_x/\varepsilon_y$	Final Strain ε_y	Final Strain ε_x	Strain ratio $-\varepsilon_x/\varepsilon_y$	Strain ε_x at 185 Ma	Strain ε_x at 280 MPa	Strain ε_y 180 MPa	Strain ε_y at 280 MPa
Test Cases	7	7	7	10	10	10	10	10	10	10
Exp. Data	-0.363	1.455	0.249	8.78	-10.9	1.24	-0.88	-2.06	1.3	2.54
Theory										
Tsai (B)	1.16	0.93	1.25	0.78	0.89	1.24	0.35	1.37	0.55	0.95
Wolfe and Butalia (B)	1.21	1.1	1.1	0.25	0.18	0.74	0.91	1	0.78	0.87
Edge	1.24	0.95	1.3	1.36	1.35	0.81	0.96	1	0.9	0.95
Rotem	2.69	0.84	3.22	0.19	0.13	0.69	0.71	0.75	0.59	0.69
Sun (L)	0.91	1	0.91	0.12	0.05	0.46	0.45	0.32	0.59	0.45
Eckold	NA	NA	NA	0.056	0.045	0.46	0.48	0.32	0.55	0.45
McCartney (B)	0.99	1.06	0.94	0.76	NA	NA	0.66	0.55	0.7	0.61
Hart-Smith (3)	1.22	0.91	1.34	0.27	0.27	0.99	2.74	1.78	1.51	1.16
Puck	1.23	0.98	1.26	0.41	0.34	0.82	0.96	1	0.9	0.95
Cuntze	1.32	1.07	1.23	0.25	0.19	0.76	0.93	0.88	0.81	0.79
Huang (B)	0.82	0.68	1.21	0.42	0.49	1.14	0.85	1.42	0.75	0.95
Mayes	1.39	1.05	1.32	0.18	0.15	0.82	1.05	1.17	0.85	0.88
Bogetti	1.05	0.95	1.1	0.25	0.18	0.74	0.85	0.98	0.75	0.85

directions) for both test case 7 and 10.

Specifically, the table C-4 and fig. C-4 od the appendix C from [36] shows that the theories which obtained the closet results to the experimental data of test case 7 were Bogetti, Sun(L)and McCartney-B theories by analysing the final strain ε_x, final strain ε_y and strain ratio $-\varepsilon_x/\varepsilon_y$ features. For the test case 10, theories with the mayor number the grade A scores by assessing normal strain, final strain and strain ratio features were first Puck approach and then, Edge and Edge-B theory. These correlations are shown in the table 3.7.

Once both the qualitative and quantitative assessments for the test cases 7 and 10 have been developed, the failure criteria most feasible can be chosen. Quantitative analysis represents the critical selection, which will be complement by the qualitative assessment.

Table 3.6 shows the second ranking category, which predict the values of the initial failure properties. Puck and Cunzte-B reached the closest SRs to value 1 (grade A) in the axial/hoop strain ratio at leakage parameter in the test case 10. On the other hand, Wolfe, Mayes and Huang-B were the theories with major agreement in the

test 7, but with a match level of ±50% in respect of the experimental values. Also, the residual thermal stresses after curing were not employed in this test due to the difficulty to obtain them. Thus, Wolfe, Mayes and Huang-B criteria can discarded by taking into account also their significant weakness from the qualitative point of view.
Table 3.7 shows the category of deformation that predict deformation of multi-directional laminates. The features analysed in the test case 10 assessed the initial and final strain and strain ratio parameters. And Puck, Edge and Edge-B reached predictions, which lie within a percentage of ±10% in respect of the experimental curves (grade A). However, the features analysed in the test 7 assessed only the final strains, where Bogetti, Sun(L) and McCartney achieved to predict with a grade A score. In consequence, these last approaches can be discarded due to the employed features in their analysis are not related directly with the initiation of damage.
Finally, it can be concluded that the two theories which have been achieved to predict the experimental data in the best way of the test cases 7 and 10 with a grade A (or grade A + B) score, are Puck and Cuntze-B theories.

3.3.2 WWFE-II criteria

By following the same assessment procedure of the WWFE-I, the first selection is carried out in order to discard the test cases involved in WWFE-II which are not related to the impact test case. For that, the material, lay-up and loading condition of the experimental case study were compared with each test case of WWFE-II from table 3.3.
The loading condition in this thesis is based on free drop of a impactor which is stopped by the top ply of the specimen. The moving body has kinetic energy which is transferred to the laminate when body comes at rest. The dissipation of this energy in the laminate divided by the local deformation (failure) is understood as impact load.
If the longitudinal, transverse and through-thickness direction of the laminate correspond with the direction-x, -y and -z respectively, the impact loading condition (regardless of shear stresses) would be the following way: $\sigma_x, \sigma_y, \sigma_z : 0, 0, 1$.
The loading conditions of WWFE-II that are related to the impact test are the test cases number 11 and 12 as shown in table 3.3.
With respect of material and lay-up part, the test case 11 and 12 keep the stacking sequence of multi-directional laminate. Thus, the test cases which will be employed from the assessment of WWFE-II, are [45]:

• Test case 11: lay-up of (0°/90°), IM7/8551/7 and stress-strain curves for σ_y:σ_x= 1:0 as loading condition.
• Test case 12: lay-up of (0°/90°), IM7/8551/7 and stress-strain curves for $\sigma_z - \varepsilon_z$,$\sigma_z - \sigma_x$ and $\sigma_z - \sigma_z$ for σ_y=σ_x=0 .

Qualitative Assessment
For this analysis, one observation per each stress ratio in each test case is explained. The problems associated with experimental results are described by showing the level strength of the theories, as shown in figure 23 of [36].

Test case 11
This test case developed associated problems in the experimental results since, the information about the initial failure and experimental data under large compressive stresses were not able to obtained (table 4 of [36]). The features analysed in this test are:
• SR:= τ_{yz}:σ_z= -1.33:1; the shear strength increases with increasing through-thickness compression.
• SR:= τ_{yz}:σ_z= -3.72:1; no apparent unbounded strength (failure envelope closed).
• SR:= τ_{yz}:σ_z= 0:1; the predicted compressive strength exceeds the measured point 552 MPa.

Test case 12
Test case 12 had a problem related to lack of understanding in the initial and final failure modes. The features involved for each stress ratio are:
• SR:= ε_x.
• SR:= ε_z.
• SR:= Poisson ratio; non-linear stress-strain behaviour in the through-thickness compression.
• SR:= Strength; the stress-strain curves exhibited stiffening effects.
• SR:= Initial modulus; strength prediction is compatible with that in Test Case 11 (or 10).
• SR:= σ at ε=3%; smooth stress-strain curves (no sudden steps or change in slope).
• SR:= Secant modulus; stress-strain curves were not fitted into the test data.
In the test case 12, the failure approaches predicted linear stress-strain curves (by Hansen, Bogetti), non-linear stress-strain curves with or without thermal stress (by Carrere, Huang, Christensen), non-linear softening behaviour (by Puck, Wolfe, Cunzte), non-linear stiffness behaviour (by Pinho, Cuntze, Hashin) and the discontinuities in the curves caused by the post-failure (by Rotem, Tsai-Ha).

Quantitative Assessment

In order to assess the prediction of different theories involved in WWFE-II, a quantitative assessment will be carried out by following the WWFE-I assessment procedure. For that, a comparison and evaluation of the magnitude of strengths and deformations will be developed by taking in to account the experimental values of the twelve test cases.

In the similar way, the WWFE authors selected various ranking cases in order to cover the four main areas in the analysis of laminates:

1. Tri-axial strength of a polymer material.
2. Tri-axial strength of UD plies.
3. Tri-axial strength of multi-directional laminates.
4. Deformation (stress-strain curves) of UD and multi-directional laminates.

The same criterion to assess the properties of these different categories was used. The ratio PCR was employed for each stress ratio and failure criterion. According to the value of PCR ratio, SR will be assigned grade 'A' or colour green (prediction lies between $\pm 10\%$ and $\pm 50\%$ of the experimental value), grade 'B' or colour yellow (prediction lies below 50% or above 150% of the experimental value) or grade 'C' or colour red (prediction lies below 50% or above 150% of the experimental value).

The test cases 11 and 12 are related to the four mentioned points, which analyse the deformation and stress-strain curves in UD and multi-directional laminates. The results for these chosen test cases are shown in the table 7 of [36]. The table contains 1000 data points which has been reduced to 220 data for the test 11 and 12, whose results are indicate in the figure 3.9 and 3.10 for the test 11 and 3.11 and 3.12 for the test 12.

Test case 11

The qualitative assessment of the test case 11 demonstrated that it had associated problems in its results. The test can not be employed to study the initiation of failure. In consequence its qualitative assessment will not carried out and thus this test case can be discarded from the analyse.

Test case 12

The results of comparing the experimental and approach results for test case 12 will be supported by bar charts and the table of correlation. On the one hand, bar charts visualise the level of under-prediction or over-prediction of the different theories, as shown in figures 3.7 and 3.8. On the other hand, the correlation between the predictions of each failure theories and the experimental data got from the test 12 is shown in the figures 3.11 and 3.12 by means of stress ratios (SRs). These SRs

were computed for the initial Young modulus, ultimate compressive strength, failure strain in the through-thickness direction and ultimate tensile failure strain in the in-plane direction.

The theories which predicted the mentioned SRs with grade A or B score by means of the tables and bar charts were Hashin-B, Cunzte-B and Carrere-B. Hashin-B achieved grade A score in the poisson ratio, strength, stress at 3%ε and secant modulus features in positioning itself as the closest criterion to the measured data. Carrere-B obtained grade A score in failure strain at ε_x and stress at 3%ε features but its bar charts showed that for the different SRs has a level very lower of under-prediction and thus it can be discarded.

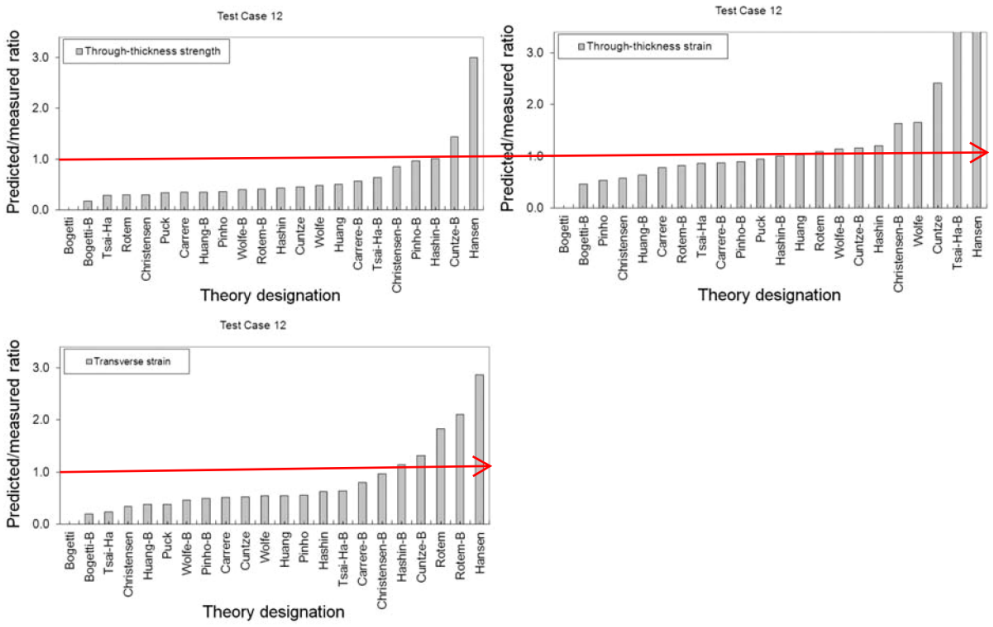

Figure 3.7 *Bar charts showing the ratio of predicted to measured properties versus theory designation of test case 12 (Through-thickness strength, through-thickness strain and transverse strain) [2].*

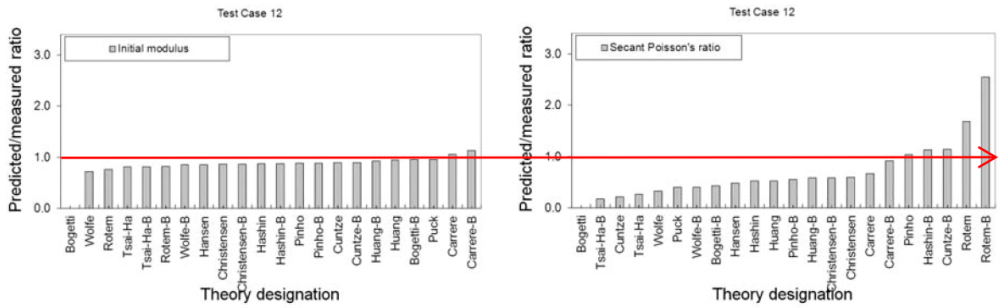

Figure 3.8 *Bar charts showing the ratio of predicted to measured properties versus theory designation of test case 12 (Inital modulus and Secant Poisson ratio) [2].*

Any failure criteria has been able to predict the SRs with grade A score. The test 12 of WWFE-II has not been able to get enough data to achieve a better level of confidence on how to predict the strength and deformation under through-thickness compression. However, the Hashin-B and Cutnzte-B theories can be established as the definitive failure criteria to model the impact case, because of theirs proximity to the experimental data by overcoming this lack in the prediction of laminates behaviour.

Stress ratio	Bogetti	Carrere	Cuntze	Tsai-Ha	Hansen	Huang	Hashin	Pinho	Puck	Rotem	Wolfe	Christensen
-1.33:1	0.60	0.83	0.74	0.71	1.18	0.98	0.80	0.85	0.78	0.70	1.12	(*)
-3.72:1	0.42	0.66	0.48	0.43	0.90	0.63	0.61	0.54	0.51	0.42	0.82	(*)
0: +1	0.93	1.01	0.74	0.79	1.83	1.13	0.85	0.94	0.93	1.17	1.48	(*)

Figure 3.9 *Ratios of predicted to measured values at various stress ratios, selected for the quantitative assessment of the various revised theories of test case 12 (Part-A criteria) [2].*

Stress ratios	Bogetti-B	Carrere-B	Cuntze-B	Tsai-Ha-B	Huang-B	Hashin-B	Pinho-B	Rotem-B	Wolfe-B	Christensen-B
-1.33:1	0.60	0.81	0.83	0.94	0.99	0.80	0.93	1.04	0.95	1.12
-3.72:1	0.42	0.86	0.86	0.83	0.55	0.61	0.80	0.71	0.65	1.10
0: +1	0.93	0.99	0.91	1.03	2.18	0.85	1.15	1.42	1.36	1.00

Figure 3.10 *Ratios of predicted to measured values at various stress ratios, selected for the quantitative assessment of the various revised theories of test case 12 (Part-B criteria) [2].*

	Bogetti	Carrere	Cuntze	Tsai-Ha	Hansen	Huang	Hashin	Pinho	Puck	Rotem	Wolfe	Christensen
Failure strain ε x	(*)	0.66	0.22	0.27	0.48	0.53	0.52	1.03	0.40	1.63	0.33	0.59
Failure strain ε z	(*)	0.52	0.53	0.23	2.86	0.55	0.63	0.56	0.38	1.78	0.54	0.34
Poisson's ratio	(*)	0.78	2.41	0.86	5.92	1.04	1.20	0.54	0.95	1.09	1.65	0.58
Strength	(*)	0.35	0.45	0.29	3.00	0.51	0.44	0.36	0.34	0.30	0.48	0.30
Initial modulus	(*)	1.06	0.89	0.81	0.85	0.95	0.87	0.89	0.96	0.76	0.72	0.87
Stress at 3% ε	(*)	0.78	0.69	0.64	0.72	0.75	0.34	0.78	0.75	0.41	0.68	0.73
Secant modulus	(*)	0.45	0.19	0.33	0.51	0.49	0.36	0.67	0.35	0.27	0.29	0.52

Figure 3.11 *Ratios (CR) between predicted and measured data for Test Case 12. Part A criteria are shown. The green colour is for ratios between 0.9 and 1.1, the yellow for 0.5-0.9 and 1.1-1.5 and red for ratios less than 0.5 or above 1.5 [45].*

	Bogetti-B	Carrere-B	Cuntze-B	Tsai-Ha-B	Huang-B	Hashin-B	Pinho-B	Rotem-B	Wolfe-B	Christensen-B
Failure strain ε x	0.43	0.91	1.14	0.18	0.58	1.12	0.55	2.54	0.40	0.59
Failure strain ε z	0.20	0.80	1.32	0.64	0.38	1.14	0.49	2.10	0.46	0.96
Poisson's ratio	0.47	0.87	1.16	3.60	0.64	1.01	0.89	0.83	1.15	1.64
Strength	0.18	0.57	1.44	0.64	0.35	1.01	0.97	0.41	0.40	0.85
Initial modulus	0.95	1.13	0.89	0.81	0.93	0.87	0.89	0.82	0.85	0.87
Stress at 3% ε	0.55	0.94	1.00	0.64	0.81	0.96	0.68	0.69	0.69	0.73
Secant modulus	0.38	0.65	1.24	0.18	0.55	0.99	1.08	0.49	0.35	0.52

Figure 3.12 *Ratios (CR) between predicted and measured data for Test Case 12. Part B criteria are shown. The green colour is for ratios between 0.9 and 1.1, the yellow for 0.5-0.9 and 1.1-1.5 and red for ratios less than 0.5 or above 1.5. [45].*

As consequence of the assessment carried out in the criteria of the WWFE-I and WWFE-II, the thesis will model the initial failure (damage onset) by means the Hashin, Puck and Cuntze-B failure criteria for the uniaxial tensile case and the impact case by using the finite element software Abaqus. The results obtained from the implementation of these criteria will be compared with the experimental results of the both tests. Thus, this thesis will analysise the mechanics of the material and predict accurately the damge onset in the cuverd specimens.

4. MATERIALS AND METHODS

The damage onset was analysed in two curved specimens by testing them through an uniaxial tensile test and 3D impact test, which are shown in this section. Modelling of the performed experimental tests was then carried out through a commercial Finite Element software (Abaqus) and threechosen failure criteria were implemented. The mathematical approach of each criterion is explained in detail in the section 4.4. The three criteria implementation into Abaqus was carried out through the Abaqus subroutines programmed with FORTRAN code (one code per criterion), which are attached in the chapter A.

4.1 Materials

The work was made as a part of Luxturrim5G (https://www.luxturrim5g.com/) project activities. The material employed in this Thesis was provided by Exel composite Ltd. company (Finland), which collaborated in the structural composites part of the project. The specimens are manufactured using E-Glass fibers and polyester matrix. The original specimen was manufactured by means of a pull-winding process by employing cylindrical mandrels. The specimen was cut by using an abrasive waterjet system in order to get specimens to the desired shape (that is, a semicylindrical shell for the impact testing and long strips for the tensile testing).

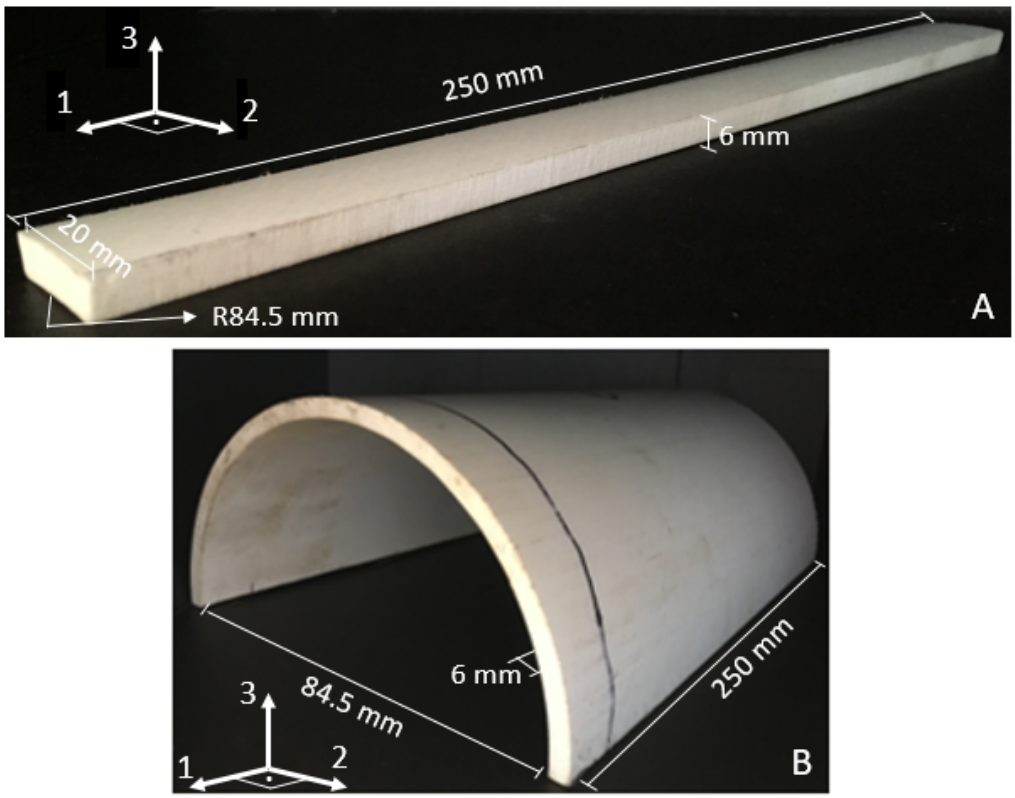

Figure 4.1 *Specimens employed in tensile (A) and impact (B) tests; Axis 1 represents the longitudinal direction; Axis 2 represents the transversal direction in-plane; Axis 3 represents the transversal through-thickness direction.*

Figure 4.1-A shows the specimen employed for the tensile test. It was cut with an outer arc (specimen width) of 20 mm from the original specimen. The dimensions of the tensile testing specimen are: length of 250 mm, thickness of 6 mm, outer radius of 84.5 mm and inner radius of 78.5 mm.
Figure 4.1-B shows the specimen employed for the impact test. The original specimen was cut by the half for obtaining a semi-cylindrical specimen. The dimensions are the same than for the previous specimen: length of 250 mm, thickness of 6 mm, outer radius of 84.5 mm and inner radius of 78.5 mm.The stacking sequence of the specimens was set up in 4 plies and in non-symmetrical way, as shown in figure 4.2:

1. Layer-1: Unidirectional ply (oriented fibers with 0° in the longitudinal direction) with thickness of 2.5 mm;

2. Layer-2: Unidirectional ply (oriented fibers with 85° in the longitudinal direction) with thickness of 0.4 mm;

3. Layer-3: Unidirectional ply (oriented fibers with 0° in the longitudinal direction) with thickness of 2.5 mm;

4. Layer-4: Non-woven fabric ply with thickness of 0.6 mm.

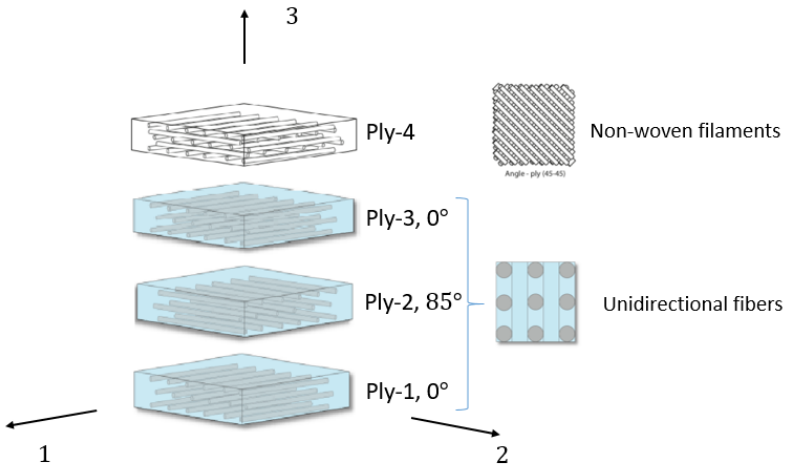

Figure 4.2 *Specimen stacking sequence.*

The grey ply in figure 4.2 represents the cover lamina, while the blue plies represent the structural ones. The global coordinate system of figure 4.2 is the same one, which was employed in the FEM software (Abaqus).
Exel composite provided the material properties for both specimens. Table 4.1 and 4.2 show the elastic mechanical properties and the ultimate stresses. These data are needed for defining the material and for implementing the three selected failure criteria into the FE analysis.

	E-Glass UD	E-Glass NNW*
E_1 (GPa)	35.00	9.60
E_2 (GPa)	7.00	9.60
E_3 (GPa)	1.20	1.20
ν_{12}	0.30	0.30
ν_{13}	0.30	0.30
ν_{23}	0.30	0.30
G_12 (GPa)	3.60	3.60
G_13 (GPa)	2.00	2.00
G_23 (GPa)	3.60	2.00

Table 4.1 *Elastic mechanical properties; *E-Glass non-woven fabric lamina.*

	E-Glass UD	E-Glass NNW*
Xt (MPa)	500	95
Xc (MPa)	200	95
Yt (MPa)	50	95
Yc (MPa)	100	95
Zt (MPa)	50	95
Zc (MPa)	100	95
Sxy (MPa)	40	36
Sxz (MPa)	26	36
Syz (MPa)	36	36

***Table** 4.2 Stress limits of the materials; *E-Glass non-woven fabric lamina.*

4.2 Experimental tests

The experimental tests constitute an important point of the research work. In this thesis, they provide results that were compared with the FE results obtained through application of the two kinds of tests: a static uniaxial tensile test and a more complex, dynamic impact test.

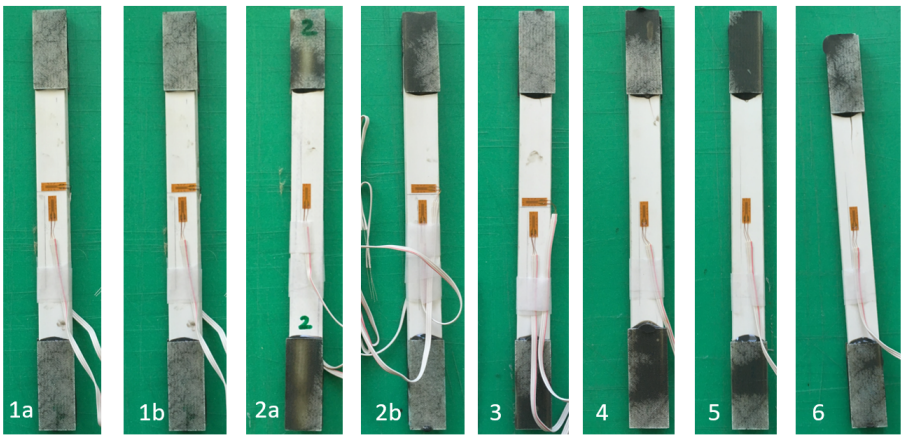

***Figure** 4.3 1- Longitudinal and transversal strain gauges in top (a) and bottom (b) area; 2- Longitudinal gauge in top (a) area and longitudinal and transversal strain gauges bottom (b) area; 3- Longitudinal and transversal strain gauges in bottom area; 4- Longitudinal strain gauges in bottom area; 5- Longitudinal strain gauges in bottom area; 6- Longitudinal strain gauges in bottom area.*

TENSILE TEST

In order to analyse the mechanical behaviour of this material, six experimental tensile tests were performed. This test allowed to study the mechanic of the material by means of force and displacement curves. The six curves showed the displacement

and force for which the damage onset and final failure of the specimen occurred. Figure 4.3 shows the six samples tested. The strain in the longitudinal direction and transversal direction were measured.

The test was displacement-controlled up to final fracture and in analysing the registered load, as shown in 4.4. Reaction force, displacement of the cross head and longitudinal and transversal strains were taken during the tensile case in each specimen.

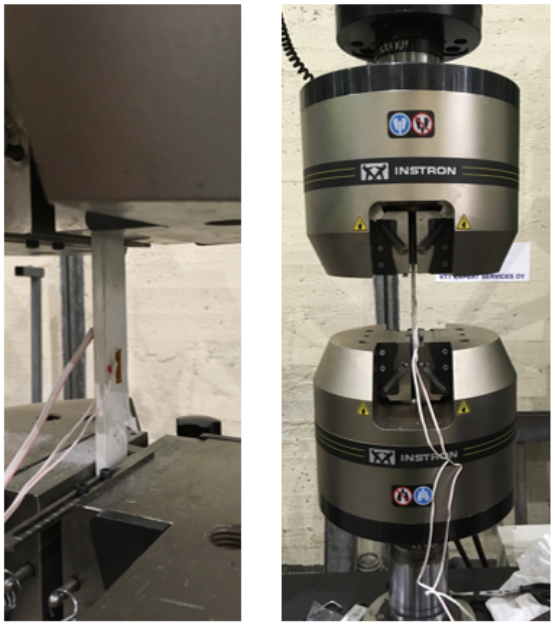

Figure 4.4 *Tensile test setting-up.*

IMPACT CASE

In order to apply dynamically a 3D complex state of stress on this structure, two impact tests were performed. The experimental outputs were analysed and compared with results of the three selected failure criteria, which were implemented through the FE software Abaqus.

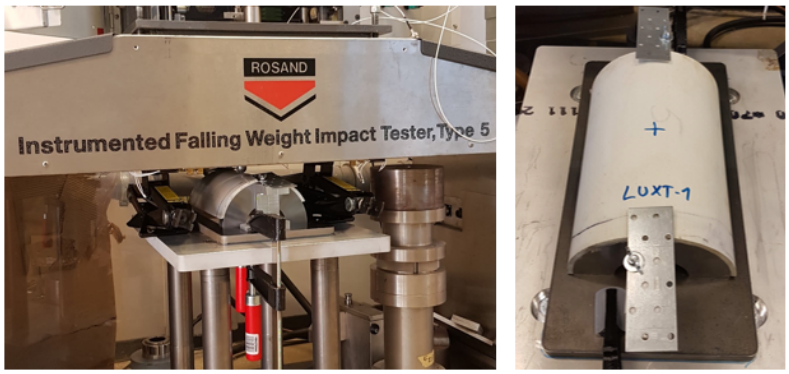

Figure 4.5 *Impact test setting-up.*

The tests consisted of free drop of the impactor of 7669 gr. from a height of 1.5 metres. The semi-cylindrical specimen was fixed on the central region of both curved ends during the test (as shown in figure 4.5). The impact load and time (in milliseconds) were stored as output data and measured through a load cell fixed on the impactor. The boundary conditions applied on the specimen are far away from the impact area and thus they do not influence the behaviour of the impact region.

4.3 FE analysis with Abaqus

Once the experimental activities have been done, the behaviour of the material could be modelled through implementation of the numerical model on finite element software. Along the same line of experimental tests, tensile case and impact case were modelled. The aim of such analyses is to obtain results that can be related to specimen mechanical behavior and failure.These analyses could then help to improve the accuracy of the elastic mechanical properties and the stress limits of the material provided by the tables 4.1 and 4.2 and to define the properties given in the selected failure criteria.

TENSILE CASE

The tensile test was modelled as a static analysis, since the imposed displacement rate was low enough. The design of the specimen was kept as similar as possible to the real one shown in section 4.1 (as shown in figure 4.6). From the structural point of view, the model was designed as a single model with three partitions, so that the four plies and their mechanical properties were could be defined in each ply. (ply 1, 2 and 3 are UD plies and ply 1 is a non-woven fabric ply).

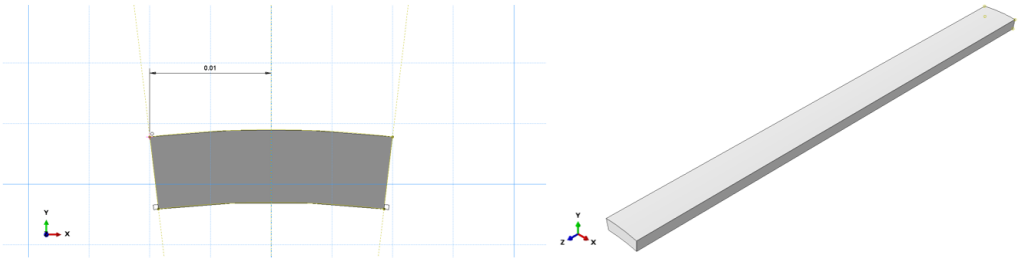

Figure 4.6 *Design module in Abaqus for the tensile case.*

Two partitions were used for applying the two boundary conditions, as shown in figure 4.7. One specimen end was fixed by the two sides in the three principal directions. At the other specimen end, the displacement along z-axis was applied on both sides and in a uniform way.

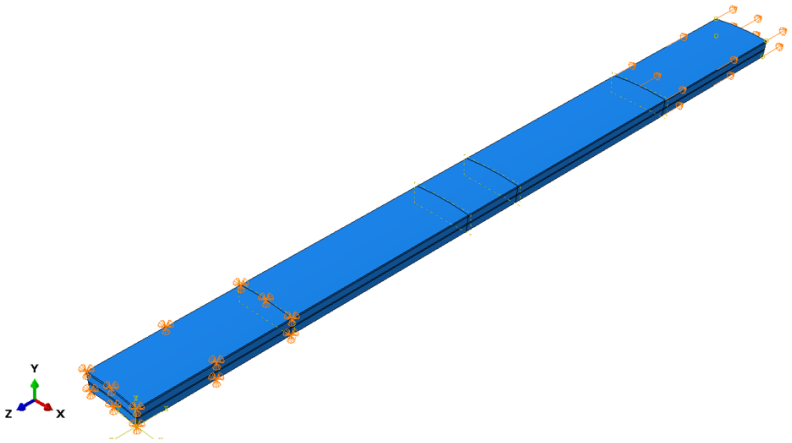

Figure 4.7 *Boundary conditions module in Abaqus for the tensile case.*

An average element size of 1 mm was used for the specimen meshing and a structured mesh were employed, as shown in figure 4.8. ply 4 and 2 have 1 element in the thickness direction and ply 1 and 3 have three and two element, respectively. The element used is a linear brick element with $2x2x2$ integrations points and eight nodes (C3D8).

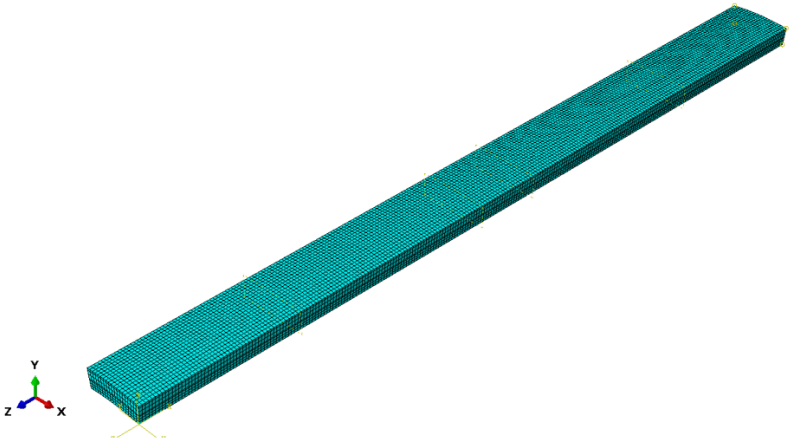

Figure 4.8 *Meshing module in Abaqus for the tensile case.*

IMPACT CASE

The finite element numerical analysis for the impact case over the semi-cylindrical specimen was carried out in Abaqus software as a dynamic analysis. Unlike the static analysis, the impact case requires the time variable to able to properly model the inertia influence of the impactor. In this model, three partitions were also applied so that the four plies separated each other and the materials and mechanical properties were defined in each ply.

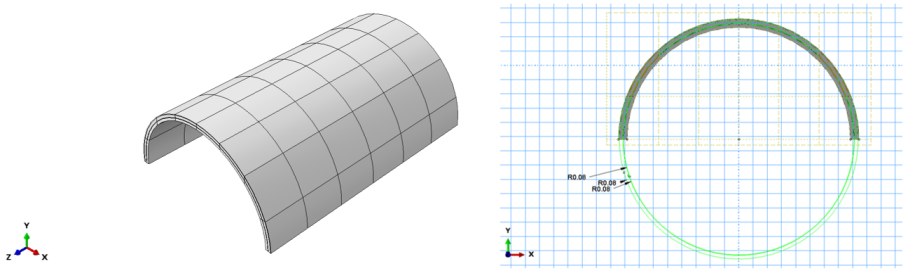

Figure 4.9 *Design module in Abaqus for the impact case.*

An initial velocity was applied as initial condition on the impactor in order to model the free fall over the impact area in the y-direction. The impactor was defined as a rigid body through a reference point, where the initial velocity was defined (the experimental test reached $5.11 m/s$). The specimen was fixed a length of 10 mm in the both specimen central ends by the two sides (top and bottoms areas). The movement was restrained in the three directions, as shown in figure 4.10. The interaction between impactor and the impact area was set. The contact properties in the tangential and normal behaviour were defined with a friction coefficient of 0.3 and a default hard contact, respectively.

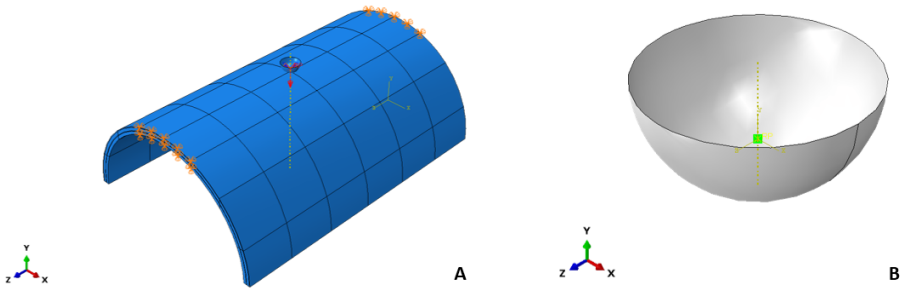

Figure 4.10 *(A) Loading and boundary conditions for the impact case in Abaqus; (B) Impactor or moving body with its defined reference point.*

The curved specimen was meshed in three areas with three different mesh dimensions. Following the figure 4.11, a uniform element size of 2 mm was used in the outer area and 1.5 mm in the middle area. In the impact area, a varied element size from 1.5 mm to 0.5 mm was applied from the middle area up to the central point of the specimen. The type of element is a linear brick element (C3D8R) with reduced integration (1 integration point).

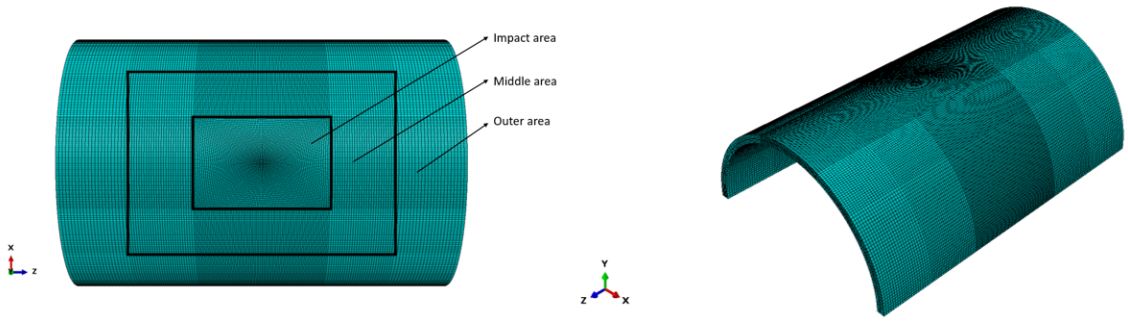

Figure 4.11 *Meshing of curved specimen for the impact case.*

4.4 Chosen failure criteria

After carrying out the qualitative and quantitative assessment in the section 5, a more specific and extent description of the selected failure criteria from the WWFE-I and WWFE-II will be developed by explaining their mathematical approaches. The main reason is to provide failure process up to the damage onset of the two specimens employed in the experimental tests (tensile and impact cases) through Abaqus software.

Through the UMAT and VUMAT subroutines connected to Abaqus Finite Element software, the anisotropic material employed in the specimens (E-Glass/Polyester) was defined as orthotropic and the three chosen failure criteria were implemented in accordance with their mathematical approaches of failure onset. Their mathematical approaches, focusing on predicting the initiation of the damage for both

experimental tests, are explained in this section.

Hashin theory

Hashin [47, 35] implemented his criterion through the failure modes by considering fibre tension/compression failure and matrix tension/compression failure. Both modes are used in the three material main directions, since the tension and compression failure in the same direction can not happen at the same time.
It is important to point out that these failure modes are defined by quadratic stress polynomials due to curve fitting considerations. The chosen approximation by author was quadratic due to curves could fit well to the data and higher approximations did not show good results.
Since the UD fibre composites are assumed as transversely isotropic with respect to

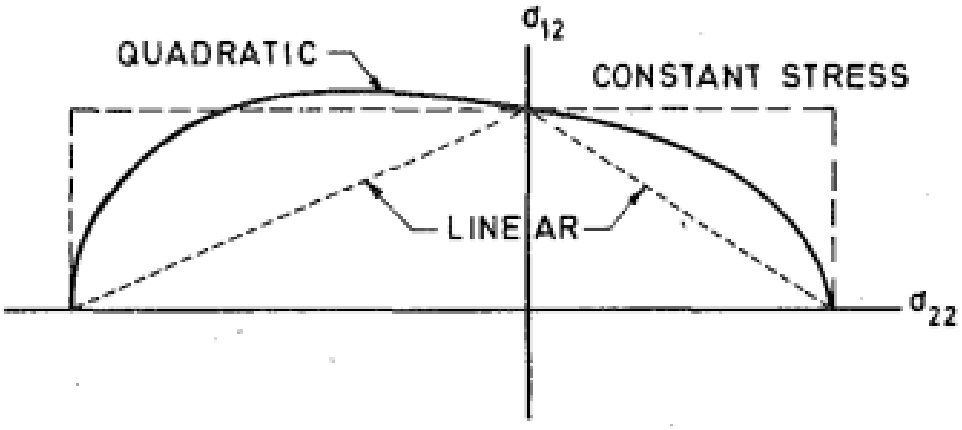

Figure 4.12 *Different approximations to experimental data [34].*

fiber direction, the failure modes are invariant under any rotation of the transverse and normal axes around fibre axe. For this reason, failure modes can be function of stress invariants under such rotations:

$$I_1 = \sigma_{11} \tag{4.1}$$

$$I_2 = \sigma_{22} + \sigma_{33} \tag{4.2}$$

$$I_3 = \sigma_{23}^2 - \sigma_{22}\sigma_{33} \tag{4.3}$$

$$I_4 = \sigma_{12}^2 + \sigma_{13}^2 \tag{4.4}$$

$$I_5 = 2\sigma_{12}\sigma_{23}\sigma_{13} - \sigma_{22}\sigma_{13}^2 - \sigma_{33}\sigma_{12}^2 \tag{4.5}$$

I_5 will not appear in the failure criterion due to the quadratic approximation. Therefore, the isotropic transversely quadratic approximation is:

$$A_1 I_1 + B_1 I_1^2 + A_2 I_2 + B_2 I_2^2 + C_{12} I_1 I_2 + A_3 I_3 + A_4 I_4 = 1 \tag{4.6}$$

Being the pure transverse and axial shear approximation:

$$A_3 = \frac{1}{\tau_T^2} A_4 = \frac{1}{\tau_A^2} \tag{4.7}$$

The fiber failure (FF) mode occurs when fiber ruptures in tension or fiber buckles

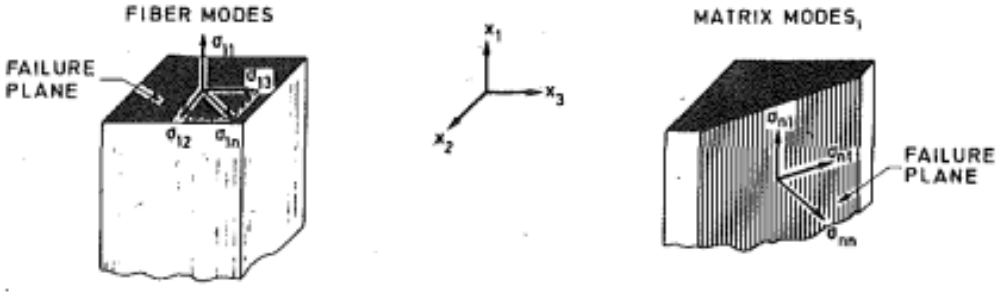

Figure 4.13 *Failure modes and planes [34].*

in compression and the matrix (or inter fiber) failure mode takes places under a parallel failure plane pto the fibers.

For the FF mode, the involved stresses are σ_{11}, σ_{12} and σ_{13}, which act over failure plane ($x_2 - x_3$ plane in figure 4.13). An interaction mechanism of these normal stresses would be necessary, since the transversal isotropic compression stress ($-\sigma$) could block the fiber buckling due to the σ_{11}. it would be need

According to the inter fiber failure (IFF) mode, figure 4.13 shows that IFF is represented by a planar failure, which is parallel to the fiber direction. The stresses, which define that plane, are σ_{nn}, σ_{nt} and σ_{ln}. σ_{nn} and σ_{nt} are defined by the stresses $\sigma_{22}, \sigma_{33} and \sigma_{23}$, while σ_{nt} is function of σ_{12} and σ_{13}.

Both failure modes combined with the approximation equations 4.6 and 4.7, the failure criterion for both modes are:

Fiber mode

$$A_f \sigma_{11} + B_f \sigma_{11}^2 + \frac{1}{\tau_A^2} * (\sigma_{12}^2 + \sigma_{13}^2) = 1 \tag{4.8}$$

Matrix mode

$$A_m(\sigma_{22}+\sigma_{33}) + B_m(\sigma_{22}+\sigma_{33})^2 + B_f * \sigma_{11}^2 + \frac{1}{\tau_T^2}(\sigma_{23}^2 - \sigma_{33}\sigma_{22}) + \frac{1}{\tau_A^2}(\sigma_{12}^2+\sigma_{13}^2) = 1 \tag{4.9}$$

Each failure mode will be discuss separately by subdividing into tensile and compressive modes due to the different obtained results experimentally.

Tensile fiber failure mode $\sigma_{11} > 0$. After the uniaxial tensile test, it can be confirmed that σ_{11}^{u}=σ_{A}^{+} to provides the coefficient A_f and B_f. Since σ_1 and σ_{12} are weakening each other, the approximation will be an ellipse quadrant with intercept A_f and B_f with the axes. In this way, equation 4.8 becomes:

$$(\frac{\sigma_{11}}{\sigma_{A}^{+}})^2 + \frac{1}{\tau_{A}^{2}}(\sigma_{12}^{2} + \sigma_{13}^{2}) = 1 \tag{4.10}$$

Compressive fiber failure mode $\sigma_{11} < 0$, The uniaxial compressive test demonstrated that $\sigma_{11}^{u} = -\sigma_{A}^{-}$. So the failure criterion in the simple maximum stress is:

$$\sigma_{11} = \sigma_{A}^{-} \tag{4.11}$$

For the matrix mode, is more complicate its modelling. Starting from (34), it has:
Tensile inter fiber failure mode $\sigma_{nn} > 0$. The experimental test demonstrates that $\sigma_{22}^{u} = \sigma_{T}^{+}$, which is introduced in equation 4.9:

$$A_{m}^{+}\sigma_{T}^{+} + B_{m}^{+}\sigma_{T}^{+2} = 1 \tag{4.12}$$

If A_{m}^{+} is assumed zero, the failure criterion for tensile mode is:

$$\frac{1}{\sigma_{T}^{+2}}(\sigma_{22} + \sigma_{33})^2 + \frac{1}{\tau_{T}^{2}}(\sigma_{23}^{2} - \sigma_{22}\sigma_{33}) + \frac{1}{\tau_{A}^{+2}}(\sigma_{12}^{2} - \tau_{13}^{2}) = 1 \tag{4.13}$$

Compressive inter fiber failure mode $\sigma_{nn} < 0$. When $\sigma_{22}^{u} = \sigma_{T}^{-}$ is introduced in the equation 4.9:

$$-A_{m}^{-}\sigma_{T}^{-} + B_{m}^{-}\sigma_{T}^{-2} = 1 \tag{4.14}$$

A_{m}^{-} and A_{m}^{+} have to be determined in terms of σ_{T}^{-} and σ. Since the material fails in transversely isotropic pressure (σ), the condition of this pressure will be $\sigma \gg \sigma_{T}^{-}$. If this condition is used for keeping the first-order terms in equation 4.9, the failure criterion for compressive mode is:

$$\frac{1}{\sigma_{T}^{-}}\left[(\frac{\sigma_{T}^{-}}{2\tau_{T}})^2 - 1\right](\sigma_{22}+\sigma_{33}) + \frac{1}{4\tau_{T}^{2}}(\sigma_{22}+\sigma_{33})^2 + \frac{1}{\tau_{T}^{2}}(\sigma_{2}3^2 - \sigma_{22}\sigma_{33}) + \frac{1}{\tau_{A}^{2}}(\sigma_{12}^{2}+\sigma_{13}^{2}) = 1 \tag{4.15}$$

For determining the sign of σ_{nn} in order to know which inter fiber mode has to be used, this mode will be expressed in function of the principal stresses σ_2 and σ_3. The normal stress σ_{nn} over the fracture plane with an orientation (θ) relative to x_2 axis is:

$$\sigma_{nn} = \sigma_{2}cos^{2}\theta + \sigma_{3}sin^{2}\theta \tag{4.16}$$

With

$$\sigma_{nn} \geq 0 \; when \; \sigma_2, \sigma_3 \geq 0 \tag{4.17}$$

$$\sigma_{nn} \leq 0 \; when \; \sigma_2, \sigma_3 \leq 0 \tag{4.18}$$

The equations 4.13 and 4.15 have to implement with the form of the equation 4.9 and the initial zero of the stress plot in σ_2-σ_3 curve [34].
Finally, the quadratic failure criteria for 3D stress state is:
Tensile Fiber Mode $\sigma_{11} > 0$:

$$(\frac{\sigma_{11}}{\sigma_A^+})^2 + (\frac{\sigma_{12}}{\tau_A})^2 + (\frac{\sigma_{13}}{\tau_A})^2 = 1 \tag{4.19}$$

Fiber Compressive Mode $\sigma_{11} < 0$:

$$(\frac{\sigma_{11}}{\sigma_A^-})^2 = 1 \tag{4.20}$$

Tensile Matrix Mode$\sigma_{22} + \sigma_{33} > 0$:

$$\frac{(\sigma_{22} + \sigma_{33})^2}{(\sigma_T^+)^2} + \frac{(\sigma_{23})^2 - \sigma_{22} * \sigma_{33}}{(\tau_T)^2} + \frac{\sigma_{12}^2 + \sigma_{13}^2}{\tau_A^2} = 1 \tag{4.21}$$

Compressive Matrix Mode $\sigma_{22} < 0$:

$$\frac{1}{\sigma_T^-}\left[(\frac{\sigma_T^-}{2\tau_T})^2 - 1\right](\sigma_{22}+\sigma_{33}) + \frac{1}{4\tau_T^2}(\sigma_{22}+\sigma_{33})^2 + \frac{1}{\tau_T^2}(\sigma_{23}^2 - \sigma_{22}\sigma_{33}) + \frac{1}{\tau_A^2}((\sigma_{12})^2 + (\sigma_{13})^2) = 1 \tag{4.22}$$

Such a failure criterion is physically realistic, since it avoids prediction of multi-axial tensile/compressive modes in terms of compressive/tensile failure stresses. The recognition of the separate modes identifies certain troublesome interaction coefficient in polynomial criteria, but they are secondary importance problems.

Puck theory

Puck theory [56] gained confidence in the community by following the Hashin criterion strategy differencing two kind of fracture in the FRP's, fibre fracture (FF) and inter-fibre fracture (IFF). Where each one of them have different load-carrying capacities in the laminate since FF always involves loss of this capacity but IFF can suggest it in certain circumstances.
In the figure 4.15, the different stresses which can occur in a ply are shown. They are compression-tension normal and shear stresses by naming with the sub-index $\parallel$ if it is parallel to the fibre direction and $\perp$ if it is perpendicularly to the fibre direction. As well for the shear stresses, which can be divide into these work in plane parallel

to fibre direction $\tau_{\perp\parallel}$ and these which work in-plane perpendicular to fibre direction $\tau_{\perp\perp}$.
Author developed this theory not only to be developed in one UD ply (figure 4.14), but also for several UD plies with different fibre orientations for achieving the best mechanical properties in the laminates.

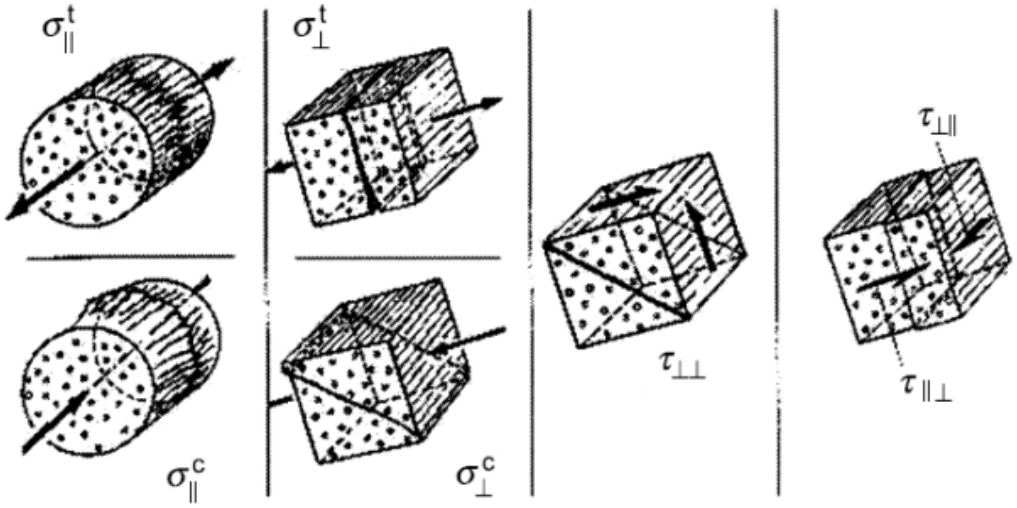

Figure 4.14 *Cigar envelope of Puck, [18].*

The different states of fracture which can occur in a FRP depend on its basis strengths, which are got by experimental tests. For the UD FRP's particularly, the fracture can produce by fibre-parallel or by perpendicular tension or compression stresses ($R_{\parallel}^{t}, R_{\parallel}^{c}, R_{\perp}^{t}$ *and* $R_{\perp}^{c}$) and by the in-plane and out of plane shear stresses ($R_{\perp\parallel}, R_{\perp\perp}$). The failure criterion is defined in the six-dimensional stress space, by including all strengths which act over the ply and predicting fractures at the all stress combinations.
Failure criteria can be based on pure mathematical considerations of surface-definition, fracture-mechanical or physical considerations by proving or contradicting itself by further experimental results. And it is important to note that Puck's theory has the most elaborated advantages of physically-based fracture conditions for the UD FPRCs [19].
Through the Puck cigar in the figure 4.15, the inventor visualized the fracture conditions for plane stress load cases. The Puck fracture cigar shows the two sub-surfaces which represent the fibre failure (end faces) and the inter-fibre failures (lateral curved surface).

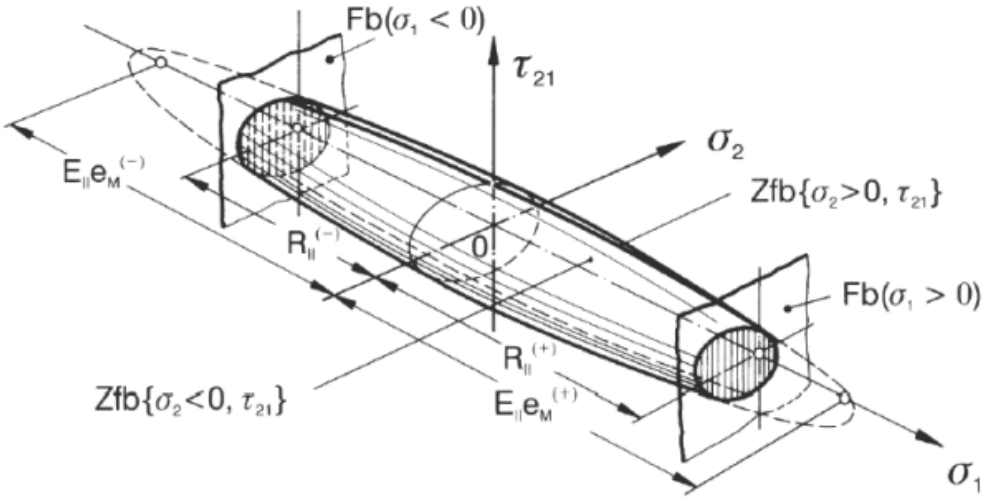

Figure 4.15 *Puck criterion cigar, [18].*

Fiber Fracture criterion

The FF is considered as independent criterion regarding the IFF. It represents two limits of stress for tension and compression (first left part of the figure 4.14). If the ply is assumed as a homogenised orthotropic continuum, the fibre fracture ratio (f_{EFF}) is considered as the stress in the ply (homogenised stress) divided between tension/compression stress at fracture of the ply ($R^t_\parallel$ and $-R^c_\parallel$). The condition of fracture would be:

$$f_{EFF} = \sigma_1 / R^t_\parallel \, for \, \sigma_{f1} > 0 \tag{4.23}$$

$$f_{EFF} = \sigma_1 / -R^c_\parallel \, for \, \sigma_{f1} < 0 \tag{4.24}$$

The fibre fracture is predicted when f_{EFF} is equal to 1.

It is important to point out that the homogenised ply stresses generate different longitudinal stresses σ_{f1} in the fibre than the uni-axial stresses. The reason is because of the transverse stresses (Posisson ratio), a local effect which is enlarged as a consequence of the in-homogeneously distributed stress on matrix. Puck took into account this local effect since transverse stress was higher than the homogenised stress in regions close to the fibre (at ply level). In consequence, the magnification factors (1.3 for GFRC and 1.1 for CFRC) were employed for this magnified stresses. The strain (ε_{1f}) in the fibre direction, due to the combined stresses, would be:

$$\varepsilon_{f1} = \frac{\sigma_{1f}}{E_{\parallel f}} - \frac{\nu_{\parallel \perp f}}{E_{\perp f}} * m_{\sigma * f1} * (\sigma_2 + \sigma_3) \tag{4.25}$$

with

$$\frac{\nu_{\parallel \perp f}}{E_{\perp f}} = \frac{\nu_{\perp \parallel f}}{E_{\parallel f}} \; and \; \varepsilon_{f1} = \varepsilon_1 \tag{4.26}$$

The longitudinal stress in the fibre is:

$$\sigma_{1f} = \varepsilon_1 * E_{\parallel f} + \nu_{\perp\parallel f} m_{\sigma_f}(\sigma_2 + \sigma_3) \tag{4.27}$$

The ε_1 is replaced from the equation 4.27 by the elastic law of the UD-lamina:

$$\varepsilon_1 = \frac{\sigma_1}{E_\parallel} - \frac{\nu_{\perp\parallel}}{E_\parallel}(\sigma_2 + \sigma_3) \tag{4.28}$$

And then, by using the fibre stress (σ_{1f}) as the fracture resistance of fibre $R_{\parallel f}$ (with $\varepsilon_{FF_f} = \varepsilon_{FF}$):

$$R_{\parallel f} = E_{\parallel f} * \varepsilon_{FF_f} \; and \; R_\parallel = E_\parallel * \varepsilon_{FF} \longrightarrow R_{\parallel f} = \frac{E_{\parallel f}}{E_\parallel} * R_\parallel \tag{4.29}$$

Finally, the FF condition for UD ply would be:

$$f_{EFF} = \frac{1}{R_\parallel^{t,c}} \left[\sigma_1 - (\nu_{\perp\parallel} - \nu_{\perp\parallel f} * m_{\sigma_1} \frac{E_\parallel}{E_{\parallel f}})(\sigma_2 + \sigma_3)\right] = 1 \; for \; \sigma_{f1} > 0 \tag{4.30}$$

$$f_{EFF} = \frac{1}{-R_\parallel^{t,c}} \left[\sigma_1 - (\nu_{\perp\parallel} - \nu_{\perp\parallel f} * m_{\sigma_1} \frac{E_\parallel}{E_{\parallel f}})(\sigma_2 + \sigma_3)\right] = 1 \; for \; \sigma_{f1} < 0 \tag{4.31}$$

From the plane-stress point of view, Puck criterion demonstrated that the FF conditions from the equations 4.23 and 4.24 and the equations 4.30 and 4.31 differ each other a few percent [18]. But, the transverse stresses on FF can have an important influence where the combined compressive σ_2^c and σ_3^c with similar magnitude (by a factor of up 4 according to experiments).

Inter-Fiber Fracture criterion

Recently, great develops have been achieved in the failure conditions for the inter-fibre failure. Many scientists implemented failure criteria for brittle composite (just like UD layers, particularly at inter-fibre failure) by following the yield criteria of Von Mises or Hill [61], which was applied for the ductile materials. However, Hashin started to use the failure criteria of Mohr, more appropriate for brittle characteristics, on UD composites. Through this develop based on physical foundations and that the fracture is created by the stresses of the fracture plane, not only the angle of fracture can be obtained but also a less computer capacity is required.

The inter-fibre failure mode (IFF) occurs due to matrix and fibre/matrix-interface are affected by the stresses $(\sigma_2, \sigma_3, \tau_{23}, \tau_{31}, \tau_{21})$ which are in the planes parallel to the fibres. Where it is necessary to single out the two coordinate systems for understanding this criterion:

$\{\sigma\} = \{\sigma_1, \sigma_1, \sigma_1, \tau_{23}, \tau_{31}, \tau_{21}\}^T \longrightarrow$ Fibre coordinate system.

$\{\sigma'\} = \{\sigma_x, \sigma_y, \sigma_z, \tau_{yz}, \tau_{xz}, \tau_{xy}\}^T \longrightarrow$ Laminate or component COS.

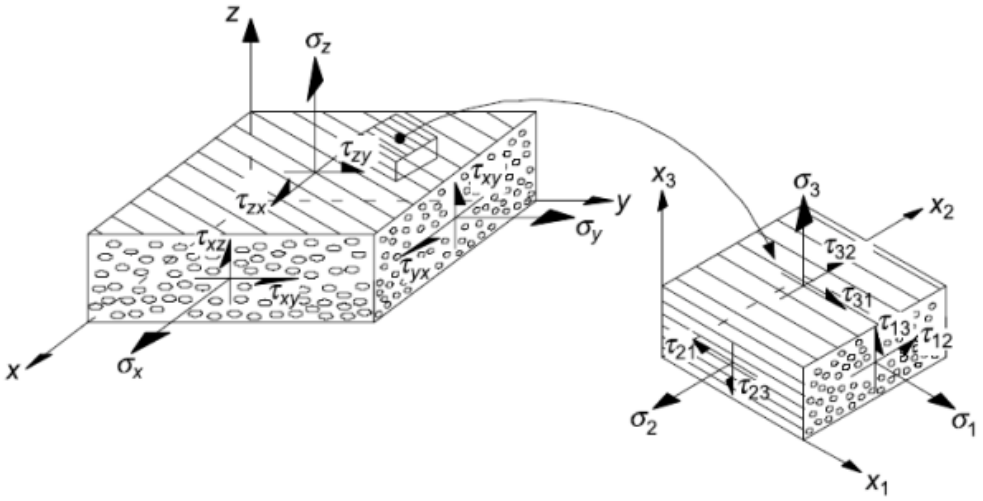

Figure 4.16 *3D stressing in local COS and laminate COS-, [18].*

Puck failure criterion is based on that the fracture is determined by stresses which, are placed in a action plane. The kind of fracture and where action and fracture plane occurs are the important point for the criterion. The stresses acting on the action plane are related to the strengths of the same action plane by means the fracture resistance R^A. This parameter constituents the resistance by which an action plane can resist its own fracture produced by stresses ($\sigma_\perp^{t/c}, \tau_{\perp\parallel}$ or $\tau_{\perp\perp}$) on the same action plane, as shown in 4.17.

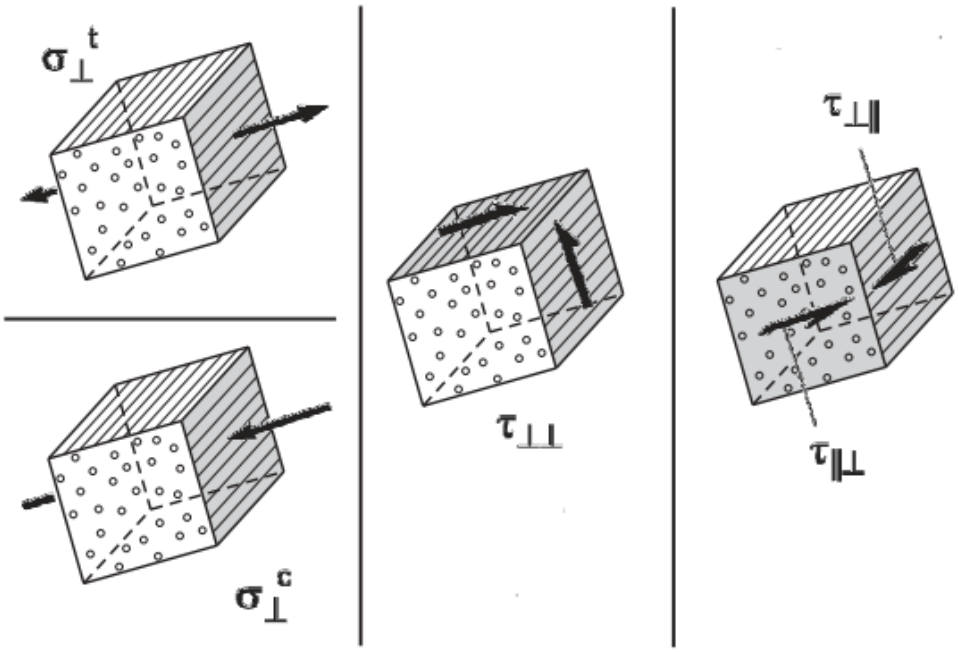

Figure 4.17 *Stresses of Ud-ply and their action planes (grey), [18].*

After observing experimentally where action plane coincided with the fracture plane [19], Puck determined that there can be only three stresses acting on an action plane ($\sigma_{\perp}^{t/c}, \tau_{\perp\parallel}$ or $\tau_{\perp\perp}$) and thus three fracture resistances ($R_{\perp}^{At}, R_{\perp}\parallel^{A}$ or $R_{\perp}\perp^{A}$) on the same plane. The two first fracture resistances are derived from the strengths of the material, but $R_{\perp\perp}^{A}$ requires a experimental observation. Which demonstrated that $\sigma_{\perp}^{t}$ in the action plane decreases the bearable shear and $\sigma_{\perp}^{t}$ increases the fracture resistance when $\tau_{\perp\parallel}$ and/or $\tau_{\perp\perp}$ act.

The two kind of stresses which define any action plane are the normal (σ) ans shear (τ) stress. From a micro-mechanical scale, the shear vector is examined by means τ_{nt} and τ_{n1} which have to be differed due to their differences in terms of shear fracture. The index-n indicates that both act on the same plane and the index-t and index-1 indicate that they are acting in transverse and fibre direction, respectively. However, their combined representation from the force point of view would be:

$$\tau_{n\psi} = \sqrt{\tau_{nt}^2 + \tau_{n1}^2} \tag{4.32}$$

The normal stress σ_n and shear stress $\tau_{n\psi}$ are shown in the figure 4.18. But the $\tau_{\psi n}$ which acts in a plane intersecting the fibres, do not play a role in the fracture criteria due to the planes resistance are higher than of fibre-parallel action planes.

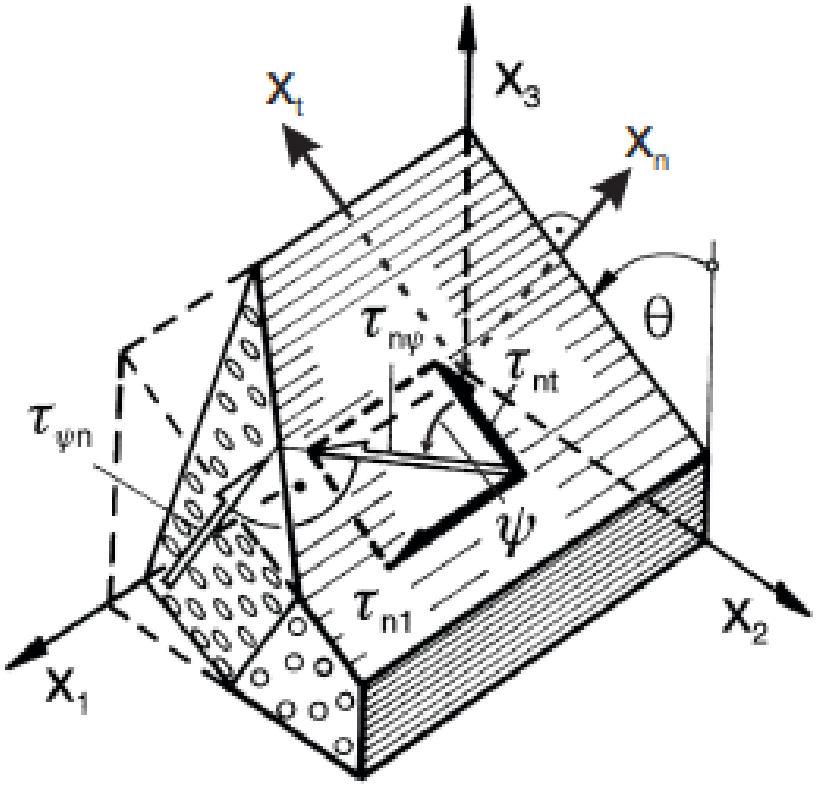

Figure 4.18 *Shear stresses in section plane, [18].*

Therefore, only the three stresses on the same action plane can appear in the fracture criteria and these stresses have to be related to adequate action plane-related strength measures when the fracture is on the common action plane.
The action plane with the highest risk of fracture must be known before the fracture stresses were calculated. For that, the stretch factor f_S is employed for 180 sections in the laminate between $\theta = [-90°, 90°]$ by increasing the stress vectors ($\sigma_{\perp}^{t/c}(\theta), \tau_{\perp\parallel}(\theta)$ or $\tau_{\perp\perp}(\theta)$) up to the failure. This factor is between stresses acting to specific action plane and the fracture limit in this plane.

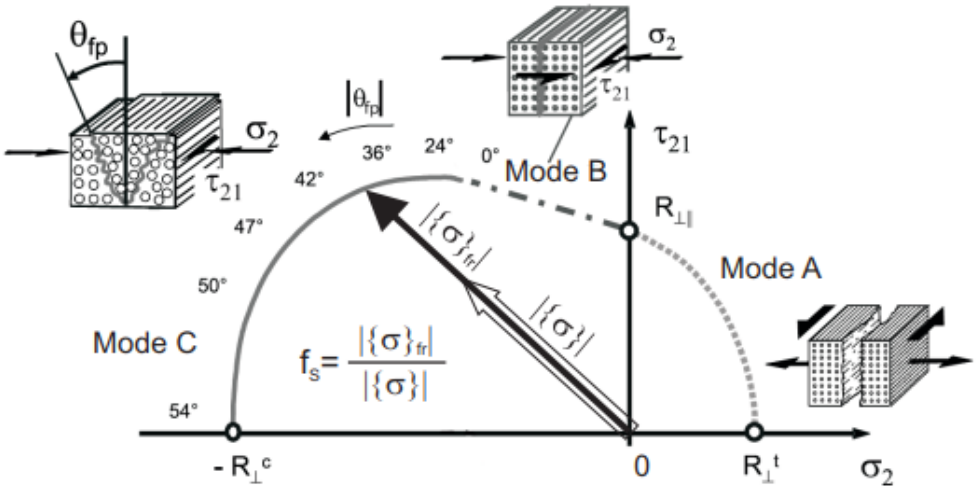

Figure 4.19 *f_S of plane states of stress, [18].*

When the action planes is under only compressive stress σ_n, f_S takes the infinite value with $\theta = -45°$ (figure 4.20). The stress exposure f_E represents directly the risk of fracture under the following equation:

$$f_E = \frac{1}{f_S} = \frac{length of the actual stress vector \vec{\sigma}}{length of the vector \vec{\sigma_{fr}} of the stresses leading to fracture} \tag{4.33}$$

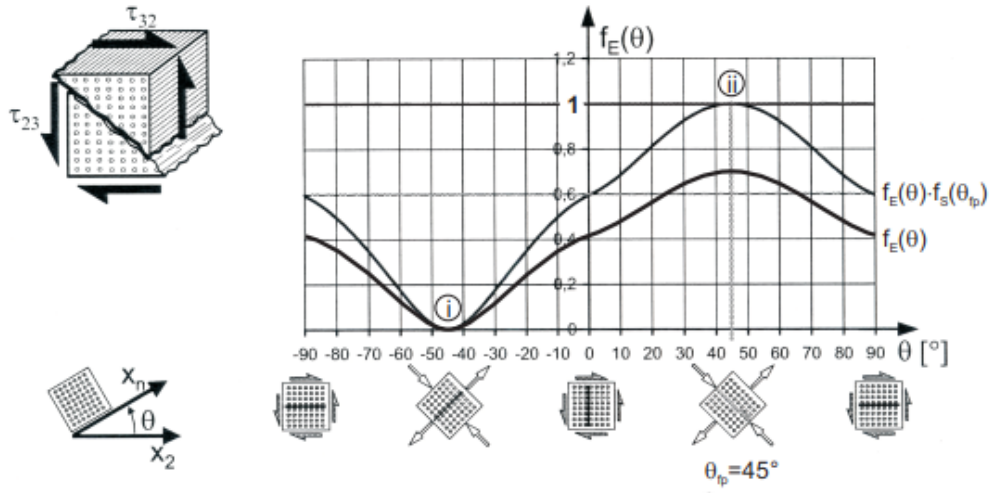

Figure 4.20 *Stress exposure, [18].*

The plane under the mentioned loading stress at θ_{fp}, it needs the lowest stretch factor (f_{Smin}) to fracture. This would be possible if the external stress was increased by f_{Smin} while the rest of the plane with $f_s > f_{Smin}$ are below.
The stresses on the action plane came from the applied stresses as:

$$\begin{aligned} \sigma_n(\theta) &= \sigma_2 \cdot cos^2\theta + \sigma_3 \cdot sin^2\theta + 2\tau_{23} \cdot sin\theta \cdot cos\theta \\ \tau_{nt}(\theta) &= -\sigma_2 \cdot sin\theta \cdot cos\theta + \sigma_3 \cdot sin\theta \cdot cos\theta + \tau_{23} \cdot (cos^2\theta - sin^2\theta) \\ \tau_{n1} &= \tau_{31} \cdot sin\theta + \tau_{21} \cdot cos\theta \end{aligned} \tag{4.34}$$

These three stresses provide $\sigma_\perp, \tau_{\perp\perp}, \tau_{\perp\parallel}$ stresses, respectively. Thus, three fracture resistances of the action plane were obtained $R^{At}_\perp, R^A_{\perp\perp}$ or $R^A_{\perp\parallel}$. Since Puck assumed the brittle behaviour of the material, the following relationships were taken as valid:

$$R^{At}_\perp = R^t_\perp \tag{4.35}$$

$$R^A_{\parallel\perp} = R_{\parallel\perp} \tag{4.36}$$

$$R^A_{\perp\perp} = \frac{R^c_\perp}{2(1 + p^c_{\perp\perp})} \tag{4.37}$$

The representation of the inter fiber failure mode in the 3D state od stress of the action plane, is shown through the Master Fracture Body (MFB). Which tries to show as $(\sigma_n, \tau_{nt}, \tau_{n1})$-combinations as possible.

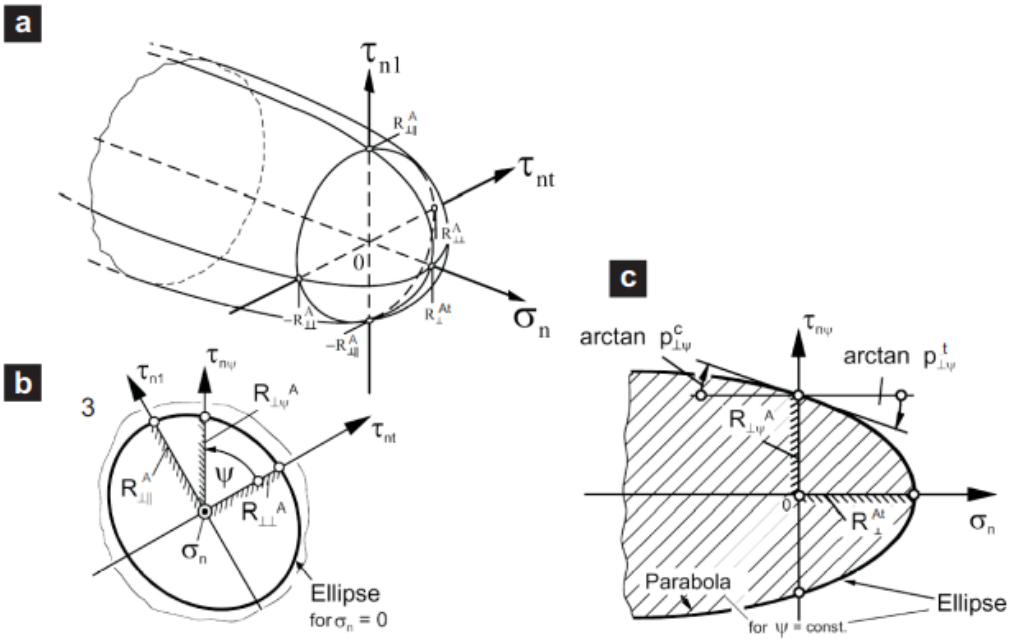

Figure 4.21 *The Master Fracture Body [20].*

Since τ_{nt}, τ_{n1} cause a stress acting on action plane parallel to the fiber (i.e. $R^A_{\parallel\perp}$ and $R^A_{\perp\perp}$), a ellipctical fracture criterion for $\tau_{n\psi}$-state of stress at $\sigma_n = 0$ is assumed:

$$(\frac{\tau_{n\psi}}{R^A_{\perp\psi}})^2 = (\frac{\tau_{nt}}{R^A_{\perp\perp}})^2 + (\frac{\tau_{n1}}{R^A_{\perp\parallel}})^2 = 1 \, for \, \sigma_n = 0 \tag{4.38}$$

On the other hand, the line, which describes the contour of the MFB, represents an ellipse for $\sigma_n \geq 0$ half space and a parabola for $\sigma_n < 0$ half space:

$$(\frac{\tau_{n\psi}}{R^A_{\perp\psi}})^2 + c_1(\frac{\sigma_n}{R^{At}_{\perp}})^2 + c_2(\frac{\sigma_n}{R^{At}_{\perp}})^2 = 1\, for\, \sigma_n = 0 \tag{4.39}$$

$$(\frac{\tau_{n\psi}}{R^A_{\perp\psi}})^2 + c\sigma_n = 1\, for\, \sigma_n = 0 \tag{4.40}$$

The points $(\sigma_n, \tau_{n\psi}) = (R^{At}_{\perp}, 0)$ on σ_n-axis and $(\sigma_n, \tau_{n\psi}) = (0, +- R^{At}_{\perp})$ on $\tau_{n\psi}$-axis are anchored to plot the ellipse. Taking the equation 4.32 and the relations $\tau_{nt} = \tau_{n\psi} cos\psi$ and $\tau_{n1} = \tau_{n\psi} sin\psi$, the equation 4.38 becomes:

$$R^A_{\perp\psi} = ((\frac{cos\psi}{R^A_{\perp\perp}})^2 + (\frac{sin\psi}{R^A_{\perp\parallel}})^2)^{\frac{1}{2}} \tag{4.41}$$

The ellipse crosses the $\tau_{n\psi}$-axis with a inclination with the following inclination parameters:

$$(\frac{\delta\tau_{n\psi}}{\delta\sigma_n})^{ellipse}_{\sigma_n=0} = -p^t_{\perp\psi}\, for\, \tau_{n\psi} > 0 \tag{4.42}$$

$$(\frac{\delta\tau_{n\psi}}{\delta\sigma_n})^{ellipse}_{\sigma_n=0} = p^t_{\perp\psi}\, for\, \tau_{n\psi} < 0 \tag{4.43}$$

The parabola inclination differs from the ellipse inclinations at the point $(\sigma_n = 0, \tau_{n\psi} = +- R^A_{\perp\psi})$:

$$(\frac{\delta\tau_{n\psi}}{\delta\sigma_n})^{parabola}_{\sigma_n=0} = -p^c_{\perp\psi}\, for\, \tau_{n\psi} > 0 \tag{4.44}$$

$$(\frac{\delta\tau_{n\psi}}{\delta\sigma_n})^{parabola}_{\sigma_n=0} = p^c_{\perp\psi}\, for\, \tau_{n\psi} < 0 \tag{4.45}$$

With these conditions, the constants c_1, c_2 and c are:

$$c_1 = 2\frac{p^t_{\perp\psi} R^{At}_{\perp}}{R^A_{\perp\psi}} \tag{4.46}$$

$$c_2 = 1 - 2\frac{p^t_{\perp\psi} R^{At}_{\perp}}{R^A_{\perp\psi}} \tag{4.47}$$

$$c = 2\frac{p^c_{\perp\psi}}{R^A_{\perp\psi}} \tag{4.48}$$

Puck used the values shown in table 4.3 for the $p^t_{\perp\psi}$ and $p^c_{\perp\psi}$.

	$p^t_{\perp\parallel}$	$p^c_{\perp\parallel}$	$p^t_{\perp\perp}, p^c_{\perp\perp}$
GFRP	0.30	0.25	0.2O to 0.25
CFRP	0.35	0.30	0.25 to 0.30

Table 4.3 *Puck inclination parameters.*

Taking the equation 4.39 and 4.40 in terms of fracture condition, The Puck inter fiber failure mode for 3D state of stresses is:

$$f_{EIFF}(\theta) = \sqrt{((\frac{1}{R^{At}_{\perp}} - \frac{p^t_{\perp\psi}}{R^A_{\perp\psi}})\sigma_n(\theta))^2 + (\frac{\tau_{nt}(\theta)}{R^A_{\perp\perp}})^2 + (\frac{\tau_{n1}\theta}{R^A_{\perp\parallel}})^2} + \frac{p^t_{\perp\psi}}{R^A_{\perp\psi}}\,\sigma_n(\theta)\, for\, \sigma_n > 0 \tag{4.49}$$

$$f_{EIFF}(\theta) = \sqrt{(\frac{\tau_{nt}\theta}{R^A_{\perp\perp}})^2 + (\frac{\tau_{n1}(\theta)}{R^A_{\perp\parallel}})^2 + (\frac{p^c_{\psi\perp}}{R^A_{\perp\psi}})^2} + \frac{p^c_{\perp\psi}}{R^A_{\perp\psi}}\,\sigma_n(\theta)\, for\, \sigma_n < 0 \tag{4.50}$$

with

$$\frac{p^{t,c}_{\perp\psi}}{R^A_{\perp\psi}} = \frac{p^{t,c}_{\perp\perp}}{R^A_{\perp\perp}}\, cos^2\psi + \frac{p^{t,c}_{\perp\parallel}}{R^A_{\perp\parallel}}\, sin^2\psi \tag{4.51}$$

Finally, the angle (θ_{fp}) of the fracture plane with respect to the stacking direction can be get:

$$[f_{EIFF}(\theta)]_{max} = f_{EIFF}(\theta_{fp}) \tag{4.52}$$

Cuntze theory

Cuntze [12] developed a model, named as failure mode concept (FMC)[12, 13, 14, 16]. If a change in one failure mode would has to be made, it would affect the domain of another independent mode; the author set a failure mode-related fitting, which required failure conditions for each mode:

$$A\ set\ of\ mode\ failure\ conditions: F^{mode}\left(\{\sigma\}, R^{mode}\right) = 1(FMCprinciple) \tag{4.53}$$

where $\{\sigma\} = \{\sigma_1, \sigma_2, \sigma_3, \sigma_{23}, \sigma_{31} and \sigma_{21}\}^{\{T\}}$ and $R^{\{mode\}}$ as mode strength.
For a UD material with symmetries of the transversally isotropic material, there are five basic (mode) strengths and five elasticity properties only, whose characterisation require five independent basic ply strengths:

- $R^t_{\parallel}(= X^c)$ as tensile and compression strength parallel to the fibres.
- $R^t_{\perp}(= Y^t)$ and $R^c_{\perp}(= Y^c)$ as tensile and compressive strength transversal to the fibre direction and $R^c_{\perp}(= S)$ as in-plane shear strength.

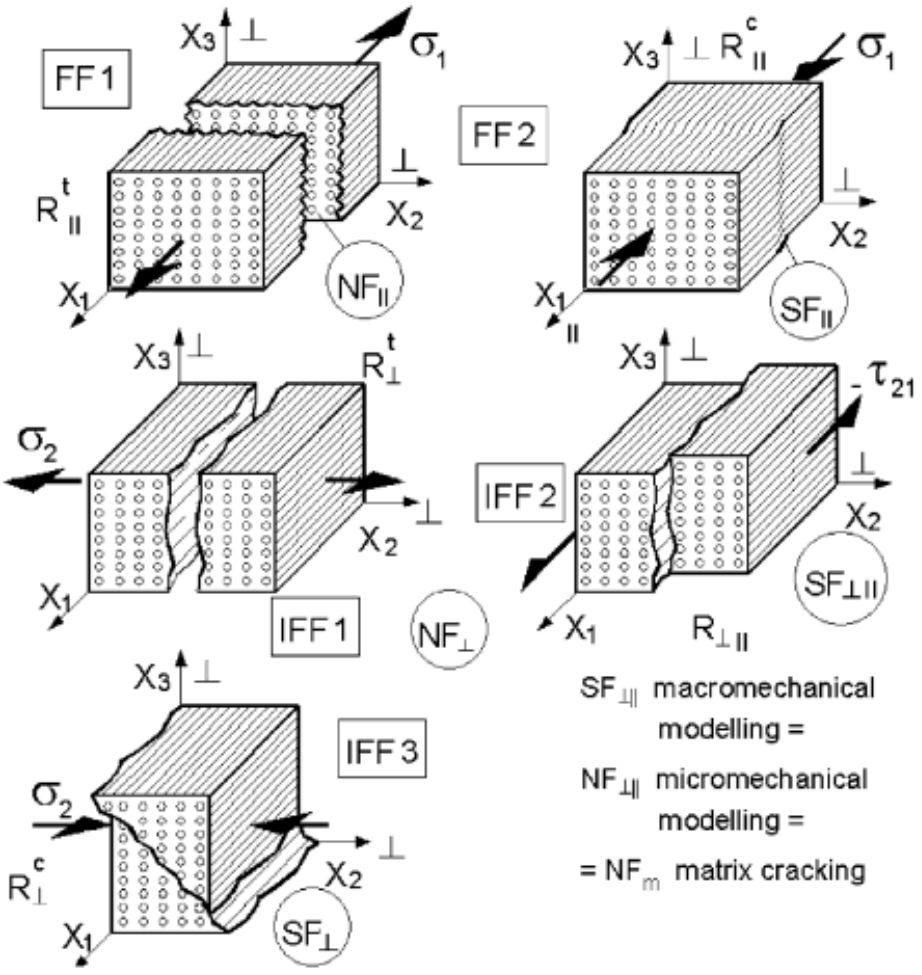

Figure 4.22 *Types of fracture of Cuntze criterion [15].*

Strength criteria ($F \leftrightarrow 1$) or failure conditions ($F = 1$) is formulated by invariants based on the macro-mechanical UD-stresses. The material symmetry-based UD invariants used in FMC are [4]:

$$I_1 = \sigma_1 \tag{4.54}$$

$$I_2 = \sigma_2 + \sigma_3 \tag{4.55}$$

$$I_3 = \tau_{31}^2 + \tau_{21}^2 \tag{4.56}$$

$$I_4 = \{\sigma_2 - \sigma_3\}^2 + 4\tau_{23}^2 \tag{4.57}$$

$$I_5 = (\sigma_2 - \sigma_3) * \left(\tau_{31}^2 - \tau_{21}^2\right) - 4 * \tau_{23} * \tau_{31} * \tau_{21} \tag{4.58}$$

The approached model of Cunzte consists of five failure modes: two fibre failure (FF) modes (FF1 and FF2, which respectively stand for tension and compression mode) and three inter-fiber failure (IFF) modes (with IFF1 as transverse tension, IFF2 as transverse compression and IFF3 shear). These modes are called

inter-fiber failure modes since they indicate failure in the interface region between matrix and fiber.
Due to the micro-mechanical nature of this model, its basic parameters are not only the macroscopic values of strength in the different directions; consequently, it also employs two friction-related parameters ($b_{\parallel\perp}$, $b^t_{\parallel\perp}$ and $b^t_{\perp}$). These parameters are defined as follows:

$$b^{\tau}_{\perp} = \frac{1 + (\sigma_2^{c,t} + \sigma_3^{ct})/R^c_{\perp}}{(\sigma_2^{c,t} + \sigma_3^{ct})/R^c_{\perp} + (\sigma_2^{c,t} - \sigma_3^{ct})/R^{c2}_{\perp}} \tag{4.59}$$

$$b_{\perp\parallel} = \frac{1 - (\tau_{21}^{\perp\parallel}/R\perp\parallel)^2}{2\sigma_2^c\,\tau_{21}^{\perp\parallel\,2}/R^3_{\parallel\perp}} \tag{4.60}$$

$$b^{\tau}_{\perp\parallel} = 1 - (b^{\tau}_{\perp} - 1)\sigma^c_{2\perp\parallel}t/R_{\perp\parallel} - b^{\tau}_{\perp}(\sigma^{ct}_{2\perp\parallel}/R_{\perp\parallel})^2 \tag{4.61}$$

However, there are a range for each parameter on the safe side for GFRP and CFRP that they are assumed to be:

$$0.05 < b_{\perp\parallel} < 0.15, \, , 1.0 < b^{\tau}_{\perp} < 1.6, \, , 0.0 < b^{\tau}_{\perp\parallel} < 0.4, \tag{4.62}$$

An equivalent stress σ_{eq} let to describe all actual load stresses and residual stresses that are acting together in a given failure mode. Its vector is read as:

$$\left\{\sigma^{mode}_{eq}\right\} = \left\{\sigma^{\sigma,\parallel}_{eq}, \sigma^{\parallel,t}_{eq}, \sigma^{\perp,\sigma}_{eq}, \sigma^{\perp,\sigma}_{eq}, \sigma^{\perp,\sigma}_{eq}, \sigma^{\perp,\parallel}_{eq}\right\}^T \tag{4.63}$$

And employing mode strength R^{mode}, its equivalent stress σ^{mode}_{eq} and the equation 9 according to the general equation of the stress effort of UD-ply in a distinct failure mode: $E^{mode}_{ff} = \sigma^{mode}_{eq}/\bar{R}^{mode}$, the following set of formulas to describe the different failure mode are:

$$FF1 : E^{\sigma\parallel}_{ff} = \frac{\sigma_1}{R^t_{\parallel}} = \, with\, \sigma_1 \, = \varepsilon^t_1 * E_{\parallel} \tag{4.64}$$

$$FF2 : E^{\parallel\tau}_{ff} = \frac{-\sigma_1}{R^c_{\parallel}} = \, with\, \sigma_1 \, = \varepsilon^c_1 * E_{\parallel} \tag{4.65}$$

$$IFF1 : E^{\sigma\perp}_{ff} = \frac{(\sigma_2 + \sigma_3) + (\sqrt{(\sigma_2 - \sigma_3)^2 + 4\tau^2_{23}})}{2\,R^c_{\perp}} \tag{4.66}$$

$$IFF2 : E^{\sigma\parallel}_{ff} = \frac{(b^{\tau}_{\perp} - 1)(\sigma_2 + \sigma_3) + b^{\tau}_{\perp}(\sqrt{(\sigma_2 - \sigma_3)^2 + 4\tau^2_{23}})}{R^c_{\perp}} \tag{4.67}$$

$$IFF3 : E^{\sigma\parallel}_{ff} = [\frac{b_{\parallel\perp}I_{23-5} + \sqrt{b^2_{\perp\parallel}I^2_{23-5} + 4R^2_{\perp\parallel}(\tau^2_{31} + \tau^2_{21})^2}}{2\,R^3_{\perp\parallel}}]^{0.5} \tag{4.68}$$

with

$$I_{23-5} = 2\sigma_2\tau_{21}^2 + 2\sigma_3\tau_{31}^2 + 4\tau_{23}\tau_{31}\tau_{21} \tag{4.69}$$

Above stresses include the non-linearly load-dependent load stresses $\{\sigma\}_L$ and the equally non-linearity-dependent residual stresses $\{\sigma\}_R$.
It is important to note that each failure mechanism is affected by an associated stress state, where the mode effort has to become zero if the mode driving stress is zero. Due to IFF, the curing stresses decay in parallel to the degradation. The not design driving stresses of a mode might increase or decrease the stress effort of the design driving one, this is pronounced by σ_{eq}.
According the interaction of failure modes, 5 are the parts that form the full failure surfaces (FFs and IFFs). On the one hand, Cuntze describes the failure mode interactions though of simple probabilistically 'series springs model' approach. On the other hand, the current model describes the ply failure system as a series failure system, which fails if any of its elements fails. Each failure mode explained previously is an element of the system and is independent of the others. The interaction between FF and IFF modes as well as between the various IFF modes acts as rounding-off procedure linked to the determination of the desired values for the resultant (global) stress effort of all interacting failure modes E_{ff}. This effort involves the sum of all the proportionate mode stress efforts according with the following equation:

$$E_{ff}^m = \left(E_{ff}^{\sigma}\|\right)^m + \left(E_{ff}^{\|}\tau\right)^m + \left(E_{ff}^{\sigma}\perp\right)^m + \left(E_{ff}^{\perp}\tau\right)^m + \left(E_{ff}^{\perp}\|\right)^m \; for UD = 1 = 100\% \, if \; failure. \tag{4.70}$$

The iteration of the partial surfaces involves all stresses efforts and each one is a portion of load-carrying of the material. For 2D level, two of five modes would interact each other. Where the interaction exponent m is obtained by curve-fitting of test data in the interaction zones.

5. RESULTS AND DISCUSSION

This chapter shows the results from both the experimental tests and the finite element analysis. They could be performed once the failure criteria were implemented and the sampled tests cases were simulated into Abaqus. Results are explained and discussed in order to compare them and to achieve a validation of the failure modes according to the experimental ones.

5.1 Comparison with the experimental results

This section shows the experimental outputs and the numerical results of the tensile and impact tests.

TENSILE CASE
As commented in the section 4.2, six specimen were tested under a uniaxial tensile loading. Figure 5.1 shows the force versus displacement curve of each specimen.

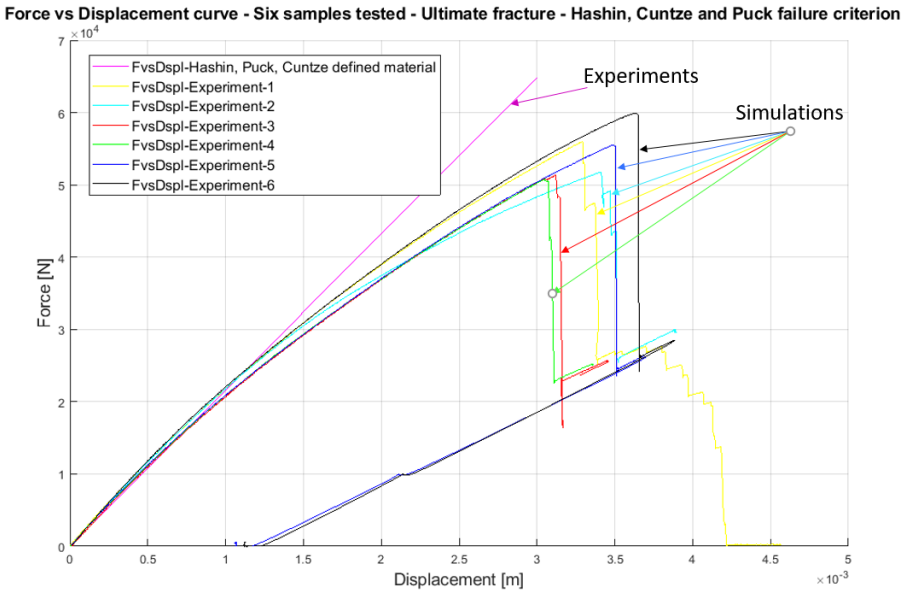

Figure 5.1 *Final fracture in force vs displacement curve of the six experimental specimens; Figure A, B, C, D, E, F and G correspond with the specimen 1, 2, 3, 4, 5 and 6, respectively.*

These curves allowed to know the level of load and displacement for which the six

specimens reached the ultimate failure under tensile case. Since, in each experiment a different ultimate failure was detected, an average of each value was made. Thus, the average ultimate failure of the six specimens occurred at 54124±3509 N and 3.41±0.24 mm. The purple curve represents the linear mechanical behavior as modelled in Abaqus, while the rest of the non-linear curves show failure when reaching the ultimate load.
Figure 5.2 represents a magnification of the force versus displacement curves, which were previously shown in figure 5.1. This magnification focuses on values close to the damage onset point.

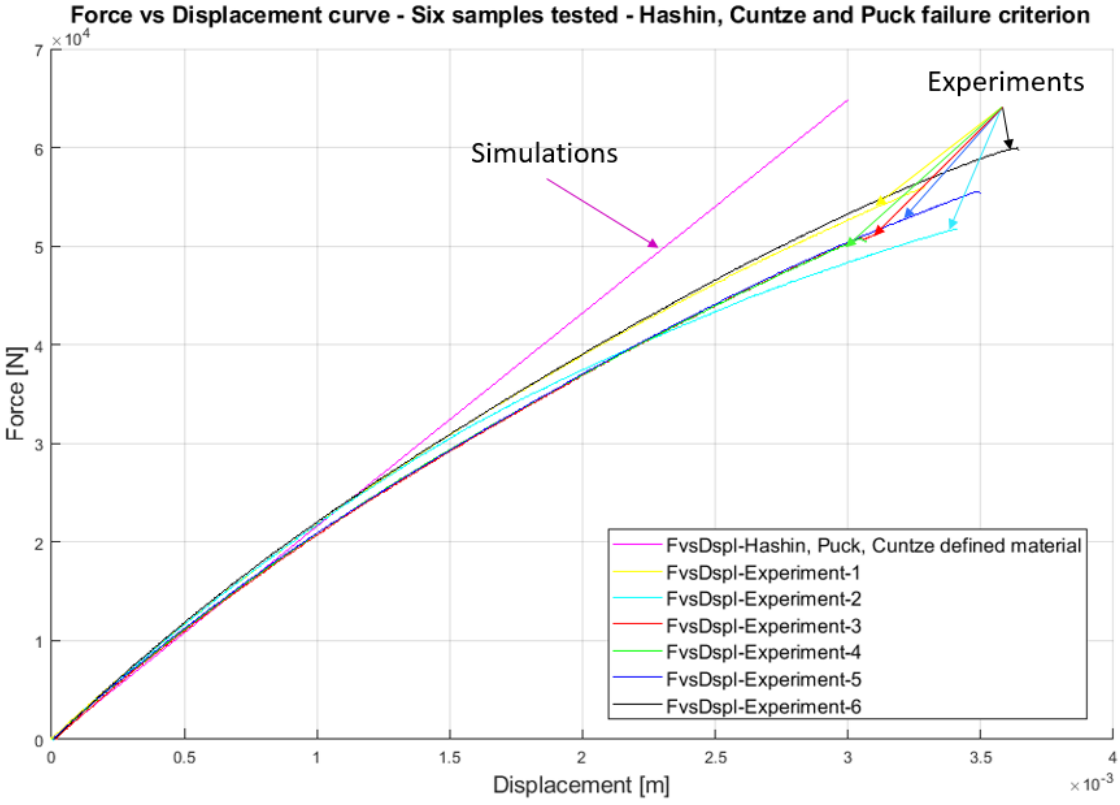

Figure 5.2 *Initiation of damage in force vs displacement curve of the specimen -1, -2, -3, -4, -5 and -6.*

The damage onset was determined approximately at the point where the linear curve (colour purple) and non-linear ones (rest of colours) separated each other. The linear curve plotted the evolution, force versus displacement under tensile load as obtained through definition of the material as a linear elastic one, while the non-linear curves represented the evolution, force versus displacement of each sampled experiment under tensile load. In order to simplify the analysis, an average of each damage onset from the six specimens was obtained at a force value of 21048±3756 N and a specimen displacement of 0.98±0.17 mm.

Figure 5.3 shows two of the the post-tested specimens under tensile load and the types of failures occurred in the regions (plies) where the boundary conditions were not applied.

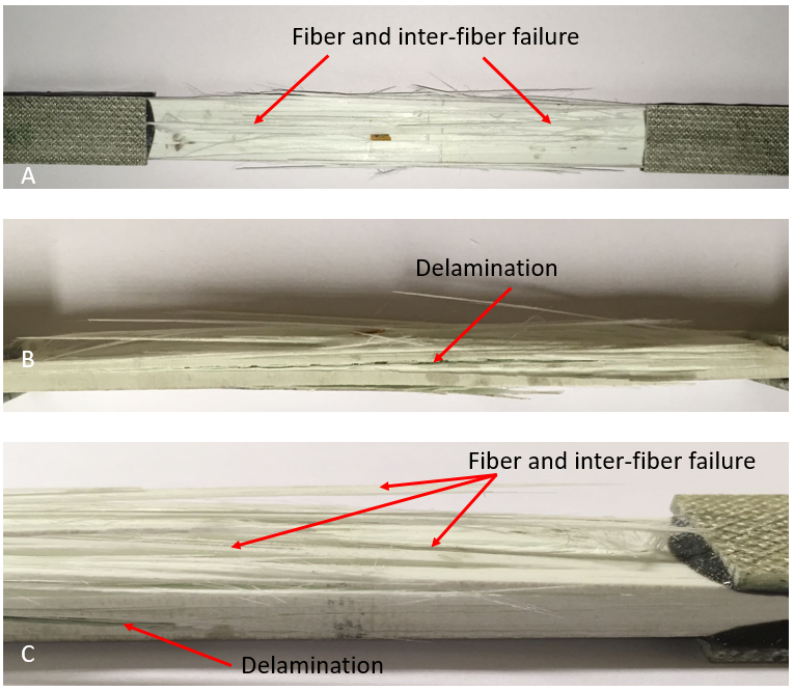

Figure 5.3 *(a) Fiber and inter-fiber failure on the critical area (Top view of specimen); (b) Delamination between plies (Front view of specimen); (c) Fiber and inter-fiber failure and delamination.*

The fiber and the inter-fiber failure can be seen in the figure 5.3-A and -C, in the top and bottom plies. Delamination, although out of the scope for this study, occurred between plies 1 and 3, as shown in figure 5.3-B.

IMPACT CASE

Figure 5.4 shows the force and displacement curves of the two experimental impact tests of the semi-cylindrical specimens. It allowed knowing the level of force and displacement, which the specimens were subjected to through the experiment.

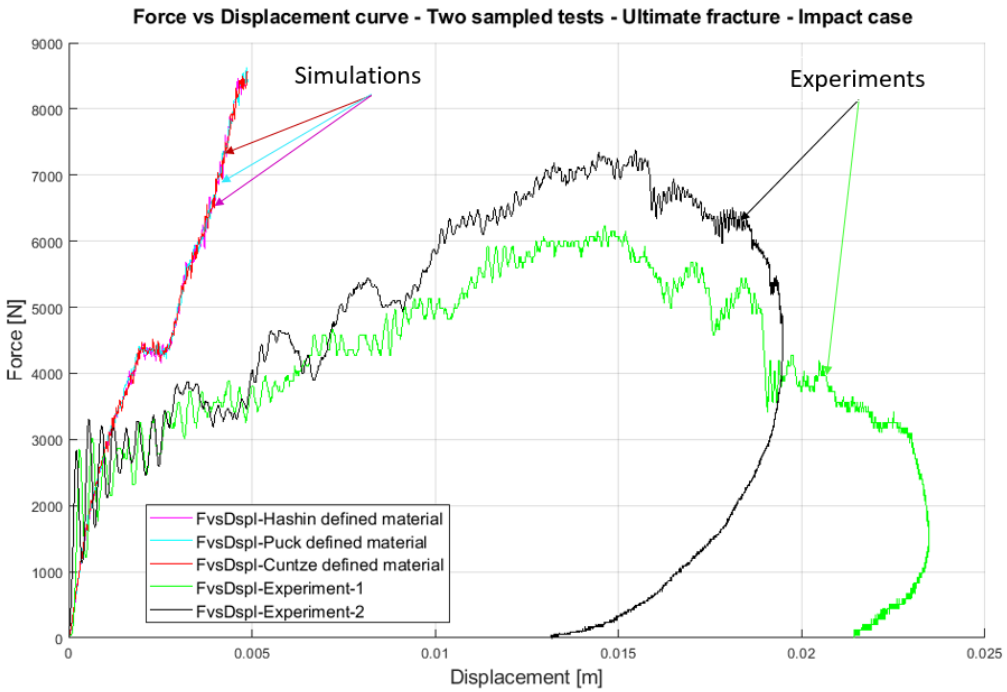

Figure 5.4 *Force vs Displacement curve up to final fracture.*

The average ultimate force of the experiment 1 and experiment 2 reached a force of 6803±811 N with an impactor displacement of 15±0.60 mm in the y-direction. These curves represent the relation between force and displacement through the whole impact test and its evolution. Experiment 1 reached damage onset at 6230 N and 14.8 mm and experiment 2 at 7377 N and 15.47 mm, as shown in the curves green and black of the figure 5.4. The force versus displacement FE curve of the material were plotted by using the linear mechanical properties as in the tensile test. This together figure 5.5 allowed determining the the initiation of damage and the ultimate fracture. The damage onset of each experiment is determined in figure 5.5, which shows the force vs displacement curves for both two experiments and FE test under the impact load.

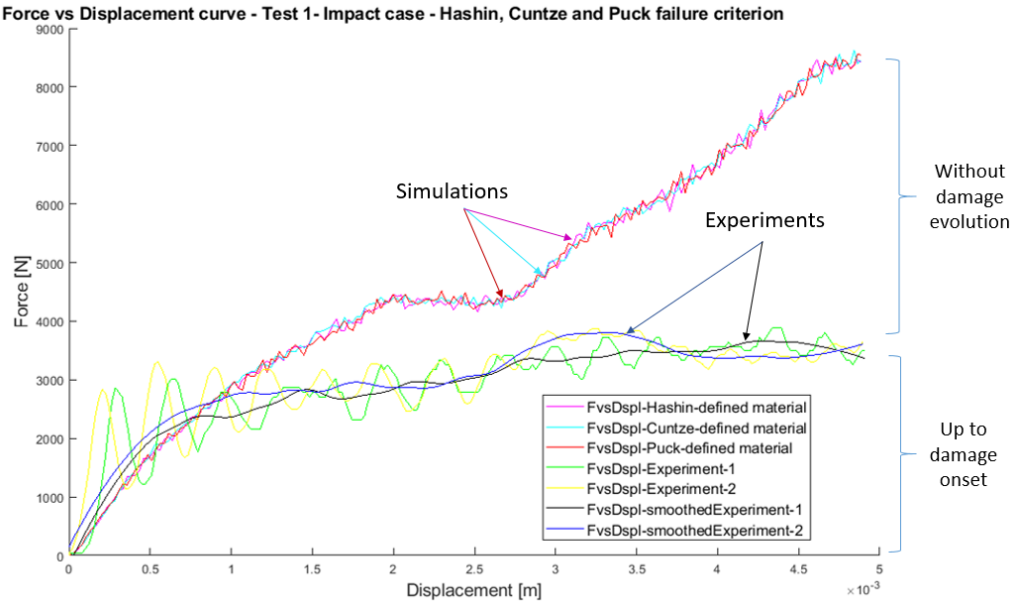

Figure 5.5 *Force vs Displacement curve before and after the damage onset.*

These comparisons between experimental and FE curves show at which force and displacement the damage onset occurs approximately. The average damage onset value of the experiment 1 and 2 occurred at a force of 2507±194 N and an impactor displacement of 0.85±0.09 mm. These values were used to approximately determine where to analyse damage onset in the FE analyses.

The experimental curves of force versus displacement show a damping effect along the displacement data (x-axis). This effect occurs because of the impact fixtures (impactor head, weight and metal supports) vibrates during the test. In consequence, experimental curves were smoothed by using an Matlab function. It was employed in order to reduce the experimental damping data and capable to compare with the finite element data in a easier way. The employed function required to a span factor of 0.2 and 'rloess' method to smooth experimental data according to the FEM numerical curves.

Regarding to the finite element data, the three material definition curves of the three failure criteria shows also small damping; This is because of mass concentration in one point (reference point) of the impactor during the finite element analysis.

The finite element curves (in colours purple, light blue and red) were plotted by defining the material lineal mechanical properties without material degradation. These curves modelled the force versus displacement evolution of the impact test up to the damage onset. After this point, they separated each other from the two smoothed experimental curves, which carried out the evolution with the material degradation caused over the tested specimens.

Figure 5.6 shows the semi-cylindrical specimen employed in the impact test and

the failures caused during the test.

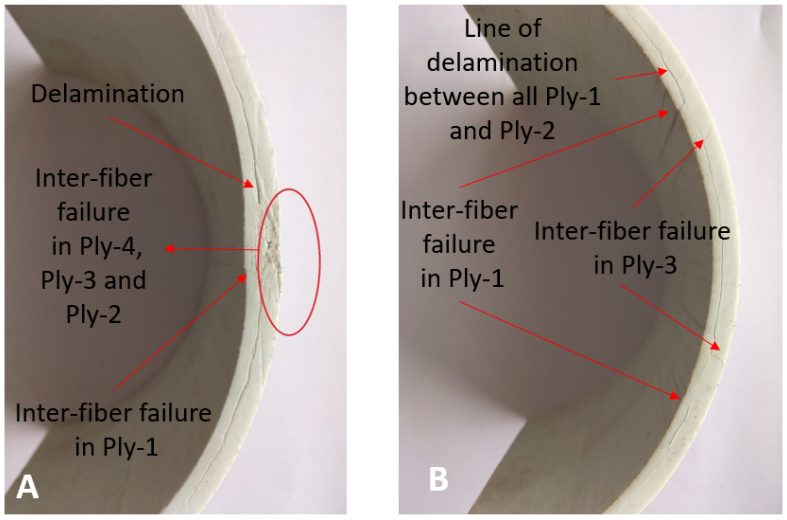

Figure 5.6 *(a) Impact region failures (Cross section of specimen); (b) Zone B (constrained region) failures (Front view of specimen).*

Figure 5.6-A shows specimen cut transversally by the half to show the damages through the impact region in the stacking direction. Inter fiber failure with a fracture plane angle in several directions took place in the ply 3. The ply 1 presented a few inter fiber failures, which are caused in a fracture plane parallel to the stacking direction. Delamination occurs between ply 3 and ply 1 by separating the impact region between two damaged zones as typical case of low velocity impact [62]. The closest ply to the first impact, presents a most quantity of failure due to the absorbed impact energy, while the farthest plies have a less quantity of failure.
Figure 5.6-B shows the failure occurred in the fixed region by the metal supports (boundary conditions). The failure is not so concentrated than in the impact region but both inter fiber failure and delamination thrive. ply 1 and ply 3 show the inter fiber failures with a fracture plane parallel to the stacking direction. Delamination takes places between ply 1 and ply 3.

5.2 Damage onset analyses of the different criteria

After determining failures and their modes into the different regions and plies of the specimen, finite element analysis results were simulated and compared with the experimental ones. Since two kind of experimental tests were made, two different simulations were carried out, first tensile test and then impact test.
The damage over the specimen was represented by the solution-dependent state variables outputs (SDVs) as failure indexes in Abaqus through UMAT/VUMAT

subroutines. The SDVs were analyzed in each element of the finite element model. SDVs were named with different numbers for each failure mode.
Hashin and Puck criteria failure modes are fiber failure (FF) and inter fiber failure (IFF). IFF mode takes places on a fracture plane, which depends on normal stress to the plane and two shear stresses on the plane (axial and transverse to the fiber direction). The fracture plane has an orientation with respect to the thickness direction axis [34, 10].
Cuntze criterion failure modes are based on two fiber failure (tension and compression), three inter fiber failure modes and a final effort mode as accumulated damage. IFF1 and IFF2 modes represent the fracture plane due to the two principal tension and compression transverse stresses in the parallel direction to the fiber, respectively. IFF3 mode represents the fracture plane angled with respect to the fiber direction as a result of the two principal compression transverse stresses [16].
For the tensile case, Abaqus employed SDV1 and SDV2 as fiber and inter fiber failure indexes for both Hashin and Puck failure criteria. The Cuntze criterion FF, IFF1, IFF2 and IFF3 modes are fixed as SDV2, SDV3, SDV4 and SDV5, respectively.
For the impact case, Abaqus used SDV7 and SDV8 as fiber and inter fiber failure indexes for both Hashin and Puck failure criteria. The Cuntze criterion FF, IFF1, IFF2 and IFF3 modes are fixed as SDV7, SDV8, SDV9 and SDV10, respectively. The final Cuntze variable (Effort), which determines the contribution and interaction of each failure mode, is fixed as SDV11. Effort variable will be used to study the overall failure level, between criteria, at 1 mm of longitudinal displacement and impactor displacement for the tensile and impact case, respectively. The correlation between the solution-dependent state variables with the failure modes of each criterion is shown in the tables 5.1 and 5.2.

Failure criterion	Fiber Failure (FF)	Inter-fiber failure (IFF)	Effort
Hashin	SDV1	SDV2	–
Puck	SDV1	SDV2	–
Cuntze	SDV2	SDV3, SDV4 and SDV5	SDV1

Table 5.1 *Solution-dependent state variables for the tensile case.*

Failure criterion	Fiber Failure (FF)	Inter-fiber failure (IFF)	Effort
Hashin	SDV7	SDV8	–
Puck	SDV7	SDV8	–
Cuntze	SDV7	SDV8, SDV9 and SDV10	SDV11

Table 5.2 *Solution-dependent state variables for the impact case.*

The ply 4 (Non-woven fabric material) covers the external structure of the original composite part. Its main function is not related to mechanical behaviour of the specimen and thus, the initiation of damage will not be studied on that ply for both tensile and impact case.

TENSILE CASE

In order to simplify the analysis, the tensile test specimen was divided into three regions, as shown in figure 5.7. The regions are zone A or critical area (region between free and constrained areas), zone B (constrained area by boundary conditions) and zone C (free area).

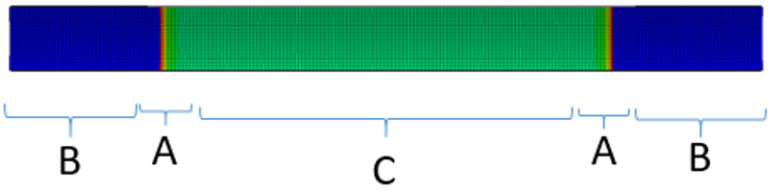

Figure 5.7 *Ply areas for the tensile case; Zones A correlate with area of joint between free and fixed regions; Zones B correlate with constrained areas; Zone C correlates with the free area.*

Figure 5.8 shows the damage onset points of the experimental test and the three ones reached by the three selected criteria over the finite element curve, force versus displacement.

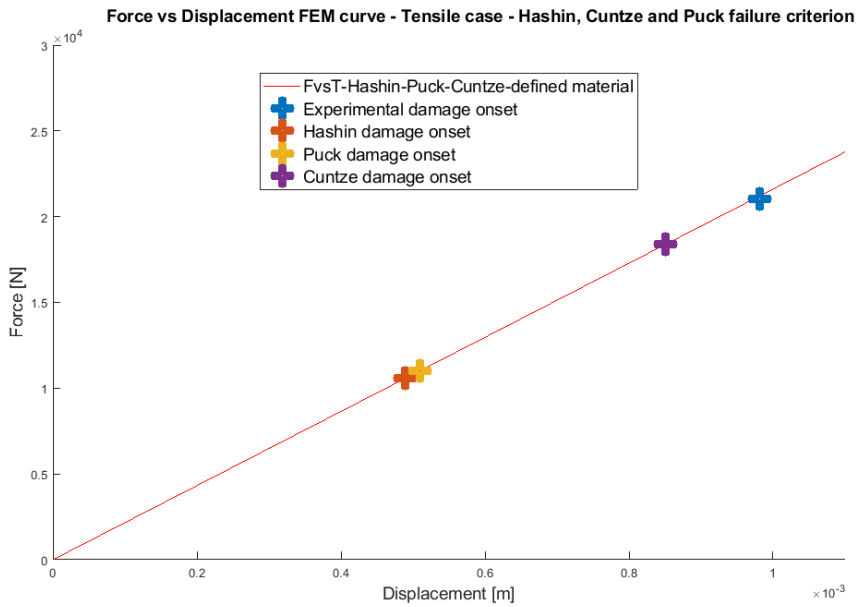

Figure 5.8 *Force versus displacement FEM curve for the selected failure criteria; Experimental damage onset; Hashin damage onset; Puck damage onset; Cuntze damage onset.*

The curve in figure 5.8 allows to know when does the damage occurs in the three criteria and when is it identified in to the experimental tests. For that, the curves of figures 5.9, 5.10 and 5.11 together with the curve of the figure 5.8 are used and compared to determine the damage onsets of the three criteria. Figures 5.9, 5.10 and 5.11 show the failure indexes distribution over each ply when SDVs reach 1.

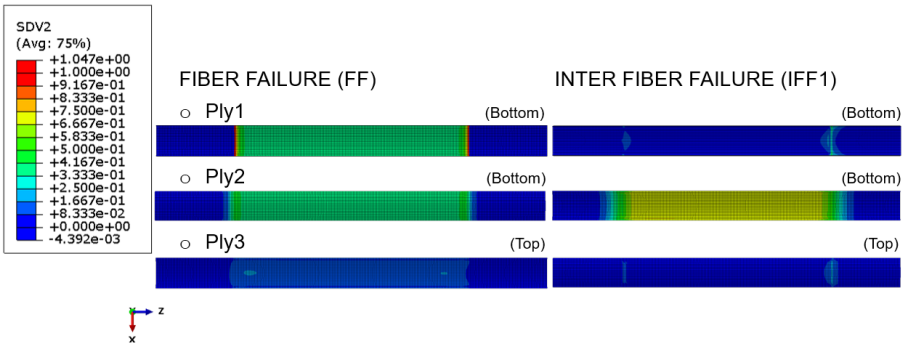

Figure 5.9 *Damage onset indexes of Hashin failure criterion.*

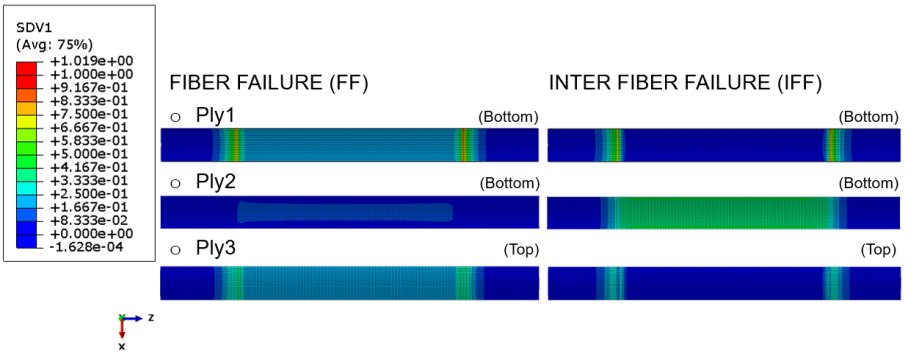

Figure 5.10 *Damage onset indexes of Puck failure criterion.*

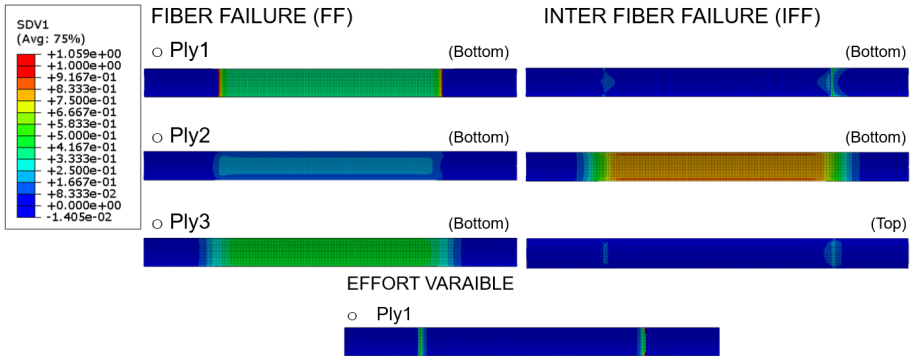

Figure 5.11 *Damage onset indexes of Cuntze failure criterion.*

Hashin damage onset took places at the lowest displacement of the specimen and then Cuntze and Puck failure criteria. Hashin criterion SDV (SDV1) was over the value one at a load of 10784.7 N and a displacement of 0.49 mm as fiber failure in the bottom part of the ply 1, as shown in figures 5.9 and 5.8. The Puck onset damage was reached at a load of 11223.3 N and a displacement of 0.51 mm as inter-fiber failure (SDV2) in the bottom part of the ply 1, as shown in figures 5.10 and 5.2. In the same way, Cuntze onset damage is reached at a load of 21050 N and a displacement of 0.85 mm in its effort variable (SDV1) in the bottom part of the ply 1, as shown in figures 5.11 and 5.8.

Hashin failure criterion demonstrated to be the one that predicted the furthest damage onset from the experimental value at the lowest displacement of the specimen. The second position was ranked by Puck failure criterion and finally, Cuntze failure criterion constituted the closest criterion to the experimental damage onset. Cuntze criterion achieved first failure at the highest displacement of the specimen. It is almost double of the one applied for the Hashin criterion.

With the objective of determining which criterion has the highest failure indexes for a fixed level of applied load, figures 5.12, 5.13 and 5.14 show a second numerical analysis that was carried out by applying one displacement in the longitudinal direction of 1 mm to the specimen. In this analysis, failure modes, failure absolute

and relative indexes and zones where the damage takes place will be assessed.

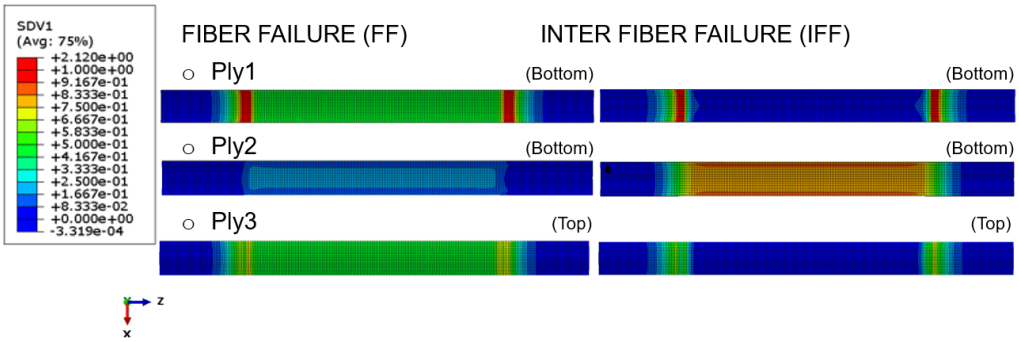

Figure 5.12 *Hashin failure criterion indexes (FF and IFF) at 1mm of displacement in longitudinal direction.*

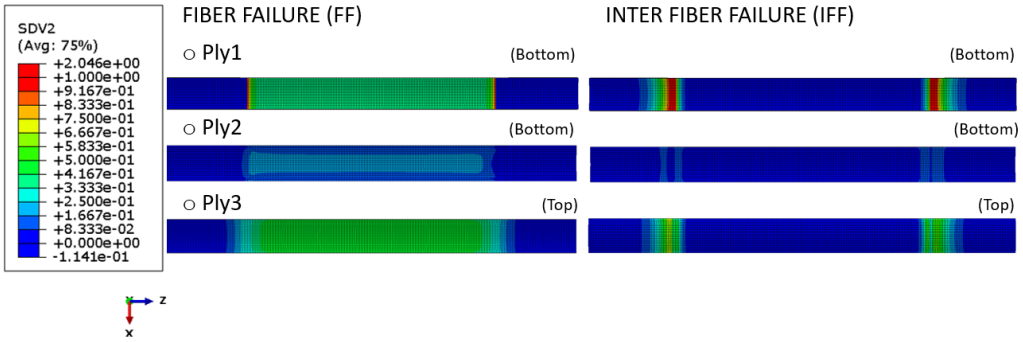

Figure 5.13 *Puck failure criterion indexes (FF and IFF) at 1mm of displacement in longitudinal direction.*

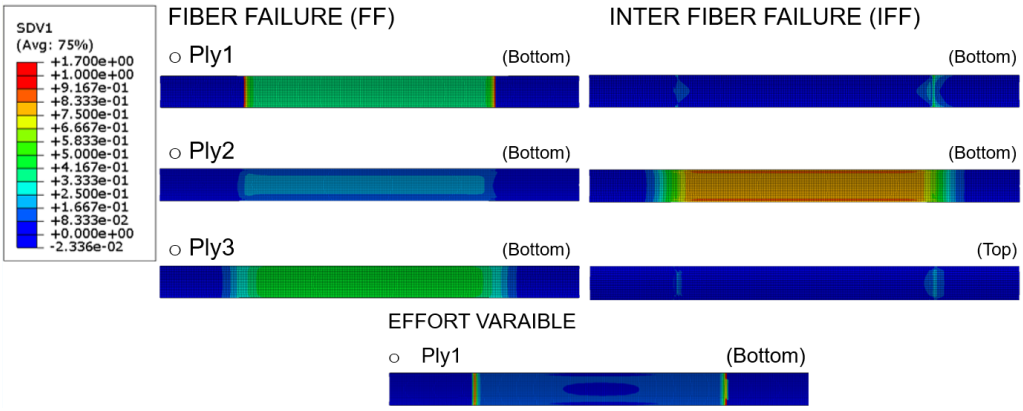

Figure 5.14 *Cuntze failure criterion indexes (Effort, FF and IFF) at 1mm of displacement in longitudinal direction.*

Hashin criterion had one failure maximum absolute index (SDV1=2.12) as FF and one relative maximum index (SDV2=2.069) as IFF in the same area than Cuntze and Puck, as shown in figure 5.12. Puck criterion reached its maximum absolute

failure index (SDV8=2.046) as IFF and one relative maximum index (SDV7=1.2) as FF in the ply 1 zone A, as shown in figure 5.13. The Cuntze criterion reached its maximum absolute failure index (SDV1=1.7) with the effort variable and its maximum relative index (SDV2=1.2) as fiber failure in the critical area of the ply 1, as shown in figure 5.14.

For the FF mode, ply 1 got the highest failure value on the area A. The ply 2 had the lowest value of failure in the central part (area C) of the all specimen, and their fibers were not so stressed than fibers of ply 1 and ply 3. ply 3 fibers were arranged in the same direction as ply 1, but its failure indexes are lower in the critical area (zone A).

For the IFF mode, failure occurred in each ply in different ways. ply 1 got the damage onset in the critical area under Hashin and Puck criteria. ply 2 failure indexes had its maximum value in the zone C bottom area for Hashin and Cuntze criteria. Puck criterion set its maximum damage in the critical area with a value close to zero. The Hashin and Puck authors coincided in both failure indexes and places (critical area top area) for the ply 3. On the other hand, ply 3 fibers have the same orientation angle than the ply 1 with respect to the longitudinal direction, but its failure indexes are different in the zone A. This is because of stacking sequence of the specimen and the ply 2 which can better support the transversal compression stresses (global coordinate system).

Figures 5.12, 5.13 and 5.14 demonstrated that Cuntze Effort variable value (SDV1) reached the highest failure index again inter fiber failure index (SDV2) of Puck criterion and fiber failure index (SDV1) of Hashin criterion. In the same way, the results show that Cuntze criterion is the most accurate criterion in predicting the damage onset for the tensile case. It is followed by Puck criterion and Hashin criterion.

It is important to point out that the first analysed damage over the specimen is in the critical area between the free and constrained regions. That means half of nodes of elements placed in the critical area are constrained (in movement) due to the boundary conditions and the other half of the nodes are free. This implies that the failure indexes obtained by the different criteria could be distorted with a certain percentage. The pressure of end tabs of the tension machine and effect of the boundary conditions might influence the obtained results.

In the most failure tensile tests, the width of the specimen central part is reduced, or a hole is made in the central part to rise the possibilities of failure occurring in the central part of the specimen (afar from the clamped edges). This would allow an assessment of the failure without constrains in the element [66, 27].

IMPACT CASE

The curved specimens have been divided into three relevant regions to simplify the

results discussion like in the tensile case. Figure 5.15 shows the chosen regions, namely zone A or impact area, external top region or zone B (constrained area by boundary conditions) and lateral curved region or zone C.

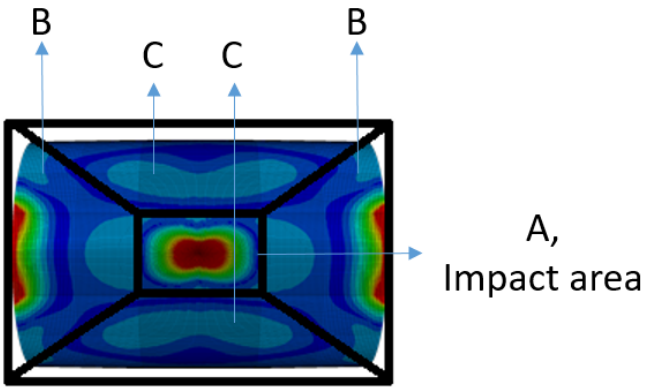

Figure 5.15 *ply areas for the impact case; Zone A or impact area; Zone B or external top region; Zone C or lateral curved region.*

Different results were discussed in the impact area (zone A) at an impactor displacement of 1 mm by considering figure 5.5-A, which is based on the cut-off point from the experimental curve. Then, damage was analysed outside of impact area (zone B and C) at an impactor displacement higher of 2 mm and 5 mm. Figures 5.16, 5.17 and 5.18 show the failure indexes of each criterion and in each ply over the impact region of the semi-cylindrical specimen.

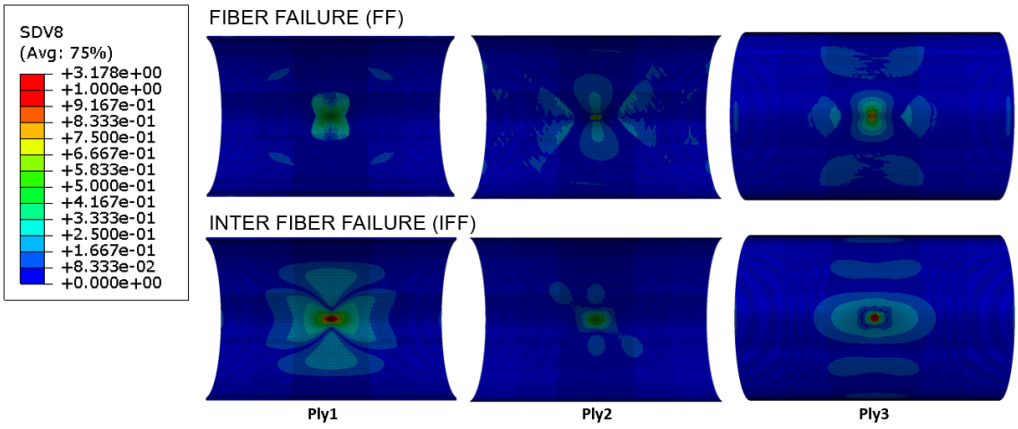

Figure 5.16 *Hashin failure criterion indexes (FF and IFF) at 1mm of displacement in Thickness direction.*

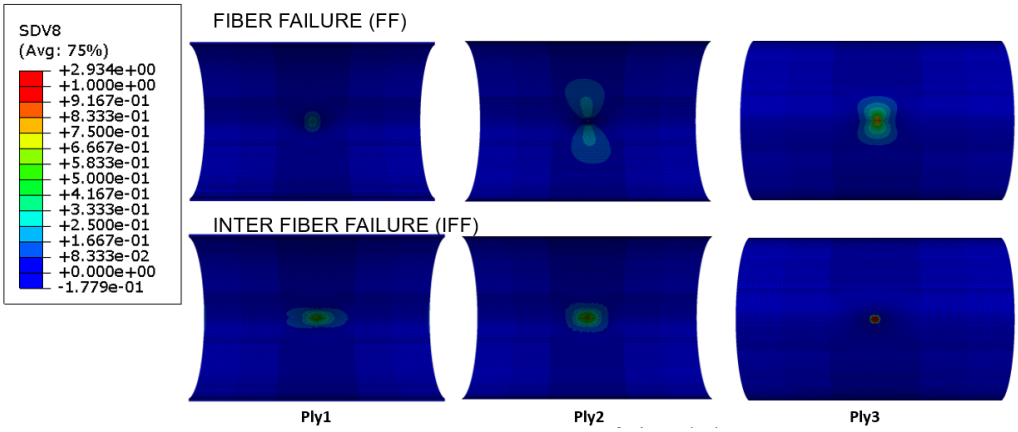

Figure 5.17 *Puck failure criterion indexes (FF and IFF) at 1mm of displacement in Thickness direction.*

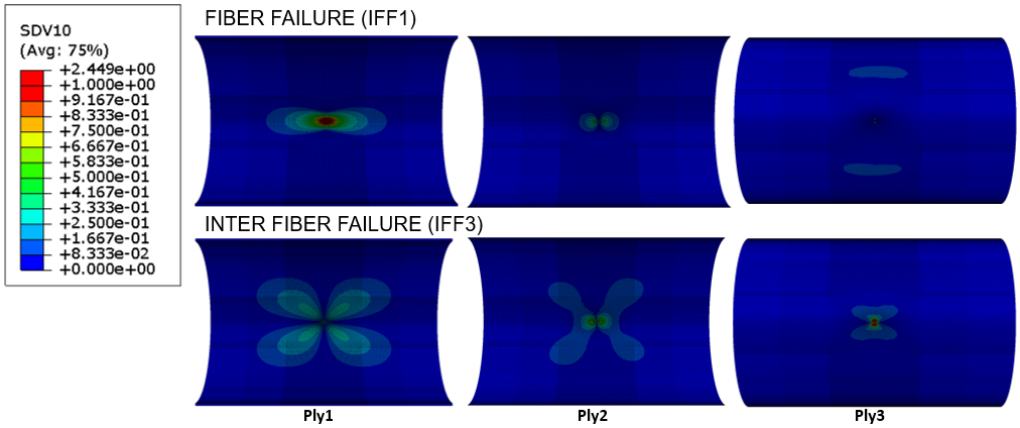

Figure 5.18 *Cuntze failure criterion indexes (IFF1 and IFF3) at 1mm of displacement in Thickness direction.*

Hashin failure criterion reached the maximum failure index (SDV8 = 3.178) on the ply 3 top area as IFF mode (figure 5.16). In the same ply 3 top area, Puck and Cuntze criterion obtained their maximum failure indexes (SDV8 = 2.934 and SDV10 = 2.449) as IFF (figures 5.17 and 5.18). Cuntze IFF is referred to the IFF3, which analyses the damage occurred in a slant fracture plane because of transversal compressive stresses. Therefore, damage is dominated under IFF mode for the impact area due to the compression reactions in plane and in thickness direction of the plies. Hashin criterion obtained the damage at the lowest impactor displacement in the ply 3 top impact area as inter fiber failure. Puck and Cuntze criteria also reached that failure mode over the ply 3 top area. The failures obtained from the impact section (ply 1, ply 2 and ply 3 cut though the thickness direction) of the experimental specimen, shown in 5.6, have been predicted by the three failure criteria. The main difference between them resides in the value of the analysed damage variables.

Cuntze criterion Effort variable is constituted by the sum of all its failure modes; it determines the contribution and the interaction of each mode for total damage. For this reason, the Cuntze Effort parameter can not be compared with the failure modes of Hashin and Puck criteria. Figure 5.19 shows that Cuntze Effort variable reached the maximum total failure index (SDV11 = 16.01) in the ply 3 top area at a displacement of 1 mm.

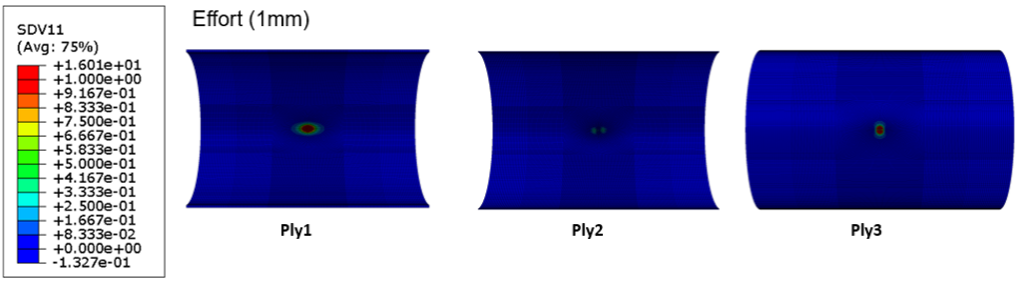

Figure 5.19 *Cuntze Effort variable (Effort) at 1mm of displacement in thickness direction.*

Figure 5.19 showed that Cuntze criterion reached the highest failure index at 1 mm of displacement by taking into account the contribution and interaction between the five Cuntze failure modes in the ply 3 top area. Hashin criterion and then Puck failure criterion followed it. Figure 5.20 shows the three types of Cuntze inter fiber failure modes that occur in the impact region in the thickness direction.

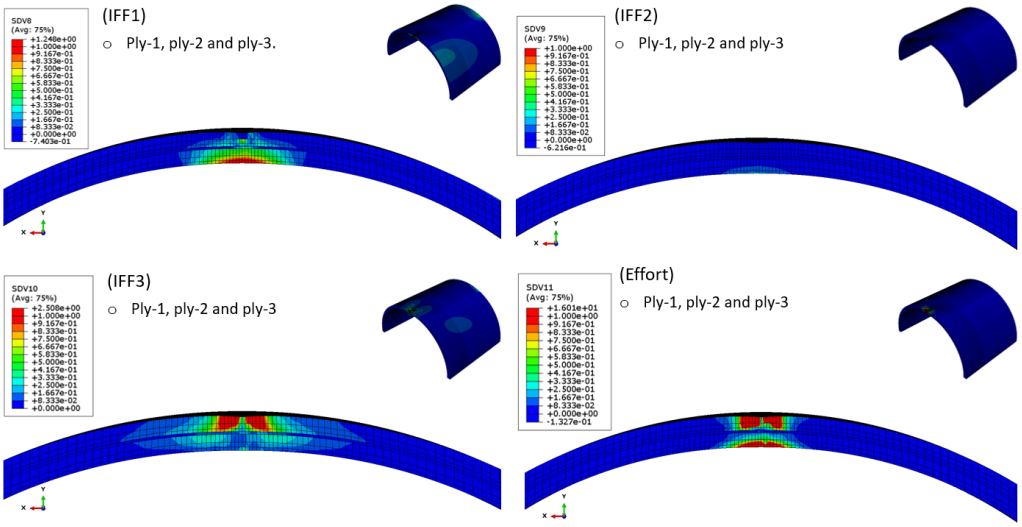

Figure 5.20 *Cuntze Effort and inter fiber failures variables at 1mm of impactor displacement (Front view of specimen cut in half).*

IFF1 and IFF3, which are consequence of transversal tensile stresses, predominate in the this region as the experimental results are shown in figure 5.6. IFF1 mode,

which occurs in the ply 1, reaches failure indexes higher than IFF3 mode, which occurs in the ply 2. Both inter fiber failures modes are represented by the effort variable as sum of them. This kind of failure, in the different mentioned plies, corresponds with low velocity impact case. Therefore, the finite element results predicted the same failures which took place over the real semi-cylindrical specimen (figure 5.6). The IFF2 mode did not predict any damage for the impact area.
In order to show the damage on the constrained regions of the specimen, impactor displacement has been fictitious increased in the specimen well over the damage initiation level. This allows to virtually analyze what would be the next damage points without introducing damage evolution. Thus, analysis of the system at a displacement of 2 and 5 mm is shown here. This allows to assess damage behaviour in regions B and C of the specimen.
Figures 5.22, 5.23 and 5.24 show the impact test at a impactor displacement of 2 mm in the constrained area by the boundary conditions.

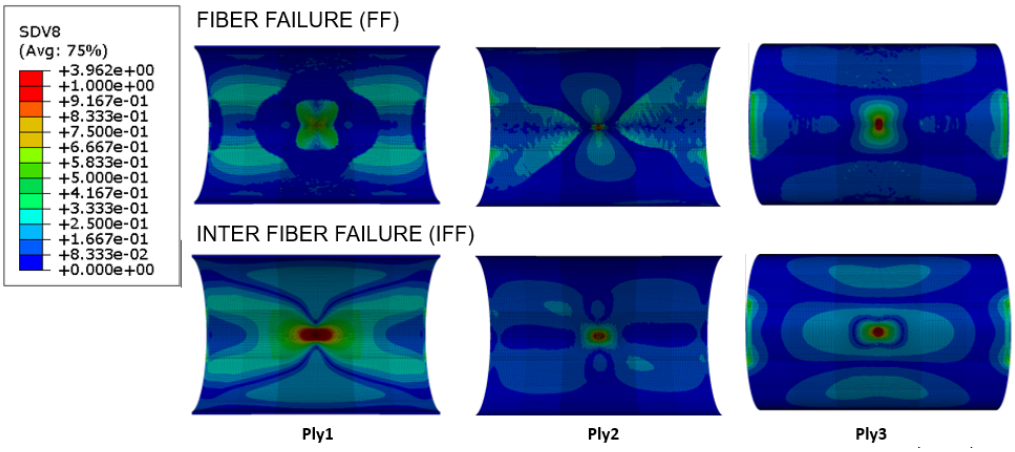

Figure 5.21 *Hashin failure criterion indexes (FF and IFF) at 2mm of displacement in thickness direction.*

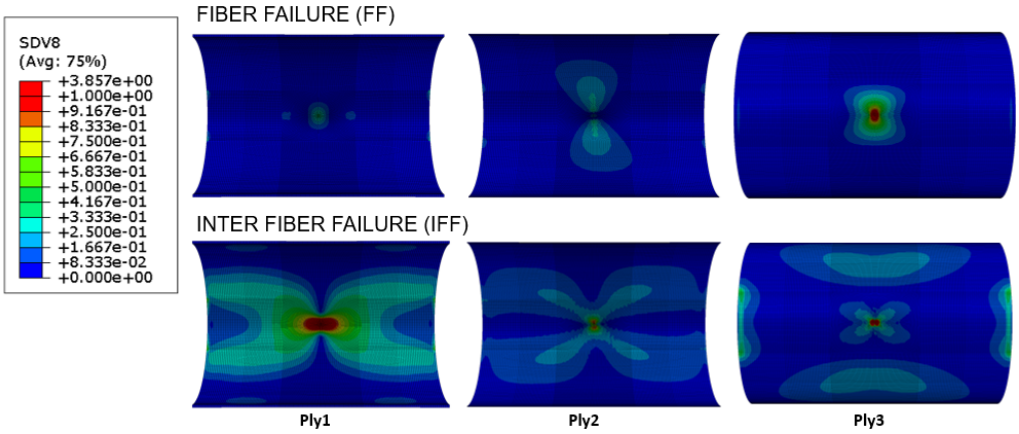

Figure 5.22 *Puck failure criterion indexes (FF and IFF) at 2mm of displacement in thickness direction.*

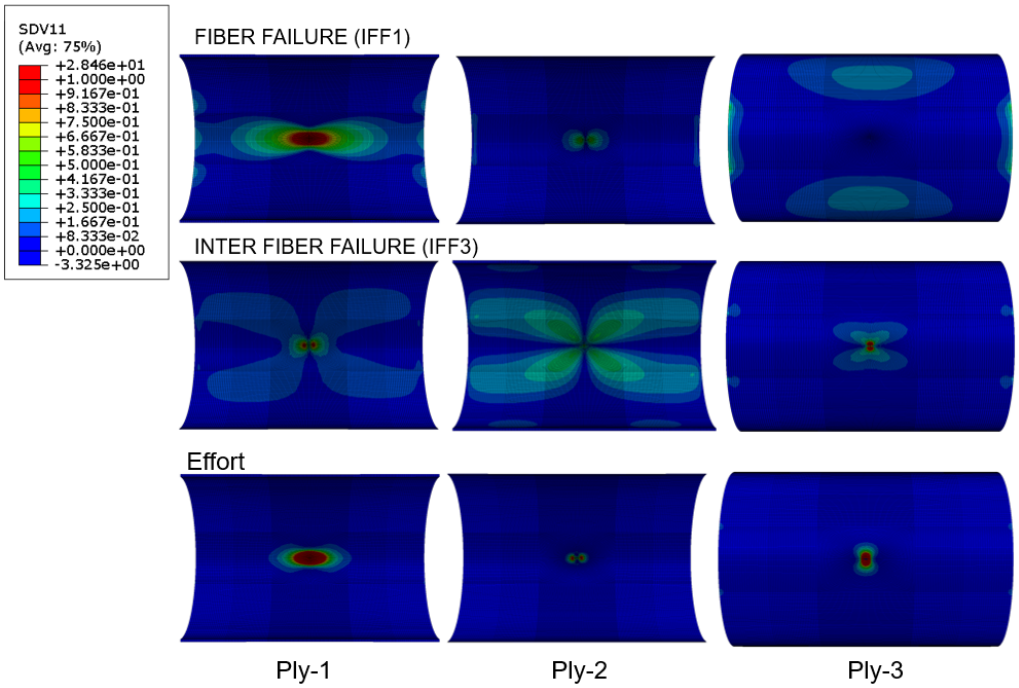

Figure 5.23 *Cuntze failure criterion indexes (Effort, IFF1 and IFF3) at 2mm of displacement in thickness direction.*

Hashin, Puck and Cuntze criteria did not reach any failure outside of impact area, even either in the area where the boundary conditions are applied (bolt/plate attachment). Figures 5.22, 5.23 and 5.24 show the impact test at a impactor displacement of 5 mm in the constrained area by the boundary conditions.

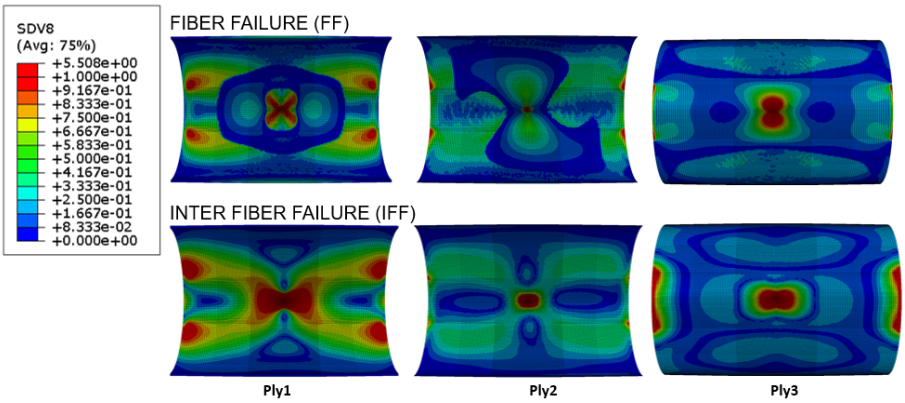

Figure 5.24 *Hashin failure criterion indexes (FF and IFF) at 5mm of displacement in thickness direction.*

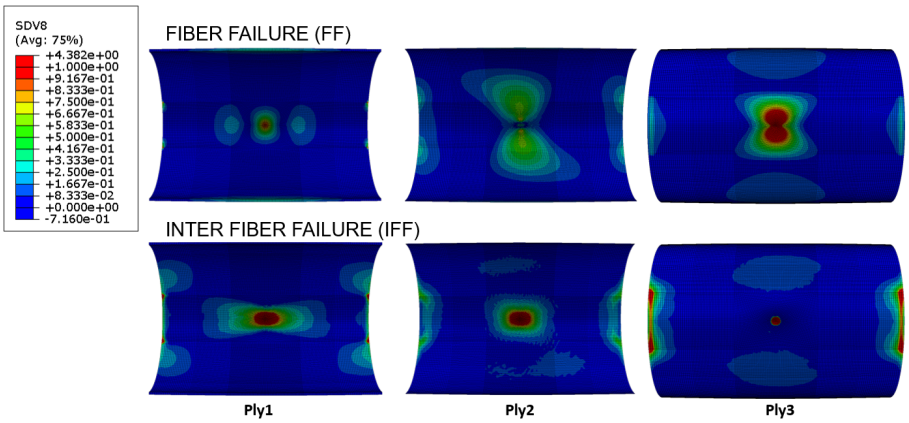

Figure 5.25 *Puck failure criterion indexes (FF and IFF) at 5mm of displacement in thickness direction.*

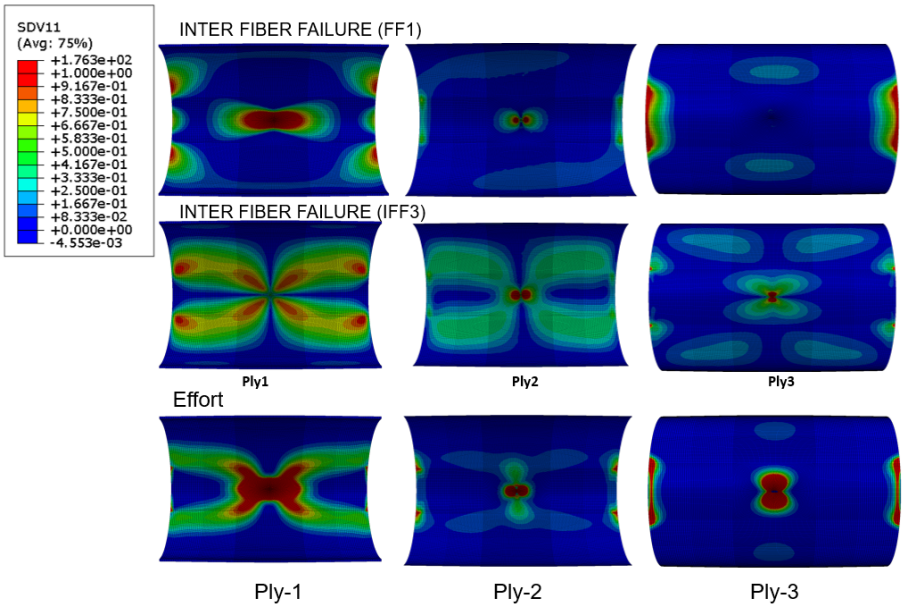

Figure 5.26 *Cuntze failure criterion indexes (Effort, IFF1 and IFF3) at 5mm of displacement in thickness direction.*

Hashin and Cuntze criteria predicted the damage onset failure in the constrained section of ply 3 (maximum failure indexes) and in the ply 1 (maximum relative indexes) as IFF modes. Hashin criterion was only one in predicting damage in the ply 2, even though damage occurred also in both the adjacent plies (ply 1 and ply 3). Figure 5.24 and 5.26 demonstrate that the main difference between Hashin and Cuntze for the inter-fiber failure is the level of failure index in the plies, since Hashin failure indexes are higher than Cuntze ones, as in the tensile case. However, Puck criterion did not predict any IFF neither in the zone B and C (5.25).
The inter fiber failures detected over the post-impacted specimen (figure 5.6) in the constrained area (zone B) through the thickness direction (front view of specimen) have been predicted by Hashin and Cuntze criterion. This inter fiber failure through the three plies was predicted by Cuntze failure with higher failure indexes than Hashin.
It is important to point out that the damage of zone B occurred between free and constrained regions. And thus, the failure indexes obtained with the different criteria could be distorted due to half of element nodes of the meshing are fixed. However, from the implementation point of view of the different criteria, these both analyses (at 2 and 5 mm of impactor displacement) have served to investigate failure onset and its development inside of the semi-cylindrical specimens.

6. CONCLUSIONS

The theory basis from the World Wide Failure Exercise provided the information needed to determine which theories predicted the damage onset for tensile and impact cases. The assessment concluded that Hashin, Puck and Cuntze failure criteria were the best ones to analyse the damage in the two curved specimens, whose principal components are E-Glass/Polyester material and with three uni-directional and structural plies as lay-up.

Two experimental tests were carried out to compare the FE analysis results which allowed to predict the damage onset in the two curved structures. The experimental tensile test achieved successfully to analysis of the correlation between experimental and theoretical material properties in longitudinal direction. Therefore, it allowed to know the initiation of damage and the type of failure modes caused in the tested specimen. The experimental impact test was also developed successfully and the failure in both impact and constraint region allowed to assess the performances of the three selected failure criteria.

The implementation procedure of the three failure criteria was managed through the Abaqus UMAT and VUMAT subroutines. The elastic mechanical properties of the material and the mathematical approaches of the criteria allowed to model both experiments and were used to obtain the results discussed in chapter 5.

For the tensile case, Cuntze failure criterion showed to predict the damage onset in the most accurate way without overtaking the experimental one as a sum of the fiber and inter fiber failures. It occurs at the highest displacement of the specimen and with the lowest failure indexes in the specimen elements. It is followed by first Puck and the Hashin failure criteria as inter fiber failure and fiber failure, respectively. Cuntze criterion is considered to be the least conservative one, since it reached the lowest failure indexes at the same force and displacement in specimen than Puck and Hashin criteria. Unlike Hashin and Cuntze criteria, Puck failure criterion predicted failure indexes with values close to zero or even no damage in any part of ply 2 (fibers oriented at 85°).

For the impact case, Cuntze failure criterion reached the highest failure indexes at a impactor displacement of 1 mm through the effort variable in the impact region. Cuntze criterion predicted failure topology of the low velocity impact case, caused over the three plies of the real specimen impact region, through its three kinds of inter fiber failure modes and the effort variable. This was possible just with Cuntze

criterion, which allowed to analyse the damage in more detail than Hashin and Puck criteria, which instead presented only one inter fiber failure variable. At much lower values than the experimental damage onset (at beginning on the force versus displacement curve), Hashin, Puck and Cuntze failure indexes had values, which went from the highest to lowest ones, respectively. However, Cuntze failure indexes reached the highest values just after the impactor displacement reached 1 mm (just after when the damage onset occurs in the experiments). Hashin and Puck criteria, instead kept their ranking since the Hashin failure indexes were higher than the ones in the Puck criterion.
Outside of the impact area, both Hashin and Cuntze failure criteria detected the inter fiber failures, which took places along of the constrained regions thickness direction, as the post-tested specimen shows. Cuntze criterion predicted failure with higher damage indexes than Hashin criterion. On the other hand, Puck failure criterion did not predict damage in any of plies in the constrained region.

FUTURE TASKS

The analysis of damage onset has allowed to know the mechanic of materials with a specific lay-up and under a loading condition. As it was mentioned before, the analysing of the damage in tensile cases requires of specimen parts which are prone to start cracks for preventing damaged and constrained elements in the meshing. For that, the experimental tensile case would need of a hole or a reduced section in the central part of the curved specimen. This modification would allow to assess the damage in regions of the specimen where the meshing elements would be free of boundary conditions and of high points of stresses. Another important point is the joint of the end tabs with the specimen, since they were pressured in the stacking direction by the tensile machine. Anyway, both the experimental tensile and impact cases would benefit from the use of additional equipment to analyse damage in side the sample, such as X-ray methods for analysing the matrix failure in models. Ultrasound techniques would also be beneficial to detect failure in the whole composite part. Digital Image Correlation could be useful to compare the strain field of the damaged elements in the meshing with the experimental results.
The specimen tested at tensile and impact loads presented the inter laminar failure of delamination, which was not analysed in this thesis. However, this kind of failure will be studied in order to assess the mechanical behaviour of the ply 2 with more precisely, since the delamination occurred between the mentioned ply and the two adjacent ones. In order to predict the experimental force and displacement curves and failure caused after the damage onset, the damage evolution would have to develop and implement through UMAT and VUMAT by degradation of the material (mechanical properties) after the damage onset. This degradation would consist on

reducing progressively the stiffness of the material after this point by means the factors implemented for each criterion in a different way.
The fracture angle of the Puck failure criterion was implemented in this Thesis. However, it would needs of a major development by following the new algorithm developed in [24].

BIBLIOGRAPHY

[1] *Abaqus 6.17 documentation. 3D SIMULIA. Abaqus User Subroutines References Guide.*

[2] M. J. H. A. S. Kaddour, "Challenging lessons from the second world-wide failure exercise (wwfe-ii): Predicting failure in polymer composite laminates under 3d states of stress." *INTERNATIONAL CONFERENCE ON COMPOSITE MATERIALS*, 2013.

[3] J. R. Blacklock and R. M. Richard, "Finite element analysis of inelastic structures." *AIAA Journal*, vol. 7, no. 3, pp. 432–438, mar 1969.

[4] J. P. Boehler and J. Raclin, "Failure criteria for glass-fiber reinforced composites under confining pressure," *Journal of Structural Mechanics*, vol. 13, no. 3-4, pp. 371–393, jan 1985.

[5] T. A. Bogetti, C. P. R. Hoppel, V. M. Harik, J. F. Newill, and B. P. Burns, "Predicting the nonlinear response and progressive failure of composite laminates," *Composites Science and Technology*, vol. 64, no. 3-4, pp. 329–342, mar 2004.

[6] T. A. Bogetti, C. P. Hoppel, V. M. Harik, J. F. Newill, and B. P. Burns, "Predicting the nonlinear response and failure of composite laminates: correlation with experimental results," *Composites Science and Technology*, vol. 64, no. 3-4, pp. 477–485, mar 2004.

[7] T. A. Bogetti, J. Staniszewski, B. P. Burns, C. P. Hoppel, J. W. Gillespie, and J. Tierney, "Predicting the nonlinear response and progressive failure of composite laminates under triaxial loading: Correlation with experimental results," *Journal of Composite Materials*, vol. 47, no. 6-7, pp. 793–804, oct 2012.

[8] T. S. Butalia and W. E. Wolfe, "A strain-energy-based non-linear failure criterion: comparison of numerical predictions and experimental observations for symmetric composite laminates," *Composites Science and Technology*, vol. 62, no. 12-13, pp. 1697–1710, sep 2002.

[9] N. Carrere, F. Laurin, and J.-F. Maire, "Micromechanical-based hybrid mesoscopic 3d approach for non-linear progressive failure analysis of composite structures," *Journal of Composite Materials*, vol. 46, no. 19-20, pp. 2389–2415, sep 2012.

[10] S.-k. K. D.-M. R. J.-M. L. Chi-Seung Lee, Jeong-Hyeon Kim, "Inital and progressive failure analyses for composite laminates using puck failurecriterion and damage-coupled finite element method," *Elservier Ltd*, 2014.

[11] R. M. Christensen, "Mechanics of composite materials," *Mineloa*, 2005.

[12] R. Cuntze, "The predictive capability of failure mode concept-based strength conditions for laminates composed of unidirectional laminae under static triaxial stress states," *Journal of Composite Materials*, vol. 46, no. 19-20, pp. 2563–2594, sep 2012.

[13] R. G. Cuntze, "The predictive capability of failure mode concept-based strength criteria for multi-directional laminates—part b," *Composites Science and Technology*, vol. 64, no. 3-4, pp. 487–516, mar 2004.

[14] ——, "Comparison between experimental and theoretical results using cuntze failure mode concept model for composites under triaxial loadings. part b of the seconf world-wide failure exercise," *Journal of Composite Materials*, vol. 47, no. 6-7, pp. 893–924, aug 2012.

[15] R. G. Cuntze and A. Freund, "The predictive capability of failure mode concept-based strength criteria for multidirectional laminates," *Composites Science and Technology*, vol. 64, no. 3-4, pp. 343–377, mar 2004.

[16] R. Cuntze, "Efficient 3d and 2d failure conditions for UD laminae and their application within the verification of the laminate design," *Composites Science and Technology*, vol. 66, no. 7-8, pp. 1081–1096, jun 2006.

[17] H. M. Deuschle and B.-H. KrÃ¶plin, "Finite element implementation of puck failure theory for fibre-reinforced composites under three-dimensional stress," *Journal of Composite Materials*, vol. 46, no. 19-20, pp. 2485–2513, sep 2012.

[18] H. M. Deuschle and A. Puck, "Application of the puck failure theory for fibre-reinforced composites under three-dimensional stress: Comparison with experimental results," *Journal of Composite Materials*, vol. 47, no. 6-7, pp. 827–846, mar 2013.

[19] M. Deuschle, *3D failure analysis of UD fibre reinforced composites : Puck theory within FEA*, 2010.

[20] ——, "3d failure analysis of ud fibre reinforced composites: Puck theory within fea," Ph.D. dissertation, Institute of Statics and Dynamics of Aerospace Structures Universitat Stuttgart, 2010.

[21] G. Eckold, "Failure criteria for use in the design environment," *Composites Science and Technology*, vol. 62, no. 12-13, pp. 1561–1570, sep 2002.

[22] E. Edge., "Stress-based grantsanders method for predicting failure of composite laminates." *Composites Science and Technology, Elsevier BV,*, 1998.

[23] E. C. Edge, "A comparison of theory and experiment for the stress-based grantsanders method," in *Failure Criteria in Fibre-Reinforced-Polymer Composites*. Elsevier, 2004, pp. 739–769.

[24] L. K. F. H. F.J. Schirmaier, J. Weiland, "A new efficient and reliable algorithm to determine the fracture angle for puck's 3d matrix failure criterion for ud composites," *Elsevier Ltd.*, 2014.

[25] P. Gotsis, "Prediction of composite laminate fracture: micromechanics and progressive fracture," *Composites Science and Technology*, vol. 58, no. 7, pp. 1137–1149, jul 1998.

[26] P. Gotsis, C. Chamis, and L. Minnetyan, "Application of progressive fracture analysis for predicting failure envelopes and stress–strain behaviors of composite laminates: a comparison with experimental results," *Composites Science and Technology*, vol. 62, no. 12-13, pp. 1545–1559, sep 2002.

[27] G. S. H. BENZAAMA, M. MOKHTARI, "Using xfem technique to predict the damage of unidirectional cfrp composite notched under tensile load," *CongrÃ¨s FranÃ§ais de MÃ©canique*, 2017.

[28] S. K. Ha, Y. Huang, H. H. Han, and K. K. Jin, "Micromechanics of failure for ultimate strength predictions of composite laminates," *Journal of Composite Materials*, vol. 44, no. 20, pp. 2347–2361, aug 2010.

[29] A. C. Hansen, E. E. Nelson, and D. J. Kenik, "A comparison of experimental data with multicontinuum failure simulations of composite laminates subjected to tri-axial stresses," *Journal of Composite Materials*, vol. 47, no. 6-7, pp. 805–825, feb 2013.

[30] L. J. Hart-Smith, "Expanding the capabilities of the ten-percent rule for predicting the strength of fibre polymer composites," *Composites Science and Technology*, vol. 62, no. 12-13, pp. 1515–1544, sep 2002.

[31] ——, "Comparison between theories and test data concerning the strength of various fibre-polymer composites," in *Failure Criteria in Fibre-Reinforced-Polymer Composites*. Elsevier, 2004, pp. 770–809.

[32] ——, "Predictions of a generalized maximum-shear-stress failure criterion for certain fibrous composite laminates," *Composite science and Technology*, pp. 219–263, 2004.

[33] L. Hart-Smith, "The truncated maximum strain composite failure model," *Composites*, vol. 24, no. 7, pp. 587–591, oct 1993.

[34] Z. Hashin, "Failure criteria for unidirectional fiber composites," *Journal of Applied Mechanics*, vol. 47, no. 2, p. 329, 1980.

[35] ——, "Fatigue failure critera for unidirectional fiber composites," *Journal of Applied Mechanics*, vol. 48, no. 4, p. 846, 1981.

[36] M. Hinton, P. D. Soden, and A.-S. Kaddour, *Failure Criteria in Fibre Reinforced Polymer Composites: The World-Wide Failure Exercise.* Elsevier Science and Technology Ltd., 2004.

[37] M. J. Hinton and A. S. Kaddour, "The second world-wide failure exercise: Benchmarking of failure criteria under triaxial stresses for fibre-reinforced polymer composites." *QunetiQ Ltd International conference of composite material*, 2007.

[38] M. Hinton, "Failure criteria in fibre reinforced polymer composites: Can any of the predictive theories be trusted ?" *NAFEMS World Congress*, 2011.

[39] O. Hoffman, "The brittle strength of orthotropic materials," *Journal of Composite Materials*, vol. 1, no. 2, pp. 200–206, apr 1967.

[40] Y. Huang, C. Jin, and S. K. Ha, "Strength prediction of triaxially loaded composites using a progressive damage model based on micromechanics of failure," *Journal of Composite Materials*, vol. 47, no. 6-7, pp. 777–792, sep 2012.

[41] Y. Huang, L. Xu, and S. K. Ha, "Prediction of three-dimensional composite laminate response using micromechanics of failure," *Journal of Composite Materials*, vol. 46, no. 19-20, pp. 2431–2442, jun 2012.

[42] Z.-M. Huang, "Correlation of the bridging model predictions of the biaxial failure strengths of fibrous laminates with experiments," *Composites Science and Technology*, vol. 64, no. 3-4, pp. 529–548, mar 2004.

[43] A. C. H. J. Steven Mayes, "Composite laminate failure analysis using multicontinuum theory," in *Failure Criteria in Fibre-Reinforced-Polymer Composites.* Elsevier, 2004, pp. 490–517.

[44] K.-K. Jin, Y. Huang, Y.-H. Lee, and S. K. Ha, "Distribution of micro stresses and interfacial tractions in unidirectional composites," *Journal of Composite Materials*, vol. 42, no. 18, pp. 1825–1849, jul 2008.

[45] A. Kaddour and M. Hinton, "Maturity of 3d failure criteria for fibre-reinforced composites: Comparison between theories and experiments: Part b of WWFE-II," *Journal of Composite Materials*, vol. 47, no. 6-7, pp. 925–966, mar 2013.

[46] A. K. Kaw, *Mechanics of Composite Materials*, Second, Ed. Taylor and Francis Group, LLC, 2006.

[47] G. Kress, "Examination of hashin's failure criteria for part b of the second world-wide failure exercise: Comparison with test data," *Journal of Composite Materials*, vol. 47, no. 6-7, pp. 867–891, sep 2012.

[48] E. M. Krokosky, "Fundamental aspects of fiber reinforced plastic composites, edited by r. t. schwartz and h. s. schwartz, interscience publishers." *Journal of Polymer Science Part B: Polymer Letters*, vol. 8, no. 1, pp. 55–56, jan 1970.

[49] K. Liu, "A progressive quadratic failure criterion for a laminate," *Composites Science and Technology*, vol. 58, no. 7, pp. 1023–1032, jul 1998.

[50] J. S. Mayes and A. C. Hansen, "A comparison of multicontinuum theory based failure simulation with experimental results," in *Failure Criteria in Fibre-Reinforced-Polymer Composites*. Elsevier, 2004, pp. 1026–1044.

[51] L. McCartney, "Prediction of ply crack formation and failure in laminates," *Composites Science and Technology*, vol. 62, no. 12-13, pp. 1619–1631, sep 2002.

[52] E. E. Nelson, A. C. Hansen, and J. S. Mayes, "Failure analysis of composite laminates subjected to hydrostatic stresses: A multicontinuum approach," *Journal of Composite Materials*, vol. 46, no. 19-20, pp. 2461–2483, jun 2012.

[53] S. Pinho, R. Darvizeh, P. Robinson, C. Schuecker, and P. Camanho, "Material and structural response of polymer-matrix fibre-reinforced composites," *Journal of Composite Materials*, vol. 46, no. 19-20, pp. 2313–2341, sep 2012.

[54] S. Pinho, G. Vyas, and P. Robinson, "Material and structural response of polymer-matrix fibre-reinforced composites: Part b," *Journal of Composite Materials*, vol. 47, no. 6-7, pp. 679–696, feb 2013.

[55] A. Puck and H. Schurmann, "Failure analysis of FRP laminates by means of physically based phenomenological models," *Composites Science and Technology*, vol. 62, no. 12-13, pp. 1633–1662, sep 2002.

[56] ——, "Failure analysis of frp laminates by means of physically based phenomenological models," in *Failure Criteria in Fibre-Reinforced-Polymer Composites*. Elsevier, 2004, pp. 832–876.

[57] A. Puck and H. M. Deuschle., "Progress in the puck failure theory for fibre reinforced composites: Analytical solutions for 3d-stress."

[58] K. Reifsnider, G. Sendeckyj, S. Wang, W. Johnson, W. Stinchcomb, N. Pagano, and M. Nahas, "Survey of failure and post-failure theories of laminated fiber-renforced composites," *Journal of Composites Technology and Research*, vol. 8, no. 4, p. 138, 1986.

[59] A. Rotem, "3d Rotem failure criterion for fibrous laminated composite materials: Comparison with experiments," *Journal of Composite Materials*, vol. 47, no. 6-7, pp. 733–741, aug 2012.

[60] ——, "The rotem failure criterion for fibrous laminated composite materials: Three-dimensional loading case." *Journal of Composite Materials*, vol. 46, no. 19-20, pp. 2379–2388, Jun. 2012.

[61] G. P. Sendeckyj, Ed., *Mechanics of Composite Materials: Volume 2*. Academic Press, 1974. [Online]. Available: https://www.amazon.com/Mechanics-Composite-Materials-G-Sendeckyj/dp/0121365026?SubscriptionId=AKIAIOBINVZYXZQZ2U3A&tag=chimbori05-20&linkCode=xm2&camp=2025&creative=165953&creativeASIN=0121365026

[62] Y. Shi, T. Swait, and C. Soutis, "Modelling damage evolution in composite laminates subjected to low velocity impact," *Composite Structures*, vol. 94, no. 9, pp. 2902–2913, sep 2012.

[63] C. Sun, J. Tao, and A. Kaddour, "The prediction of failure envelopes and stress/strain behavior of composite laminates: comparison with experimental results," *Composites Science and Technology*, vol. 62, no. 12-13, pp. 1673–1682, sep 2002.

[64] S. W. Tsai and E. M. Wu, "A general theory of strength for anisotropic materials," *Journal of Composite Materials*, vol. 5, no. 1, pp. 58–80, jan 1971.

[65] J. R. Vinson and R. L. Sierakowski, Eds., *The Behavior Of Structures Composed Of Composite Materials*. Springer Netherlands, 2002.

[66] Y. Wang, M. Tong, and S. Zhu, "Three dimensional continuum damage mechanics model of progressive failure analysis in fibre-reinforced composite laminates," in *50th AIAA/ASME/ASCE/AHS/ASC Structures, Structural Dynamics, and*

Materials Conference. American Institute of Aeronautics and Astronautics, may 2009.

[67] W. Wolfe, "A strain-energy based failure criterion for non-linear analysis of composite laminates subjected to biaxial loading," *Composites Science and Technology*, vol. 58, no. 7, pp. 1107–1124, jul 1998.

[68] J. Ye and D. Zhang, "Prediction of failure envelopes and stress–strain curves of fiber composite laminates under triaxial loads," *Journal of Composite Materials*, vol. 46, no. 19-20, pp. 2417–2430, jun 2012.

[69] B. Zand, T. S. Butalia, W. E. Wolfe, and G. A. Schoeppner, "A strain energy based failure criterion for nonlinear analysis of composite laminates subjected to triaxial loading," *Journal of Composite Materials*, vol. 46, no. 19-20, pp. 2515–2537, sep 2012.

[70] D. Zhang, L. Xu, and J. Ye, "Prediction of failure envelopes and stress–strain curves of fiber composite laminates under triaxial loads: Comparison with experimental results," *Journal of Composite Materials*, vol. 47, no. 6-7, pp. 763–776, mar 2013.

[71] P. A. Zinoviev, S. V. Grigoriev, O. V. Lebedeva, and L. P. Tairova, "The strength of multilayered composites under a plane-stress state," *Composites Science and Technology*, vol. 58, no. 7, pp. 1209 – 1223, 1998.

[72] P. A. Zinoviev, O. V. Lebedeva, and L. P. Tairova, "A coupled analysis of experimental and theoretical results on the deformation and failure of composite laminates under a state of plane stress," *Composites Science and Technology*, vol. 62, no. 12-13, pp. 1711–1723, sep 2002.

A. APPENDIX

This section shows the FORTRAN codes of the three selected failure criteria in order to predict the damage onset of the employed specimens at uniaxial tensile load (UMAT subroutine) and impact load (VUMAT subroutine). The codes contain the definition of the material lineal mechanical properties and its limit stresses shown in section 4.1, and the implementation of the criteria mathematical approaches studied in section 4.4.

A.1 UMAT subroutine codes

The user subroutine UMAT allows implementing the failure criteria under static loading conditions. This subroutine can be written in FORTRAN code, which is attached in the finite element software Abaqus. The mechanical constitutive behaviour of the material is defined through the Jacobian matrix ($\partial \triangle \sigma / \partial \triangle \varepsilon$) and the SDVs and stresses are updated at the end of the increment [1].

Hashin failure criterion

```
c ——————— SUBROUTINE UMAT OF HASHIN FAILURE CRITERION ———————
      subroutine UMAT(STRESS,STATEV,DDSDDE,SSE,SPD,SCD,
     1 RPL,DDSDDT,DRPLDE,DRPLDT,
     2 STRAN,DSTRAN,TIME,DTIME,TEMP,DTEMP,PREDEF,DPRED,CMNAME,
     3 NDI,NSHR,NTENS,NSTATV,PROPS,NPROPS,COORDS,DROT,PNEWDT,
     4 CELENT,DFGRD0,DFGRD1,NOEL,NPT,LAYER,KSPT,JSTEP,KINC)
c
      INCLUDE 'ABA_PARAM.INC'
c
      CHARACTER*80 CMNAME
      DIMENSION STRESS(NTENS),STATEV(NSTATV),
     1 DDSDDE(NTENS,NTENS),DDSDDT(NTENS),DRPLDE(NTENS),
     2 STRAN(NTENS),DSTRAN(NTENS),TIME(2),PREDEF(1),DPRED(1),
     3 PROPS(NPROPS),COORDS(3),DROT(3,3),DFGRD0(3,3),DFGRD1(3,3),
     4 JSTEP(4)
c ——————— DEFINITION OF MATERIAL LINEAL MECHANICAL PROPERTIES
c           AND LIMIT STRESSES ———————
      PARAMETER(ONE=1.0D0,TWO=2.0D0,THREE=3.0D0,FOUR=4.0D0)
          E1=PROPS(1)
```

```
      E2=PROPS(2)
      E3=PROPS(3)
        ANNU12=PROPS(4)
      ANNU13=PROPS(5)
      ANNU23=PROPS(6)
      G12=PROPS(7)
      G23=PROPS(8)
      G31=PROPS(9)
      Xt= PROPS(10)
      Xc= PROPS(11)
      Yt= PROPS(12)
      Yc= PROPS(13)
      Zt= PROPS(14)
      Zc= PROPS(15)
      Sxy= PROPS(16)
      Sxz= PROPS(17)
      Syz= PROPS(18)
      ANNU21=(E2/E1)*ANNU12
      ANNU31=(E3/E1)*ANNU13
      ANNU32=(E3/E2)*ANNU23
      S=1-ANNU12*ANNU21-ANNU23*ANNU32-ANNU13*ANNU31
     & -TWO*ANNU21*ANNU32*ANNU13
c ------- Stiffness matrix of material -------
          DO I=1,NTENS
            DO J=1,NTENS
            DDSDDE(I,J)=0.0D0
            ENDDO
          ENDDO
              DDSDDE(1,1)=((1-ANNU23*ANNU32)*E1)/S
              DDSDDE(2,2)=((1-ANNU13*ANNU31)*E2)/S
              DDSDDE(3,3)=((1-ANNU12*ANNU21)*E3)/S
              DDSDDE(4,4)=G12
              DDSDDE(5,5)=G23
              DDSDDE(6,6)=G31
              DDSDDE(1,2)=((ANNU21+ANNU31*ANNU23)*E1)/S
              DDSDDE(1,3)=((ANNU31+ANNU21*ANNU32)*E1)/S
              DDSDDE(2,3)=((ANNU32+ANNU31*ANNU12)*E2)/S
              DDSDDE(2,1)=((ANNU21+ANNU31*ANNU23)*E1)/S
              DDSDDE(3,1)=((ANNU31+ANNU21*ANNU32)*E1)/S
              DDSDDE(3,2)=((ANNU32+ANNU31*ANNU12)*E2)/S
c ------- Vector of stress -------
          DO I=1,NTENS
              DO J=1,NTENS
              STRESS(I) = STRESS(I) + DDSDDE(I,J)*DSTRAN(J)
              ENDDO
          ENDDO
c ------- IMPLEMENTATION OF DAMAGE INITIATION CRITERIA -------
```

```
c ------- 3D Hashin Failure Criterion in quadratic stress -------
c ------- Fiber tension or compression failure mode ------------
            IF (STRESS(1) .GT. 0.0D0) THEN
              F_f = SQRT((STRESS(1)/Xt)**2 +
     &       (STRESS(4)**2 + STRESS(5)**2)/(Sxy)**2
     &           )
            ELSEIF (STRESS(1) .LT. 0.0D0) THEN
              F_f = SQRT((STRESS(1)/Xc)**2)
            ENDIF
            STATEV(1) = F_f
c ------- Inter-fiber tension or compresion failure mode -------
            IF ((STRESS(2) + STRESS(3)) .GT. 0.0D0) THEN
       F_m= SQRT((STRESS(2)+STRESS(3))**2/(Yt**2) -
     &  (STRESS(2)*STRESS(3))/(Syz)**2 + (STRESS(4))**2/(Syz)**2 +
     & (STRESS(5))**2/(Sxy)**2 + (STRESS(6))**2/(Sxy)**2
     &           )
            ELSEIF ((STRESS(2) + STRESS(3)) .LT. 0.0D0) THEN
       F_m = SQRT( (STRESS(2)+STRESS(3))**2 / (FOUR*(Syz)**2) +
     & (abs((STRESS(2)+STRESS(3)))/Yc)*((Yc/(TWO*Syz))**2 - 1) -
     & abs(STRESS(2)*STRESS(3))/(Syz)**2 + (STRESS(4))**2/(Syz)**2  +
     & (STRESS(5))**2/(Sxy)**2 + (STRESS(6))**2/(Sxy)**2
     &           )
            ENDIF
       STATEV(2) = F_m
c
        RETURN
       END
```

Puck failure criterion

```
c ------- SUBROUTINE UMAT OF PUCK FAILURE CRITERION -------
       subroutine UMAT(STRESS,STATEV,DDSDDE,SSE,SPD,SCD,
     1 RPL,DDSDDT,DRPLDE,DRPLDT,
     2 STRAN,DSTRAN,TIME,DTIME,TEMP,DTEMP,PREDEF,DPRED,CMNAME,
     3 NDI,NSHR,NTENS,NSTATV,PROPS,NPROPS,COORDS,DROT,PNEWDT,
     4 CELENT,DFGRD0,DFGRD1,NOEL,NPT,LAYER,KSPT,JSTEP,KINC)
c
       INCLUDE 'ABA_PARAM.INC'
c
       CHARACTER*80 CMNAME
       DIMENSION STRESS(NTENS),STATEV(NSTATV),
     1 DDSDDE(NTENS,NTENS),DDSDDT(NTENS),DRPLDE(NTENS),
     2 STRAN(NTENS),DSTRAN(NTENS),TIME(2),PREDEF(1),DPRED(1),
     3 PROPS(NPROPS),COORDS(3),DROT(3,3),DFGRD0(3,3),DFGRD1(3,3),
     4 JSTEP(4)
c ------- DEFINITION OF LINEAL MECHANICAL PROPERTIES
c         AND LIMIT STRESSES -------
       REAL M, o, p, L
```

```
      DIMENSION an(32), sigman(32), taunt(32), taun1(32),
     &  cose2(32), sine2(32), a(32), b(32), FE(32)
      PARAMETER(ONE=1.0D0,TWO=2.0D0,THREE=3.0D0,FOUR=4.0D0)
       an =(/-1.5708d0,-1.4708d0,-1.3708d0,-1.2708d0,-1.1708d0,
     & -1.0708d0,-0.9708d0,-0.8708d0,-0.7708d0,-0.6708d0,
     & -0.5708d0,-0.4708d0,-0.3708d0,-0.2708d0,-0.1708d0,
     & -0.0708d0,0.0292d0,0.1292d0,0.2292d0,0.3292d0,
     & 0.4292d0,0.5292d0,0.6292d0,0.7292d0,0.8292d0,
     & 0.9292d0,1.0292d0,1.1292d0,1.2292d0,1.3292d0,
     & 1.4292d0,1.5292d0/)
          E1=PROPS(1)
        E2=PROPS(2)
        E3=PROPS(3)
          ANNU12=PROPS(4)
        ANNU13=PROPS(5)
        ANNU23=PROPS(6)
        G12=PROPS(7)
        G23=PROPS(8)
        G31=PROPS(9)
        Xt= PROPS(10)
        Xc= PROPS(11)
        Yt= PROPS(12)
        Yc= PROPS(13)
        Zt= PROPS(14)
        Zc= PROPS(15)
        Sxy= PROPS(16)
        Sxz= PROPS(17)
        Syz= PROPS(18)
        mf= PROPS(19)
        p12t= PROPS(20)
        p12c= PROPS(21)
        p23t= PROPS(22)
        p23c= PROPS(23)
        E1m= PROPS(24)
        ANNU21=(E2/E1)*ANNU12
        ANNU31=(E3/E1)*ANNU13
        ANNU32=(E3/E2)*ANNU23
        S=1-ANNU12*ANNU21-ANNU23*ANNU32-ANNU13*ANNU31
     & -TWO*ANNU21*ANNU32*ANNU13
c ------ Stiffness matrix of material ------
            DO I=1,NTENS
              DO J=1,NTENS
              DDSDDE(I,J)=0.0D0
              ENDDO
            ENDDO
                DDSDDE(1,1)=((1-ANNU23*ANNU32)*E1)/S
                DDSDDE(2,2)=((1-ANNU13*ANNU31)*E2)/S
```

```
                DDSDDE(3,3)=((1-ANNU12*ANNU21)*E3)/S
                DDSDDE(4,4)=G12
                DDSDDE(5,5)=G23
                DDSDDE(6,6)=G31
                DDSDDE(1,2)=((ANNU21+ANNU31*ANNU23)*E1)/S
                DDSDDE(1,3)=((ANNU31+ANNU21*ANNU32)*E1)/S
                DDSDDE(2,3)=((ANNU32+ANNU31*ANNU12)*E2)/S
                DDSDDE(2,1)=((ANNU21+ANNU31*ANNU23)*E1)/S
                DDSDDE(3,1)=((ANNU31+ANNU21*ANNU32)*E1)/S
                DDSDDE(3,2)=((ANNU32+ANNU31*ANNU12)*E2)/S
c ------- Vector of stress -------
          DO I=1,NTENS
              DO J=1,NTENS
              STRESS(I) = STRESS(I) + DDSDDE(I,J)*DSTRAN(J)
              ENDDO
          ENDDO
c ------- IMPLEMENTATION OF DAMAGE INITIATION CRITERIA -------
c ------- 3D Puck Failure Criterion in quadratic stress -------
       p23tnew=0.5D0*(SQRT(ONE+TWO*((p12c*Yc)/Sxy) )-ONE)
       p23cnew=0.5D0*(SQRT(ONE+TWO*((p12c*Yc)/Sxy) )-ONE)
c ------- Fiber tension or compression failure mode ----------
            IF (STRESS(1) .GT. 0.0D0) THEN
      F_f = (1/Xt)*(STRESS(1)-(ANNU12-
     &          ANNU12*mf*(E1/E1m))*(STRESS(2)+STRESS(3)))
            ELSEIF (STRESS(1) .LT. 0.0D0) THEN
      F_f = (1/-Xc)*(STRESS(1)-(ANNU12-(ANNU12*mf*(E1/E1m)))*(STRESS(2)+
     &          STRESS(3)))
            ENDIF
       STATEV(1) = F_f
c ------- Inter-fiber tension or compresion failure mode -------
       DO T=1,32,1
       DO U=-1.57D0,1.57D0,0.1d0
       sigman(T)= STRESS(2)*(cos(U))**2 + STRESS(3)*(sin(U))**2 +
     & 2*cos(U)*sin(U)*STRESS(6)
       taunt(T)= -STRESS(2)*sin(U)*cos(U) + STRESS(3)*sin(U)*cos(U) +
     & ((cos(U))**2-(sin(U))**2)*STRESS(6);
       taun1(T)= stress(5)*sin(U) + STRESS(4)*cos(U);
       R23A=(Yc)/(2*(1+p23cnew));
       cose2(T)=(taunt(T)**2)/(taunt(T)**2 + taun1(T)**2);
       sine2(T)=(taun1(T)**2)/(taunt(T)**2 + taun1(T)**2);
       a(T)=(p23t/R23A)*cose2(T) + (p12t/Sxy)*sine2(T);
       b(T)=(p23c/R23A)*cose2(T) + (p12c/Sxy)*sine2(T);
            IF (STRESS(2) .GE. 0.0D0) THEN
       FE(T) = sqrt( ((1/Yt)-a(T))**2*sigman(T)**2 + (taunt(T)/R23A)**2
     & + (taun1(T)/Sxy)**2 ) + a(T)*s22
            ELSEIF (STRESS(2) .LT. 0.0D0) THEN
       FE(T) = sqrt( (taunt(T)/R23A)**2 + (taun1(T)/Sxy)**2 +
```

```
     & (b(T)*sigman(T))**2 ) + b(T)*STRESS(2)
          ENDIF
        ENDDO
        ENDDO
        M=FE(1)
        L = an(1)
        DO o = 2,32,1
          IF (FE(o) .GT. M) THEN
            M = FE(o)
          ENDIF
        ENDDO
         STATEV(2) = M
c
         RETURN
        END
```

Cuntze failure criterion

```
c ------- SUBROUTINE UMAT OF CUNTZE FAILURE CRITERION -------
      subroutine UMAT(STRESS,STATEV,DDSDDE,SSE,SPD,SCD,
     1 RPL,DDSDDT,DRPLDE,DRPLDT,
     2 STRAN,DSTRAN,TIME,DTIME,TEMP,DTEMP,PREDEF,DPRED,CMNAME,
     3 NDI,NSHR,NTENS,NSTATV,PROPS,NPROPS,COORDS,DROT,PNEWDT,
     4 CELENT,DFGRD0,DFGRD1,NOEL,NPT,LAYER,KSPT,JSTEP,KINC)
c
      INCLUDE 'ABA_PARAM.INC'
c
      CHARACTER*80 CMNAME
      DIMENSION STRESS(NTENS),STATEV(NSTATV),
     1 DDSDDE(NTENS,NTENS),DDSDDT(NTENS),DRPLDE(NTENS),
     2 STRAN(NTENS),DSTRAN(NTENS),TIME(2),PREDEF(1),DPRED(1),
     3 PROPS(NPROPS),COORDS(3),DROT(3,3),DFGRD0(3,3),DFGRD1(3,3),
     4 JSTEP(4)
c ------- DEFINITION OF LINEAL MECHANICAL PROPERTIES
c         AND LIMIT STRESSES -------
      PARAMETER(ONE=1.0D0,TWO=2.0D0,THREE=3.0D0,FOUR=4.0D0,A=1.5D0)
         E1=PROPS(1)
        E2=PROPS(2)
        E3=PROPS(3)
         ANNU12=PROPS(4)
        ANNU13=PROPS(5)
        ANNU23=PROPS(6)
        G12=PROPS(7)
        G23=PROPS(8)
        G31=PROPS(9)
        Xt= PROPS(10)
        Xc= PROPS(11)
        Yt= PROPS(12)
```

```
      Yc= PROPS(13)
      Zt= PROPS(14)
      Zc= PROPS(15)
      Sxy= PROPS(16)
      Sxz= PROPS(17)
      Syz= PROPS(18)
      b12e= PROPS(19)
      b23e= PROPS(20)
      m = PROPS(21)
      ANNU21=(E2/E1)*ANNU12
      ANNU31=(E3/E1)*ANNU13
      ANNU32=(E3/E2)*ANNU23
      S=1-ANNU12*ANNU21-ANNU23*ANNU32-ANNU13*ANNU31
     & -TWO*ANNU21*ANNU32*ANNU13
c ------- Stiffness matrix of material -------
         DO I=1,NTENS
           DO J=1,NTENS
           DDSDDE(I,J)=0.0D0
           ENDDO
         ENDDO
              DDSDDE(1,1)=((1-ANNU23*ANNU32)*E1)/S
              DDSDDE(2,2)=((1-ANNU13*ANNU31)*E2)/S
              DDSDDE(3,3)=((1-ANNU12*ANNU21)*E3)/S
              DDSDDE(4,4)=G12
              DDSDDE(5,5)=G23
              DDSDDE(6,6)=G31
              DDSDDE(1,2)=((ANNU21+ANNU31*ANNU23)*E1)/S
              DDSDDE(1,3)=((ANNU31+ANNU21*ANNU32)*E1)/S
              DDSDDE(2,3)=((ANNU32+ANNU31*ANNU12)*E2)/S
              DDSDDE(2,1)=((ANNU21+ANNU31*ANNU23)*E1)/S
              DDSDDE(3,1)=((ANNU31+ANNU21*ANNU32)*E1)/S
              DDSDDE(3,2)=((ANNU32+ANNU31*ANNU12)*E2)/S
c ------- Vector of stress -------
         DO I=1,NTENS
              DO J=1,NTENS
              STRESS(I) = STRESS(I) + DDSDDE(I,J)*DSTRAN(J)
              ENDDO
         ENDDO
c ------- IMPLEMENTATION OF DAMAGE INITIATION CRITERIA -------
c ------- 3D Cuntze Failure Criterion in quadratic stress -------
       I1 = STRESS(1)
       I2 = ((STRESS(2)) + (STRESS(3)))
       I3 = (STRESS(4))**2 + (STRESS(6))**2
       I4 = (STRESS(2)-STRESS(3))**2 +
     &     (FOUR*(STRESS(6))**2)
       I5 = ((STRESS(2))-(STRESS(3)))*(STRESS(6)**2-STRESS(4)**2)-
     &      (FOUR*(STRESS(4))*(STRESS(5))*(STRESS(6)))
```

```
      I235 = (TWO*STRESS(2)*(STRESS(4))**2) +
     &       (TWO*STRESS(3)*(STRESS(6))**2) +
     &       (FOUR*STRESS(4)*STRESS(5)*STRESS(6))
c ------ Fiber tension or compression failure mode ----------
          IF (STRESS(1) .GE. 0.0D0) THEN
          f_FF1 = STRESS(1)/Xt
          ENDIF
          IF (STRESS(1) .LT. 0.0D0) THEN
          f_FF1 = -STRESS(1)/Xc
          f_FF2 = -STRESS(1)/Xc
          ENDIF
c ------ Inter-fiber tension or compresion failure mode ------
          IF (STRESS(2) .GE. 0.0D0) THEN
      f_IFF1e =((STRESS(2)+STRESS(3))+((STRESS(2)-STRESS(3))**2+
     & FOUR*(STRESS(6))**2)**0.5D0)/(TWO*Yt)
          ELSEIF (STRESS(2) .LT. 0.0D0) THEN
      f_IFF2e = ((b23e-1)*(STRESS(2)+STRESS(3))+
     & b23*((STRESS(2)-STRESS(3))**2+FOUR*(STRESS(6))**2)**0.5D0)*(1/Yc)
          ENDIF
      f_IFF3e = (((b12e*I235)+((b12e)**2*(I235)**2+
     & FOUR*(Sxy)**2*((STRESS(6))**2+
     & (STRESS(4))**2)**2)**0.5D0)/(TWO*(Sxy)**3))**0.5D0
c ------ Effort ------
          Eff= ((f_FF1)**m + (f_FF2)**m + (f_IFF1)**m +
     &     (f_IFF2e)**m + (f_IFF3e)**m)
          STATEV(1) = Eff
          STATEV(2) = f_FF1
          STATEV(3) = f_IFF1e
          STATEV(4) = f_IFF2e
          STATEV(5) = f_IFF3e
c
        RETURN
        END
```

A.2 VUMAT subroutine codes

The user subroutine VUMAT allows implementing the failure criteria under dynamic loading conditions. This subroutine can be written in FORTRAN code, which is attached in the finite element software Abaqus. The mechanical constitutive behaviour of the material is defined in a corotational system in which the basis system rotate with the material [1]. The SDVs can be used and updated during the implementation.

Hashin failure criterion

```
c ------- SUBROUTINE VUMAT OF HASHIN FAILURE CRITERION -------
      subroutine vumat(
c ------- Read only (unmodifiable)variables -------
     1  nblock, ndir, nshr, nstatev, nfieldv, nprops, lanneal,
     2  stepTime, totalTime, dt, cmname, coordMp, charLength,
     3  props, density, strainInc, relSpinInc,
     4  tempOld, stretchOld, defgradOld, fieldOld,
     5  stressOld, stateOld, enerInternOld, enerInelasOld,
     6  tempNew, stretchNew, defgradNew, fieldNew,
c ------- Write only (modifiable) variables -------
     7  stressNew, stateNew, enerInternNew, enerInelasNew )
c
      include 'vaba_param.inc'
c
      dimension props(nprops), density(nblock), coordMp(nblock,*),
     1  charLength(nblock), strainInc(nblock,ndir+nshr),
     2  relSpinInc(nblock,nshr), tempOld(nblock),
     3  stretchOld(nblock,ndir+nshr),
     4  defgradOld(nblock,ndir+nshr+nshr),
     5  fieldOld(nblock,nfieldv), stressOld(nblock,ndir+nshr),
     6  stateOld(nblock,nstatev), enerInternOld(nblock),
     7  enerInelasOld(nblock), tempNew(nblock),
     8  stretchNew(nblock,ndir+nshr),
     8  defgradNew(nblock,ndir+nshr+nshr),
     9  fieldNew(nblock,nfieldv),
     1  stressNew(nblock,ndir+nshr), stateNew(nblock,nstatev),
     2  enerInternNew(nblock), enerInelasNew(nblock)
c
      character*80 cmname
c ------- DEFINITION OF LINEAL MECHANICAL PROPERTIES
c         AND LIMIT STRESSES -------
      DOUBLE PRECISION e1, e2, e3, annu12, annu13,annu23,g12,g13,g23
      DOUBLE PRECISION Xt, Xc
      DOUBLE PRECISION Yt, Yc, Zt, Zc, Sxy, Sxz, Syz
      DOUBLE PRECISION annu21, annu31, annu32
```

```
      DOUBLE PRECISION s, c11, c12, c13, c22, c33, c23, c44, c55, c66
c
      parameter(zero=0.0d0,one=1.0d0,two=2.0d0,three=3.0d0,four=4.0d0,
     & half=0.5d0)
      dimension JAC(6,6), dmg(nblock,2)
      real n, a
c
      a= props(1)
      e1= props(2)
      e2= props(3)
      e3= props(4)
      annu12= props(5)
      annu13= props(6)
      annu23= props(7)
      g12= props(8)
      g13= props(9)
      g23= props(10)
      Xt= props(11)
      Xc= props(12)
      Yt= props(13)
      Yc= props(14)
      Zt= props(15)
      Zc= props(16)
      Sxy= props(17)
      Sxz= props(18)
      Syz= props(19)
      annu21=(e2/e1)*annu12
      annu31=(e3/e1)*annu13
      annu32=(e3/e2)*annu23
      s=one-(annu12*annu21)-(annu23*annu32)-(annu13*annu31)-
     & (two*annu21*annu32*annu13)
c ------ Stiffness matrix of material ------
      c11=(e1*(1.0d0-annu23*annu32))/s
      c22=(e2*(1.0d0-annu13*annu31))/s
      c33=(e3*(1.0d0-annu12*annu21))/s
      c12=(e1*(annu21+annu31*annu23))/s
      c13=(e1*(annu31+annu21*annu32))/s
      c23=(e2*(annu32+annu12*annu31))/s
      c44=g12
      c55=g13
      c66=g23
      c21=((annu21+annu31*annu23)*e1)/s
      c31=((annu31+annu21*annu32)*e1)/s
      c32=((annu32+annu31*annu12)*e2)/s
c ------ Elastic stress update ------
       do i = 1, nblock
      stressNew(i,1)= stressOld(i,1) + c11*strainInc(i,1) +
```

```
     &     c12*strainInc(i,2) + c13*strainInc(i,3)
           stressNew(i,2)= stressOld(i,2) + c21*strainInc(i,1) +
     &     c22*strainInc(i,2) + c23*strainInc(i,3)
           stressNew(i,3)=stressOld(i,3) + c31*strainInc(i,1) +
     &     c32*strainInc(i,2) + c33*strainInc(i,3)
           stressNew(i,4)=stressOld(i,4) + two*c44*strainInc(i,4)
           stressNew(i,5)=stressOld(i,5) + two*c55*strainInc(i,5)
           stressNew(i,6)=stressOld(i,6) + two*c66*strainInc(i,6)
c ------- Update back stress -------
           stateNew(i,1) = stressNew(i,1)
           stateNew(i,2) = stressNew(i,2)
           stateNew(i,3) = stressNew(i,3)
           stateNew(i,4) = stressNew(i,4)
           stateNew(i,5) = stressNew(i,5)
           stateNew(i,6) = stressNew(i,6)
c ------- IMPLEMENTATION OF DAMAGE INITIATION CRITERIA -------
c ------- 3D Hashin Failure Criterion in quadratic stress -------
           s11 = stressNew(i,1)
           s22 = stressNew(i,2)
           s33 = stressNew(i,3)
           s12 = stressNew(i,4)
           s23 = stressNew(i,5)
           s13 = stressNew(i,6)
c ------- Fiber tension or compression failure mode ----------
            IF (s11 .GT. zero) THEN
         dmg(i,1) = SQRT( (abs(s11)/Xt)**2 + (abs(s12)/Sxy)**2 +
     & (abs(s13)/Sxz) )
            ELSEIF (s11 .LE. zero) THEN
         dmg(i,1) = abs(s11)/Xc
            ENDIF
c ------- Inter-fiber tension or compresion failure mode -------
           IF ((s22 + s33) .GT. zero) THEN
         a = one/((Yt)**2)
         dmg(i,2) =SQRT( ABS(((s22+s33)**2)*a - (s22*s33)/(Syz)**2 +
     & (s12)**2/(Syz)**2 + (s13)**2/(Sxy)**2 + (s23)**2/(Sxy)**2 ))
            ELSEIF ((s22 + s33) .LE. zero) THEN
         n = one/(four*(Syz)**2)
         dmg(i,2)= SQRT( ABS( ((s22 + s33)**2)*n +
     & ((s22+s33)/Yc)*((Yc/(two*Syz))**2-one) -
     & (s22*s33)/(Syz)**2 + (s12)**2/(Syz)**2 +
     & (s13)**2/(Sxy)**2 + (s23)**2/(Sxy)**2 ))
           ENDIF
c ------- Update back failure indexes -------
           stateNew(i,7) = dmg(i,1)
           stateNew(i,8) = dmg(i,2)
             enddo
c
```

```
      return
      end
```

Puck failure criterion

```
c ------- SUBROUTINE VUMAT OF PUCK FAILURE CRITERION -------
      subroutine vumat(
c ------- Read only (unmodifiable)variables -------
     1  nblock, ndir, nshr, nstatev, nfieldv, nprops, lanneal,
     2  stepTime, totalTime, dt, cmname, coordMp, charLength,
     3  props, density, strainInc, relSpinInc,
     4  tempOld, stretchOld, defgradOld, fieldOld,
     5  stressOld, stateOld, enerInternOld, enerInelasOld,
     6  tempNew, stretchNew, defgradNew, fieldNew,
c ------- Write only (modifiable) variables -------
     7  stressNew, stateNew, enerInternNew, enerInelasNew )
c
      include 'vaba_param.inc'
c
      dimension props(nprops), density(nblock), coordMp(nblock,*),
     1  charLength(nblock), strainInc(nblock,ndir+nshr),
     2  relSpinInc(nblock,nshr), tempOld(nblock),
     3  stretchOld(nblock,ndir+nshr),
     4  defgradOld(nblock,ndir+nshr+nshr),
     5  fieldOld(nblock,nfieldv), stressOld(nblock,ndir+nshr),
     6  stateOld(nblock,nstatev), enerInternOld(nblock),
     7  enerInelasOld(nblock), tempNew(nblock),
     8  stretchNew(nblock,ndir+nshr),
     8  defgradNew(nblock,ndir+nshr+nshr),
     9  fieldNew(nblock,nfieldv),
     1  stressNew(nblock,ndir+nshr), stateNew(nblock,nstatev),
     2  enerInternNew(nblock), enerInelasNew(nblock)
c
      character*80 cmname
c ------- DEFINITION OF LINEAL MECHANICAL PROPERTIES
c         AND LIMIT STRESSES -------
      DOUBLE PRECISION e1, e2, e3, annu12, annu13,annu23,g12,g13,g23
      DOUBLE PRECISION Xt, Xc
      DOUBLE PRECISION Yt, Yc, Zt, Zc, Sxy, Sxz, Syz
      DOUBLE PRECISION annu21, annu31, annu32
      DOUBLE PRECISION s, c11, c12, c13, c22, c33, c23, c44, c55, c66
c
      parameter(zero=0.0d0,one=1.0d0,two=2.0d0,three=3.0d0,four=4.0d0,
     & half=0.5d0)
      real M, o, p
      dimension JAC(6,6), dmg(nblock,2)
      DIMENSION an(32), sigman(32), taunt(32), taun1(32),
     &  cose2(32), sine2(32), a(32), b(32), FE(32)
```

```
      an =(/-1.5708d0,-1.4708d0,-1.3708d0,-1.2708d0,-1.1708d0,
     & -1.0708d0,-0.9708d0,-0.8708d0,-0.7708d0,-0.6708d0,
     & -0.5708d0,-0.4708d0,-0.3708d0,-0.2708d0,-0.1708d0,
     & -0.0708d0,0.0292d0,0.1292d0,0.2292d0,0.3292d0,
     & 0.4292d0,0.5292d0,0.6292d0,0.7292d0,0.8292d0,
     & 0.9292d0,1.0292d0,1.1292d0,1.2292d0,1.3292d0,
     & 1.4292d0,1.5292d0/)
c Read material properties
      a= props(1)
      e1= props(2)
      e2= props(3)
      e3= props(4)
      annu12= props(5)
      annu13= props(6)
      annu23= props(7)
      g12= props(8)
      g13= props(9)
      g23= props(10)
      Xt= props(11)
      Xc= props(12)
      Yt= props(13)
      Yc= props(14)
      Zt= props(15)
      Zc= props(16)
      Sxy= props(17)
      Sxz= props(18)
      Syz= props(19)
      mf= PROPS(20)
      p12t= PROPS(21)
      p12c= PROPS(22)
      p23t= PROPS(23)
      p23c= PROPS(24)
      e1m= PROPS(25)
      annu21=(e2/e1)*annu12
      annu31=(e3/e1)*annu13
      annu32=(e3/e2)*annu23
      s=one-(annu12*annu21)-(annu23*annu32)-(annu13*annu31)-
     & (two*annu21*annu32*annu13)
c ------ Stiffness matrix of material ------
      c11=(e1*(1.0d0-annu23*annu32))/s
      c22=(e2*(1.0d0-annu13*annu31))/s
      c33=(e3*(1.0d0-annu12*annu21))/s
      c12=(e1*(annu21+annu31*annu23))/s
      c13=(e1*(annu31+annu21*annu32))/s
      c23=(e2*(annu32+annu12*annu31))/s
      c44=g12
      c55=g13
```

```
      c66=g23
      c21=((annu21+annu31*annu23)*e1)/s
      c31=((annu31+annu21*annu32)*e1)/s
      c32=((annu32+annu31*annu12)*e2)/s
c ------- Update back stress -------
       do i = 1, nblock
c---------- Elastic stress increment ----------
        stressNew(i,1)= stressOld(i,1) + c11*strainInc(i,1) +
     &   c12*strainInc(i,2) + c13*strainInc(i,3)
        stressNew(i,2)= stressOld(i,2) + c21*strainInc(i,1) +
     &   c22*strainInc(i,2) + c23*strainInc(i,3)
        stressNew(i,3)=stressOld(i,3) + c31*strainInc(i,1) +
     &   c32*strainInc(i,2) + c33*strainInc(i,3)
        stressNew(i,4)=stressOld(i,4) + two*c44*strainInc(i,4)
        stressNew(i,5)=stressOld(i,5) + two*c55*strainInc(i,5)
        stressNew(i,6)=stressOld(i,6) + two*c66*strainInc(i,6)
c---------- Update back stress ----------
        stateNew(i,1) = stressNew(i,1)
        stateNew(i,2) = stressNew(i,2)
        stateNew(i,3) = stressNew(i,3)
        stateNew(i,4) = stressNew(i,4)
        stateNew(i,5) = stressNew(i,5)
        stateNew(i,6) = stressNew(i,6)
c ------- IMPLEMENTATION OF DAMAGE INITIATION CRITERIA -------
c ------- 3D Puck Failure Criterion in quadratic stress -------
        s11 = stressNew(i,1)
        s22 = stressNew(i,2)
        s33 = stressNew(i,3)
        s12 = stressNew(i,4)
        s23 = stressNew(i,5)
        s13 = stressNew(i,6)
c ------- Fiber tension or compression failure mode ----------
          IF (s11 .GT. zero) THEN
     dmg(i,1) = (1/Xt)*(s11-(annu12-
     &         annu12*mf*(e1m/e1))*(s22+s33))
          ELSEIF (s11 .LT. zero) THEN
     dmg(i,1) = (1/-Xc)*(s11-(annu12-(annu12*mf*(e1m/e1)))*(s22+
     &         s33))
          ENDIF
c ------- Inter-fiber tension or compresion failure mode -------
      p23tnew=0.5D0*(SQRT(one+two*((p12c*Yc)/Sxy) )-one)
      p23cnew=0.5D0*(SQRT(one+two*((p12c*Yc)/Sxy) )-one)
      DO T=1,32,1
      DO U=-1.57D0,1.57D0,0.1d0
      sigman(T)= s22*(cos(U))**2 + s33*(sin(U))**2 +
     & 2*cos(U)*sin(U)*s13
      taunt(T)= -s22*sin(U)*cos(U) + s33*sin(U)*cos(U) +
```

```
     & ((cos(U))**2-(sin(U))**2)*s13;
      taun1(T)= s23*sin(U) + s12*cos(U);
      R23A=(Yc)/(2*(1+p23cnew));
      cose2(T)=(taunt(T)**2)/(taunt(T)**2 + taun1(T)**2);
      sine2(T)=(taun1(T)**2)/(taunt(T)**2 + taun1(T)**2);
      a(T)=(p23t/R23A)*cose2(T) + (p12t/Sxy)*sine2(T);
      b(T)=(p23c/R23A)*cose2(T) + (p12c/Sxy)*sine2(T);
           IF (s22 .GE. 0.0D0) THEN
      FE(T) = sqrt( ((1/Yt)-a(T))**2*sigman(T)**2 + (taunt(T)/R23A)**2
     & + (taun1(T)/Sxy)**2 ) + a(T)*s22
           ELSEIF (s22 .LT. 0.0D0) THEN
      FE(T) = sqrt( (taunt(T)/R23A)**2 + (taun1(T)/Sxy)**2 +
     & (b(T)*sigman(T))**2 ) + b(T)*s22
           ENDIF
      ENDDO
      ENDDO
c ------- Update back failure indexes -------
      M=FE(1)
      L=an(1)
      DO o = 2,32,1
           IF (FE(o) .GT. M) THEN
                M = FE(o)
           ENDIF
      ENDDO
      dmg(i,2) = M
        stateNew(i,7) = dmg(i,1)
        stateNew(i,8) = dmg(i,2)
          enddo
c
       return
      end
```

Cuntze failure criterion

```
c ------- SUBROUTINE VUMAT OF CUNTZE FAILURE CRITERION -------
      subroutine vumat(
c ------- Read only (unmodifiable)variables -------
     1  nblock, ndir, nshr, nstatev, nfieldv, nprops, lanneal,
     2  stepTime, totalTime, dt, cmname, coordMp, charLength,
     3  props, density, strainInc, relSpinInc,
     4  tempOld, stretchOld, defgradOld, fieldOld,
     5  stressOld, stateOld, enerInternOld, enerInelasOld,
     6  tempNew, stretchNew, defgradNew, fieldNew,
c ------- Write only (modifiable) variables -------
     7  stressNew, stateNew, enerInternNew, enerInelasNew )
c
      include 'vaba_param.inc'
c
```

```
      dimension props(nprops), density(nblock), coordMp(nblock,*),
     1  charLength(nblock), strainInc(nblock,ndir+nshr),
     2  relSpinInc(nblock,nshr), tempOld(nblock),
     3  stretchOld(nblock,ndir+nshr),
     4  defgradOld(nblock,ndir+nshr+nshr),
     5  fieldOld(nblock,nfieldv), stressOld(nblock,ndir+nshr),
     6  stateOld(nblock,nstatev), enerInternOld(nblock),
     7  enerInelasOld(nblock), tempNew(nblock),
     8  stretchNew(nblock,ndir+nshr),
     8  defgradNew(nblock,ndir+nshr+nshr),
     9  fieldNew(nblock,nfieldv),
     1  stressNew(nblock,ndir+nshr), stateNew(nblock,nstatev),
     2  enerInternNew(nblock), enerInelasNew(nblock)
c
      character*80 cmname
c ------ DEFINITION OF MATERIAL LINEAL MECHANICAL PROPERTIES AND LIMIT STRESSES ----
      DOUBLE PRECISION e1, e2, e3, annu12, annu13,annu23,g12,g13,g23
      DOUBLE PRECISION Xt, Xc
      DOUBLE PRECISION Yt, Yc, Zt, Zc, Sxy, Sxz, Syz
      DOUBLE PRECISION annu21, annu31, annu32
      DOUBLE PRECISION s, c11, c12, c13, c22, c33, c23, c44, c55, c66
c
      parameter(zero=0.0d0,one=1.0d0,two=2.0d0,three=3.0d0,four=4.0d0,
     & half=0.5d0)
      dimension JAC(6,6), dmg(nblock,6)
      a= props(1)
      e1= props(2)
      e2= props(3)
      e3= props(4)
      annu12= props(5)
      annu13= props(6)
      annu23= props(7)
      g12= props(8)
      g13= props(9)
      g23= props(10)
      Xt= props(11)
      Xc= props(12)
      Yt= props(13)
      Yc= props(14)
      Zt= props(15)
      Zc= props(16)
      Sxy= props(17)
      Sxz= props(18)
      Syz= props(19)
      b12e= PROPS(20)
      b23e= PROPS(21)
      m = PROPS(22)
```

```
      annu21=(e2/e1)*annu12
      annu31=(e3/e1)*annu13
      annu32=(e3/e2)*annu23
      s=one-(annu12*annu21)-(annu23*annu32)-(annu13*annu31)-
     & (two*annu21*annu32*annu13)
c ------ Stiffness matrix of material ------
      c11=(e1*(1.0d0-annu23*annu32))/s
      c22=(e2*(1.0d0-annu13*annu31))/s
      c33=(e3*(1.0d0-annu12*annu21))/s
      c12=(e1*(annu21+annu31*annu23))/s
      c13=(e1*(annu31+annu21*annu32))/s
      c23=(e2*(annu32+annu12*annu31))/s
      c44=g12
      c55=g13
      c66=g23
      c21=((annu21+annu31*annu23)*e1)/s
      c31=((annu31+annu21*annu32)*e1)/s
      c32=((annu32+annu31*annu12)*e2)/s
c ------ Elastic stress update ------
        do i = 1, nblock
c--------- Elastic stress increment ---------
        stressNew(i,1)= stressOld(i,1) + c11*strainInc(i,1) +
     &   c12*strainInc(i,2) + c13*strainInc(i,3)
        stressNew(i,2)= stressOld(i,2) + c21*strainInc(i,1) +
     &   c22*strainInc(i,2) + c23*strainInc(i,3)
        stressNew(i,3)=stressOld(i,3) + c31*strainInc(i,1) +
     &   c32*strainInc(i,2) + c33*strainInc(i,3)
        stressNew(i,4)=stressOld(i,4) + two*c44*strainInc(i,4)
        stressNew(i,5)=stressOld(i,5) + two*c55*strainInc(i,5)
        stressNew(i,6)=stressOld(i,6) + two*c66*strainInc(i,6)
c ------ Update back stress ------
        stateNew(i,1) = stressNew(i,1)
        stateNew(i,2) = stressNew(i,2)
        stateNew(i,3) = stressNew(i,3)
        stateNew(i,4) = stressNew(i,4)
        stateNew(i,5) = stressNew(i,5)
        stateNew(i,6) = stressNew(i,6)
c ------ IMPLEMENTATION OF DAMAGE INITIATION CRITERIA ------
c ------ 3D Cuntze Failure Criterion in quadratic stress ------
        s11 = stressNew(i,1)
        s22 = stressNew(i,2)
        s33 = stressNew(i,3)
        s12 = stressNew(i,4)
        s23 = stressNew(i,5)
        s13 = stressNew(i,6)
c ------ Invariant ------
      I235 = ABS((two*s22*(s12)**2) +
```

```
     &        (two*s33*(s23)**2) +
     &        (four*s12*s13*s23))
c ------ Fiber tension or compression failure mode ----------
      dmg(i,1) = s11/Xt
      dmg(i,1) = ABS(s11)/Xc
      dmg(i,2) = ABS(s11)/Xc
c ------ Inter-fiber tension or compresion failure mode ------
      dmg(i,3) = ((s22+s33)+SQRT((s22-s33)**2+
     & four*(s23)**2))/(two*Yt)
      dmg(i,4) = ((b23e-1)*(s22+s33) +
     & b23*SQRT((s22-s33)**2+four*(s23)**2))*(1/Yc)
      dmg(i,5) =SQRT( ( (b12e*I235) + SQRT((b12e)**2*(I235)**2+
     & four*(Sxy)**2*((s23)**2 + (s12)**2)**2) )/(two*(Sxy)**3))
c ------ Effort ------
      dmg(i,6)=((dmg(i,1))**m + (dmg(i,2))**m + (dmg(i,3))**m +
     &     (dmg(i,4))**m + (dmg(i,5))**m)
c ------ Update back failure indexes ------
        stateNew(i,7) = dmg(i,1)
        stateNew(i,8) = dmg(i,3)
        stateNew(i,9) = dmg(i,4)
        stateNew(i,10) = dmg(i,5)
        stateNew(i,11) = dmg(i,6)
          enddo
c
       return
      end
```